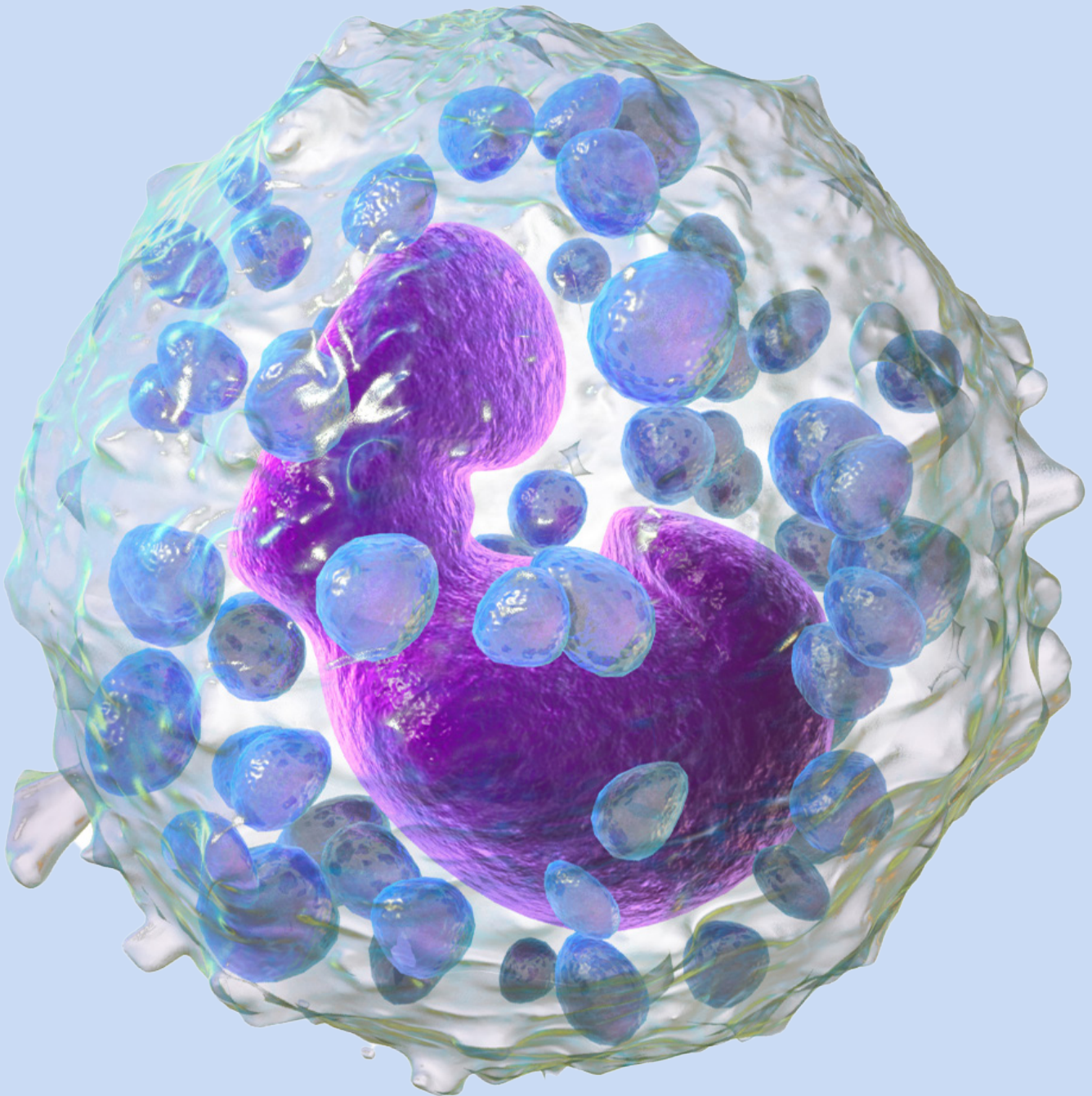


# TURKISH JOURNAL OF IMMUNOLOGY

**13**  
Volume  
**1**  
Issue



## Editor-in-Chief

### Prof. Günnur Deniz, PhD

İstanbul University, Aziz Sancar Institute of  
Experimental Medicine, Department of  
Immunology, İstanbul, Türkiye  
gdeniz@istanbul.edu.tr  
ORCID: 0000-0002-0721-6213

## Managing Editor

### Prof. Akif Turna, MD, PhD

İstanbul University-Cerrahpasa, Cerrahpasa  
Faculty of Medicine, Department of Thoracic  
Surgery, İstanbul, Türkiye  
akif.turna@gmail.com  
ORCID: 0000-0003-3229-830X

## Executive Office

### Türk İmmünoloji Derneği

Doğpa Ticaret AŞ Blok Yıldız Cad No 55  
34353 Beşiktaş - İstanbul, Türkiye  
turkimmunolojidernegi@gmail.com  
+90 212 - 414 20 97

## Publication Secretary

### Esra Dizdar

Turkish Society of Immunology  
(Türk İmmünoloji Derneği)  
turkimmunolojidernegi@gmail.com

## Assistant Editors

### Prof. Arzu Aral, MD, PhD

Yeditepe University Faculty of Medicine,  
Department of Immunology, İstanbul, Türkiye  
arzuaral@gmail.com  
ORCID: 0000-0002-7300-1624

### Prof. Ceren Çıracı, PhD

İstanbul Technical University Faculty of Science  
and Literature, Department of Molecular  
Biology and Genetics, İstanbul, Türkiye  
cerenciraci@gmail.com  
ORCID: 0000-0003-2162-0930

### Asst. Prof. Tolga Sütü, PhD

Acibadem University Faculty of Engineering  
and Natural Sciences, Department of Molecular  
Biology and Genetics, İstanbul, Türkiye  
Tolga.Sutlu@acibadem.edu.tr  
ORCID: 0000-0002-7813-8734

### Prof. Ali Önder Yıldırım, MD, PhD

Helmholtz Zentrum München, Germany  
oender.yildirim@helmholtz-muenchen.de  
ORCID: 0000-0003-1969-480X

## English Language Editor

### Rabia Ünal

DOC Tasarım ve Bilişim Ltd. Şti., İstanbul, Türkiye



## Owner

Owned by on behalf of the Turkish Society of Immunology:  
Prof. İhsan Gürsel



## Publication and Design

DOC Design and Informatics Co. Ltd.

E-mail: info@dotdoc.com.tr

Web page: www.dotdoc.com.tr

## Publishing Coordinator

Gizem Pakdil

## Design Lead

Ali Pekşen

## Software

Asim Demirağ

## Informatics

Nuh Naci Kışnişçi

## Graphic Design

Yeşim Akdeniz

## EDITORIAL BOARD

### **Prof. Ali Önder Yıldırım, MD, PhD**

Helmholtz Zentrum München, Germany  
oender.yildirim@helmholtz-muenchen.de  
ORCID: 0000-0003-1969-480X

### **Prof. Barbaros Oral, MD, PhD**

Bursa Uludag University Faculty of Medicine,  
Department of Immunology, Bursa, Türkiye  
oralb@uludag.edu.tr  
ORCID: 0000-0003-0463-6818

### **Prof. Cevayir Çoban, MD, PhD**

The Institute of Medical Science (IMSUT), The University  
of Tokyo Division of Malaria Immunology, Japan  
ccoban@ims.u-tokyo.ac.jp  
ORCID: 0000-0002-4467-7799

### **Prof. Cezmi Akdiş, MD**

Swiss Institute of Allergy and Asthma, Davos,  
Switzerland  
akdisac@siaf.uzh.ch  
ORCID: 0000-0001-8020-019X

### **Prof. Derya Unutmaz, MD**

The Jackson Laboratory, Bar Harbor, USA  
derya@mac.com  
ORCID: 0000-0001-8898-6633

### **Prof. Dicle Güç, MD, PhD**

Hacettepe University, Basic Oncology Institute, Retired  
Lecturer, Ankara, Türkiye  
dicleguc17@gmail.com  
ORCID: 0000-0003-1203-2109

### **Prof. Güher Saruhan Direskeneli, MD, PhD**

İstanbul University, İstanbul Faculty of Medicine,  
Department of Physiology, İstanbul, Türkiye  
gsaruhan@istanbul.edu.tr  
ORCID: 0000-0002-6903-7173

### **Prof. Haner Direskeneli, MD**

Marmara University Faculty of Medicine, Department  
of Internal Medicine, Department of Rheumatology,  
İstanbul, Türkiye  
hanerdireskeneli@gmail.com  
ORCID: 0000-0003-2598-5806

### **Prof. İhsan Gürsel, PhD**

Bilkent University, Department of Molecular Biology and  
Genetics, Ankara, Türkiye  
ihsangursel@bilkent.edu.tr  
ORCID: 0000-0003-3761-1166

### **Prof. Ken J. Ishii, MD, PhD**

Tokyo University, Institute of Medical Science, Division  
of Vaccine Science, Department of Microbiology and  
Immunology, Japan  
kenishii@ims.u-tokyo.ac.jp  
ORCID: 0000-0002-6728-3872

### **Prof. Mayda Gürsel, PhD**

Middle East Technical University, Department of  
Biological Sciences, Ankara, Türkiye  
mgursel@metu.edu.tr  
ORCID: 0000-0003-0044-9054

### **Prof. Moshe Arditı, MD**

Cedars-Sinai Medical Center, Department of Pediatrics,  
USA  
Moshe.Arditi@cshs.org  
ORCID: 0000-0001-9042-2909

### **Oral Alpan, MD**

Amerimmune Clinic, Fairfax, USA  
Oalpan@me.com  
ORCID: 0000-0001-7467-8541

### **Prof. Sühendan Ekmekcioğlu, PhD**

MD Anderson Cancer Center, Department of Melanoma  
Medical Oncology, Division of Cancer Medicine, Huston,  
USA  
sekmekcioglu@mdanderson.org  
ORCID: 0000-0003-4079-6632

### **Prof. Şefik Şanal Alkan, PhD**

Alkan Consulting LLC, Switzerland  
sefik.alkan@gmail.com  
ORCID: 0000-0001-8922-6337

### **Prof. Yıldız Camcioğlu, MD**

İstanbul University-Cerrahpaşa, Cerrahpaşa Faculty of  
Medicine, Department of Pediatrics, Retired Lecturer,  
İstanbul, Türkiye  
camciy@yahoo.com  
ORCID: 0000-0002-4796-6828

## ADVISORY BOARD

### **Adil Doğanay Duru, MD**

Glycostem Therapeutics, Oss, The Netherlands

### **Prof. Ahmet Özen, MD**

Marmara University Faculty of Medicine, Department of Pediatric Allergy-Immunology, İstanbul, Türkiye

### **Assoc. Prof. Ahmet Eken, PhD**

Erciyes University Faculty of Medicine, Department of Medical Biology, Kayseri, Türkiye

### **Assoc. Prof. Ayça Aslan Kıyıkım, MD**

İstanbul University-Cerrahpasa, Cerrahpasa Faculty of Medicine, Department of Pediatric Allergy-Immunology, İstanbul, Türkiye

### **Assoc. Prof. Ayça Sayı Yazgan, PhD**

İstanbul Teknik University, Department of Molecular Biology and Genetics, İstanbul, Türkiye

### **Assoc. Prof. Ayten Nalbant, PhD**

Izmir Institute of Technology, Department of Molecular Biology and Genetics, Izmir, Türkiye

### **Prof. Batu Erman, PhD**

Bogazici University Faculty of Medicine, Department of Molecular Biology and Genetics, İstanbul, Türkiye

### **Asst. Prof. Baran Erman, PhD**

Hacettepe University, Child Health Institute, Department of Pediatric Basic Sciences, HÜGEN, Can Sucak Translational Immunology Research Laboratory, Ankara, Türkiye

### **Prof. Cem Ar, MD, PhD**

İstanbul University-Cerrahpasa, Cerrahpasa Faculty of Medicine, Department of Hematology, İstanbul, Türkiye

### **Assoc. Prof. Çağman Tan, PhD**

Hacettepe University Faculty of Medicine, Child Health Institute, Department of Child Health and Diseases, Division of Pediatric Immunology, Ankara, Türkiye

### **Prof. Deniz Nazire Çağdaş Ayvaz, MD**

Hacettepe University Faculty of Medicine, Child Health Institute, Department of Child Health and Diseases, Division of Pediatric Immunology, Ankara, Türkiye

### **Asst. Prof. Diğdem Yöyen Ermiş, PhD**

Bursa Uludag University Faculty of Medicine, Department of Immunology, Bursa, Türkiye

### **Assoc. Prof. Duygu Sağ, PhD**

Dokuz Eylul University, Izmir Biomedicine and Genome Center, Izmir, Türkiye

### **Prof. Elif Aydiner, MD**

Marmara University Faculty of Medicine, Department of Pediatric Allergy-Immunology, İstanbul, Türkiye

### **Prof. Emel Ekşioğlu Demiralp, MD, PhD**

İstanbul Memorial Hospital, Tissue Type and Immunology Laboratory, İstanbul, Türkiye

### **Prof. Erdem Tüzün, MD**

İstanbul University, Aziz Sancar Institute of Experimental Medicine, Department of Neuroscience, İstanbul, Türkiye

### **Dr. Esen Şefik, PhD**

Yale University, Dr. Diane Mathis ve Dr. Christophe Benoist Laboratory, USA

### **Prof. Esin Aktaş, PhD**

İstanbul University, Aziz Sancar Institute of Experimental Medicine, Department of Immunology, İstanbul, Türkiye

### **Assoc. Prof. Fatih Kocabaş, MD**

Yeditepe University Faculty of Medicine, Department of Molecular Biology and Genetics, İstanbul, Türkiye

### **Prof. Ferah Budak, PhD**

Bursa Uludag University Faculty of Medicine, Department of Immunology, Bursa, Türkiye

### **Prof. Gaye Erten Yurdagül, MD, PhD**

İstanbul University, Aziz Sancar Institute of Experimental Medicine, Department of Immunology, İstanbul, Türkiye

### **Prof. Gülderen Yanıkkaya Demirel, MD, PhD**

Yeditepe University Faculty of Medicine, Department of Immunology, İstanbul, Türkiye

### **Prof. Güneş Esendağlı, PhD**

Hacettepe University, Basic Oncology Institute, Ankara, Türkiye

### **Assoc. Prof. Gürcan Günaydın, MD, PhD**

Hacettepe University, Cancer Institute, Department of Basic Oncology, Ankara, Türkiye

**Prof. Hasibe Artaç, MD**

Selcuk University Faculty of Medicine, Department of Immunology, Konya, Türkiye

**Assoc. Prof. Hande Canpınar, PhD**

Hacettepe University, Cancer Institute, Department of Basic Oncology, Ankara, Türkiye

**Prof. İlgin Özden, MD**

İstanbul University-İstanbul Faculty of Medicine, Department of General Surgery, İstanbul, Türkiye

**Assoc. Prof. Jülide Duymaz, PhD**

Trakya University, Vocational School of Health Services, Edirne, Türkiye

**Assoc. Prof. Leyla Pur, MD, PhD**

University of Hospitals of Leicester NHS Trust, England

**Prof. Murat İnanç, MD**

İstanbul University-İstanbul Faculty of Medicine, Department of Internal Medicine, Division of Rheumatology, İstanbul, Türkiye

**Dr. Mustafa Diken, MD**

TRON - Translational Oncology at University Medical Center of Johannes Gutenberg University, Germany

**Assoc. Prof. Neşe Akış, PhD**

Trakya University Faculty of Medicine, Department of Medical Microbiology, Edirne, Türkiye

**Prof. Neslihan Cabioğlu, MD, PhD**

İstanbul University-İstanbul Faculty of Medicine, Department of Surgery, İstanbul, Türkiye

**Prof. Nesrin Özören, PhD**

Bogazici University, Department of Molecular Biology and Genetics, İstanbul, Türkiye

**Prof. Safa Barış, MD**

Marmara University Faculty of Medicine Hospital, Department of Pediatric Allergy-Immunology, İstanbul, Türkiye

**Dr. Semir Beyaz, PhD**

Cold Spring Harbor Laboratory, Immunology, USA

**Prof. Suzan Adın Çınar, PhD**

İstanbul University, Aziz Sancar Institute of Experimental Medicine, Department of Immunology, İstanbul, Türkiye

**Asst. Prof. Timuçin Avcı, PhD**

Bahcesehir University Faculty of Medicine, Department of Medical Biology, İstanbul, Türkiye

**Prof. Tunç Akkoç, PhD**

Marmara University Faculty of Medicine, Department of Pediatric Allergy-Immunology, İstanbul, Türkiye

**Assoc. Prof. Umut Can Küçüksezer, PhD**

İstanbul University, Aziz Sancar Institute of Experimental Medicine, Department of Immunology, İstanbul, Türkiye

**Assoc. Prof. Vuslat Yılmaz, PhD**

İstanbul University, Aziz Sancar Institute of Experimental Medicine, Department of Neuroscience, İstanbul, Türkiye

## CONTENT

### EDITORIAL

- 1** **Turkish Journal of Immunology: Launching the 2025 Volume**  
Günnur Deniz

### REVIEW ARTICLE

- 2** **PANoptosis: A Coordinated Response in the Diversity of Cell Death**  
Mert Karaca, Haluk Barbaros Oral

### ORIGINAL RESEARCH

- 22** **Impact of Genetic Background and Gender on Mouse Susceptibility to H1N1- PR8: Implication of the Host Immune Responses**  
Dina Nadeem Abd-Elshafy, Mohamed Hassan Nasraa, Rola Nadeem, Mahmoud Mohamed Bahgat
- 33** **Validation and Comparative Analysis of Dihydrorhodamine 123 Oxidative Burst Measurement by Flow Cytometry in Neutrophils: A Study of Two Isolation Techniques and Two Bacterial Strains**  
Cemil Pehlivanoglu, Başak Aru, Ali Osman Gürol, Gülderen Yanıkkaya Demirel
- 43** **Fc Receptor-Like 3 Gene Polymorphism and the Risk of Lupus Nephritis in Systemic Lupus Erythematosus Patients**  
Amany Gamal Thabit, Michael Nazmi Agban, Rania Mohamed Gamal, Ahmed Mahmoud Rayan, Mona Sallam Embarek Mohamed
- 54** **Soluble HLA-G as a Novel Biomarker for the Diagnosis of Acute Lymphoblastic Leukemia**  
Sura M.Y. Al-Taee, Rojan G.M. Al-Allaff

### COMMENTARY

- 62** **Symbiotic Life is a Success of Immunity**  
Şefik Ş. Alkan

# Turkish Journal of Immunology: Launching the 2025 Volume

## Dear Colleagues,

It is our great pleasure to present the first issue of the *Turkish Journal of Immunology* for 2025.

This issue highlights the diversity and depth of current immunological research. In our **Review Article**, the emerging concept of **PANoptosis** is explored as a novel form of programmed cell death, shedding light on its intricate relationship with immune responses and inflammatory diseases.


Our **Original Research Articles** span various themes across experimental and clinical immunology. A murine study investigates how **genetic background and gender influence susceptibility to H1N1 infection**, underlining the complexity of host immune responses. Another contribution identifies **soluble HLA-G as a promising biomarker** for the diagnosis of **acute lymphoblastic leukemia**, while a third paper examines **Fc receptor-like-3 gene polymorphisms in lupus nephritis patients**, providing insight into genetic risk factors in autoimmunity. A final research article presents a **methodological comparison of oxidative burst assays** in neutrophils, offering practical guidance for laboratory immunologists working with flow cytometry.

The issue concludes with a **Commentary** titled "*Symbiotic Life is a Success of Immunity*," which reflects on the evolutionary interplay between host and microorganisms and emphasizes the immunological foundations of life's symbiotic balance.

We thank our authors, reviewers, and editorial board members for their continued commitment to scientific excellence. This issue marks not only the beginning of a new volume but also a fresh chapter for our journal as we transition to a new publishing platform. With **DOC Design and Informatics** as our new publisher, we aim to further elevate the visibility and impact of TJI within the international immunology community.

We warmly invite you to submit your research to the **Turkish Journal of Immunology**. With your valuable contributions and support, our journal will continue to grow stronger.

With warm regards,

Prof. Günnur Deniz 

On behalf of the Editorial Board  
*Turkish Journal of Immunology*

## Correspondence

Günnur Deniz

## E-mail

gdeniz@istanbul.edu.tr

## Published

April 29, 2025

## Suggested Citation

Deniz G. Turkish Journal of Immunology: launching the 2025 volume. Turk J Immunol. 2025;13(1):1.



## DOI

10.36519/tji.2025.672



This work is licensed under the Creative Commons Attribution-NonCommercial-Non-Derivatives 4.0 International License (CC BY-NC-ND 4.0).

# PANoptosis: A Coordinated Response in the Diversity of Cell Death

Mert Karaca<sup>1,2</sup> , Haluk Barbaros Oral<sup>1</sup> 

<sup>1</sup>Bursa Uludağ University Faculty of Medicine, Department of Immunology, Bursa, Türkiye; <sup>2</sup>Bursa Uludağ University Institute of Health Sciences, Department of Medical Immunology, Bursa, Türkiye

## Abstract

The recently introduced concept of PANoptosis describes a highly regulated mechanism involving the coordinated action of pyroptosis, apoptosis, and necroptosis. However, none of these three types of cell death can explain this concept alone. PANoptosis is mediated by a structure called the PANoptosome. PANoptosome components can be formed in different ways according to triggers and receptor interactions. Therefore, stimulators and regulators become central to understanding the mechanism of PANoptosis. In this review, the mechanism of PANoptosis was summarized in general, and PANoptosome regulators in the literature were discussed collectively. We aimed to contribute to the possible therapeutic approaches.

**Keywords:** PANoptosis, pyroptosis, apoptosis, necroptosis, cell death

## Introduction

Programmed cell death (PCD) mechanisms are an inherent part of protection against pathogens and cellular stress. Pyroptosis, apoptosis, and necroptosis are the best-known PCD pathways that protect the body against both internal and external risk factors (1, 2). The observation that all three cell death pathways can be activated in response to certain stimuli, such as influenza virus (IAV) infection, has raised the question of whether they are triggered independently or work in concert. In 2019, PANoptosis (P, pyroptosis; A, apoptosis; N, necroptosis), a concept that encompasses the interplay of pyroptosis, apoptosis, and necroptosis, was defined by realizing that the three PCD mechanisms are linked (3). With the discovery of the regulators of the PANoptosis mechanism, it became evident in 2020 that these three death pathways are controlled through the PANoptosome complex

### Correspondence

Haluk Barbaros Oral

### E-mail

oralb@uludag.edu.tr

### Received

December 21, 2024

### Accepted

February 24, 2025

### Published

April 29, 2025

### Suggested Citation

Karaca M, Oral HB. PANoptosis: A coordinated response in the diversity of cell death. Turk J Immunol. 2025;13(1):2-21.

### DOI

10.36519/tji.2025.573



This work is licensed under the Creative Commons Attribution-NonCommercial-Non-Derivatives 4.0 International License (CC BY-NC-ND 4.0).

(4). PANoptosis is an inflammatory PCD mechanism that highlights the important cross-talk and coordination between the three death pathways regulated by the formation of PANoptosome complexes as a result of complex interactions of different receptors and molecular signaling. It has been associated with many diseases, including infectious, neurodegenerative, autoinflammatory, cancer, and metabolic (5, 6). In particular, inflammasome elements, which act as constituents of the PANoptosome, have a pivotal function in the regulation of inflammatory responses and cell death pathways. Components such as the NOD-like receptor family and pyrin domain-containing 12 (NLRP12) also contribute to the activation of PANoptosomes, as well as the inflammasome, shaping inflammatory outcomes and cell death (7).

PANoptosome production and PANoptosis activation begin with sensing pathogen-associated molecular patterns (PAMP), damage-associated molecular patterns (DAMPs), or other risk factors. Almost all PANoptosomes share common structural components of pyroptosis, apoptosis, and necroptosis. In essence, a PANoptosome consists of three types of structures: the sensor protein, which is important for sensing and determining the type of PANoptosome; the adaptor protein region with the caspase (CASP) recruitment domain (CARD); and the effector protein, which is required for subsequent catalytic activity. In general, the initiation of PANoptosis involves sensing endogenous or exogenous danger signals by specific sensors, such as absent in melanoma 2 (AIM2), Z-DNA binding protein 1 (ZBP1), NLRP12, followed by the transduction of signals recognized by downstream adapter proteins to effector proteins. These effectors, gasdermin D (GSDMD), Casp3, Casp7, and mixed lineage kinase domain-like protein (MLKL), are activated in response to PANoptosome formation and drive PANoptosis. These are followed by pyroptosis, which is mediated by GSDMD, Casp8-dependent apoptosis, and necroptosis, which is mediated by MLKL. Amongst them, GSDMD is cleaved by Casp1 and certain other caspases. Casp3 and Casp7 are activated by Casp8, while receptor-interacting protein kinase 1 (RIPK1) interacts with RIPK3 for activation. MLKL is then phosphorylated, and PANoptosis is induced through the three death pathways (8). However, this generalization is not valid for every stimulus. The components and interactions that make up the PANoptosome vary depending on the triggers. Therefore, the PANoptosome has become a central focus for the study of the mechanism of PANoptosis (5).

An important point to consider in understanding PANoptosis is the coactivation of the three death pathways (pyroptosis, apoptosis, and necroptosis). However, this does not mean all three cell death forms occur simultaneously. In some cases, when one type of cell death in PANoptosis is inhibited, other types of cell death can be promoted (9). For example, in *Salmonella* infection, a PANoptosis mechanism can be observed in which pyroptosis and apoptosis are inhibited, and necroptosis is promoted by the down-regulation of Casp8 (10).

Awareness of the basic mechanisms of types of PCD is important for understanding the mechanism of PANoptosis and its relationship with diseases, as these processes are interconnected in PANoptosis through common regulatory proteins and signaling pathways.

## Pyroptosis, Apoptosis, Necroptosis

Each multicellular organism has a number of processes that kill its own cells. Physiologically, the reasons for this are related to defense, development, homeostasis,

### Highlights

- PANoptosis provides an integrated cell death mechanism that responds to a wide range of triggers, from viruses to fungi, supporting the immune response against invading pathogens.
- The composition of the PANoptosome varies depending on specific triggers and disease contexts; this review compiles PANoptosis regulators that have previously been discussed separately in the literature.
- Reviewing the molecular interactions among pyroptosis, apoptosis, and necroptosis, draws attention to the context-dependent roles of caspases, contributing to a better understanding of PANoptosis.
- Recent findings on macrophage polarization, dendritic cell activation, and immunogenic cell death have begun to shape our understanding of the role of PANoptosis in tumor immunity.
- The coordinated activation of pyroptosis, apoptosis, and necroptosis in PANoptosis does not necessarily indicate that all three cell death pathways occur simultaneously.

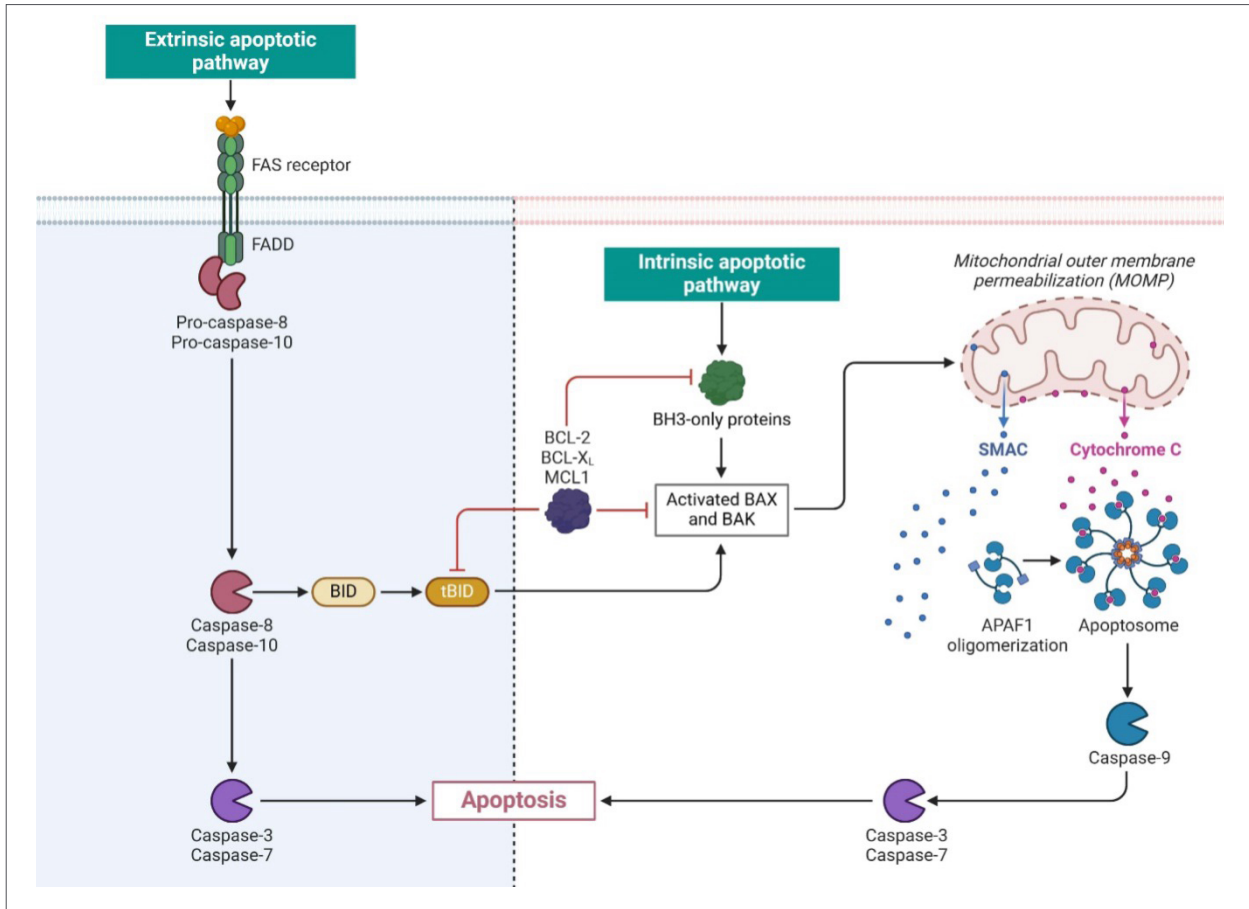


**Figure 1.** General representation of signaling molecules involved in endogenous and exogenous apoptosis pathways. While signaling molecules basically mediate apoptosis, they also play a role in the PANoptosis mechanism by cross-talking with molecules involved in pyroptosis and necroptosis. (Modified and created with BioRender.com by Karaca, M. Adapted from "Apoptosis Extrinsic and Intrinsic Pathways" by BioRender.com, 2025. Retrieved from <https://app.biorender.com/biorender-templates>)

and aging. Apoptosis is a morphologically recognizable form of cell death that can occur through multiple mechanisms (11). Apoptosis, one of the first defined PCD pathways, can occur through three pathways. Endogenous (intrinsic) apoptosis, exogenous (extrinsic) apoptosis, and the later identified endoplasmic reticulum (ER) stress pathway. Intrinsic and extrinsic pathways are summarised in Figure 1. In the endogenous apoptosis pathway, mitochondrial damage or dysfunction causes the outer membrane to become permeable, releasing several molecules, including cytochrome C (cyto-C). Subsequently, cytosolic cyto-C is recognized by Apaf-1. Casp9, an intrinsic apoptosis pathway initiator, is activated by cyto-C to mediate apoptosome formation (12). Afterward, Casp3, Casp6, and Casp7 are activated, and apoptosis occurs (13). The Bcl-2 gene family regulates this pathway (14). Binding extracellular death ligands to death receptors on the cell surface

initiates the extrinsic apoptosis pathway and triggers apoptosis. Casp8 has been identified as the initiator of this pathway (15). These ligands can be secreted by immune cells (T lymphocytes, natural killers [NKs], macrophages, and dendritic cells [DCs]). The subsequent signaling pathway differs depending on the activated ligand (16). In the stress-induced apoptosis pathway of the ER, a response termed the unfolded protein response (UPR) is triggered when the stress of the ER is experienced due to various factors. The UPR is activated by three major ER stress-integrated proteins: inositol requiring enzyme-1 (IRE1), protein kinase RNA-like endoplasmic reticulum kinase (PERK), and activating transcription factor 6 (ATF6). This is followed by a process in which the pro-apoptotic proteins Bcl-2 associated X protein (BAX), Bcl-2 associated agonist of cell death (BAD), and Bcl-2 antagonist/killer (BAK) are activated (17). Killer caspases have the ability to initiate apopto-

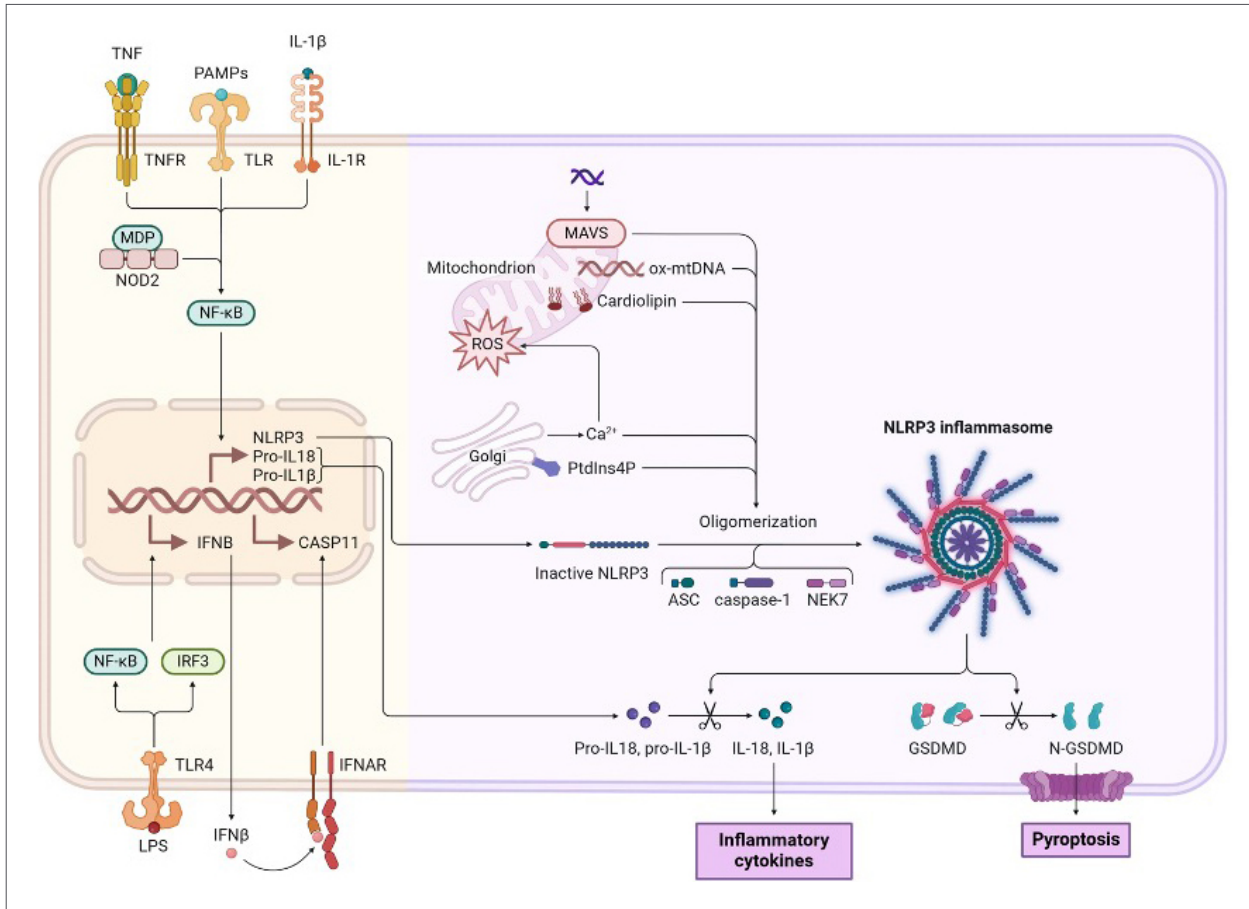


**Figure 2.** Structures involved in NLRP3 inflammasome-mediated pyroptosis mechanism. (Modified and created with BioRender.com by Karaca, M. Adapted from “NLRP3 Inflammasome Activation” by BioRender.com, 2025. Retrieved from <https://app.biorender.com/biorender-templates>)

sis by acting on chaperones and approximately a thousand substrates. The morphological characterization of apoptotic cells is also well-known (18).

Pyroptosis was first reported in 1992 as Casp1-mediated cell death (19). However, its mechanism was elucidated in the following years with the realization that GSDMD is a target for cleavage by different caspases (20, 21). Thus, pyroptosis was identified as a GSDMD-driven lytic and inflammatory-driven cell death program. GSDMD is a lethal protein that is proteolytically cleaved and activated by pro-inflammatory caspases (Casp1/4/5/11), forming cytoplasmic membrane pores (19). Pro-inflammatory caspases are localized in inflammasomes, which are large cytosolic protein complexes that can cleave and activate protein substrates. Inflammasomes are a complex that executes pyroptosis of multimeric protein structures formed in a cell to regulate host defense mechanisms against infectious agents and physiological

perturbations (22). Some NOD-like receptors (NLRs) and other sensors, such as AIM2, act as sensors for assembling inflammasomes. Inflammasomes often contain the apoptosis-associated speck-like (ASC) adaptor protein, which has both the pyrin domain (PYD) and CARD. Following the formation of the inflammasome, inactive pro-IL-1 $\beta$ , and pro-IL-18 cytokines are cleaved and released in their mature and bioactive form as IL-1 $\beta$  and IL-18, similar to GSDMD, and pyroptosis is initiated (23), summarised in Figure 2. According to distinct molecular mechanisms, it can occur in four ways: canonical, non-canonical, Casp3/8-mediated, and granzyme-mediated (24). Pyroptosis occurs mainly in professional phagocytes of the myeloid lineage but is also seen in some other cell types, such as CD4<sup>+</sup> T lymphocytes and neurons (25). Furthermore, while GSDMD is the most well-known executioner protein of pyroptosis, it is not the only gasdermin capable of inducing pyroptotic cell death (26).

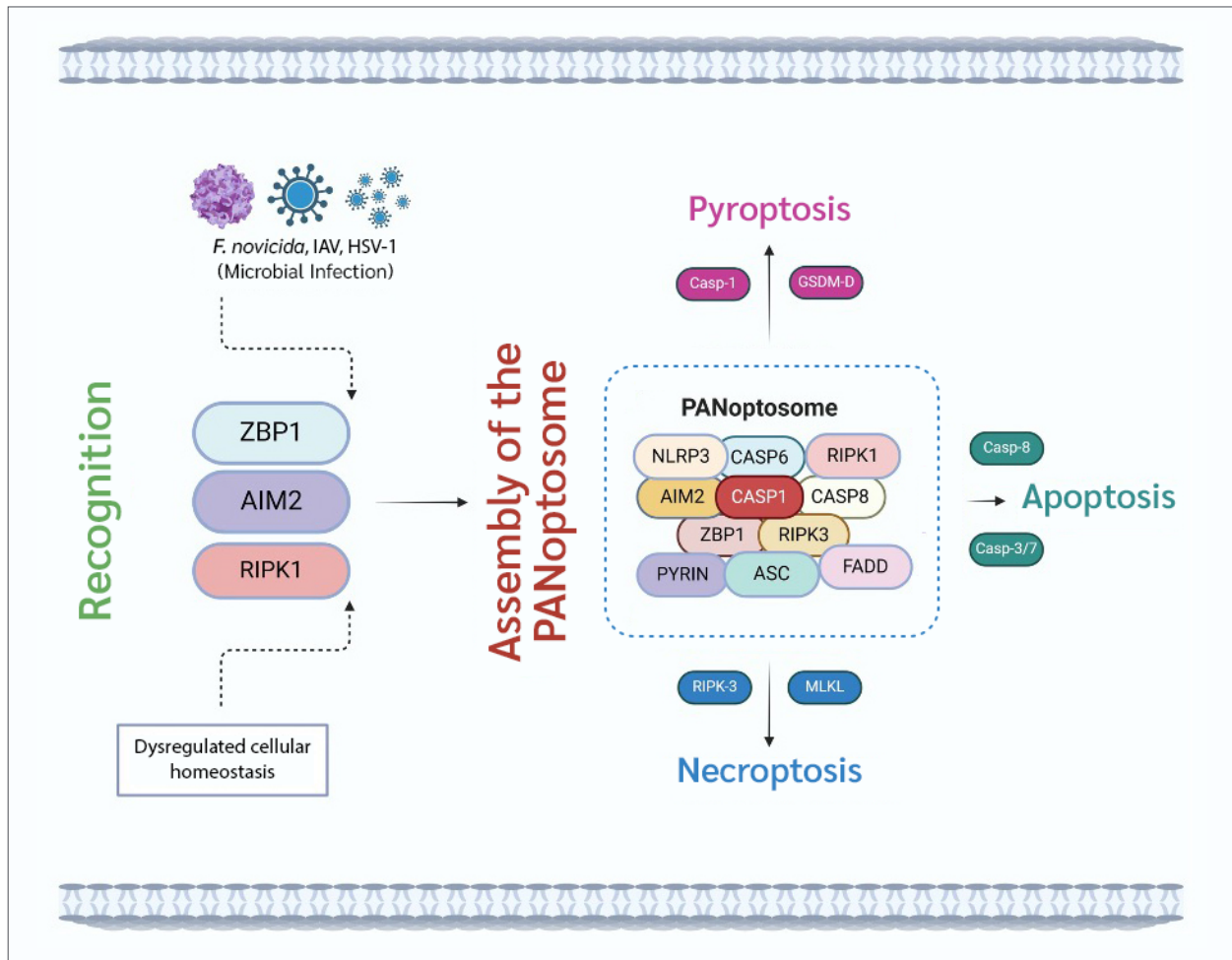


**Figure 3.** Components involved in PANoptosome formation. The components depicted in the figure do not coexist in this exact arrangement during PANoptosome formation. Variations in formation are seen according to the type of PANoptosome. Therefore, both sensor molecules and stimulus diversity are essential. PANoptosome structure should be evaluated specific to the pathogen and should not be generalised. (Created with BioRender.com by Karaca, M., 2025)

Although necroptosis is activated by MLKL phosphorylation mediated by RIPK1 and RIPK3 oligomerization rather than caspase cleavage, its initiation requires Casp-8 inhibition. Nevertheless, unlike apoptosis and pyroptosis, it is generally considered caspase-independent (27). It is a regulated form of necrosis in which the dying cell releases its intracellular components, which can trigger an innate immune response (28). Necroptosis is typically caused by tumor necrosis factor (TNF), Fas, or lipopolysaccharide (LPS) activating RIPK3 kinase, allowing the subsequent phosphorylation of the pseudokinase MLKL. It is triggered by Casp8-mediated disruption of apoptosis and depends on receptor-interacting protein kinases (RIPK1/3) and the mixed lineage kinase domain to form the necroptosome. The release of cytosolic contents and cell death-associated molecular patterns (CDAMPs) can

trigger innate immune responses and promote acquired immune responses (29).

These three death pathways have a more complex mechanism than outlined above and are regulated by many additional factors not mentioned here (1, 18). The focus of this review is PANoptosis, which arises from the interactions among these three death pathways that act together, as well as the connections between the PANoptosome and diseases and the associated regulatory molecules.

## PANoptosome Component

The PANoptosome serves as an integrative platform for the simultaneous interaction of the active elements of

the three death pathways. This flexible, multiprotein complex consists of several proteins, including serine/threonine kinases, caspases, and specific death domains. Various stimuli such as IAV, vesicular stomatitis virus, *Listeria monocytogenes*, and *Salmonella enterica* serovar Typhimurium activate sensors such as ZBP1 that trigger the formation of PANoptosome. Once the PANoptosome is formed, it promotes the activation of executors in each death pathway, including apoptosis mediated by Casp3/7, pyroptosis via GSDMD/E, and necroptosis driven by RIPK1/MLKL (4, 30-38). (Figure 3 summarises the structures mainly involved in PANoptosome formation.) Sensors encountering stimuli interact with various molecules to form PANoptosomes. The components of PANoptosomes vary depending on the stimulus and the sensor. The known types of PANoptosomes are summarized in Figure 4.

It was initially shown that the PANoptosome is composed of RIPK1, CARD, NLRP3, and caspases (39). Further studies showed that RIPK3, Casp6, ZBP1, and Casp1 are also involved in the PANoptosome formation triggered by IAV infection (32). Understanding the diversity of these molecules and how they interact reveals that the three types of PCD are interconnected, constituting PANoptosis. Rather than being activated separately, they are regulated together by the PANoptosome complex, inducing cell death (3, 4, 39). In some cases, inhibition of pyroptosis allows Casp8 to activate the inflammasome, which may trigger both apoptosis and a Casp8-dependent form of cell death known as secondary pyroptosis (4, 40, 41). Moreover, the inhibition of Casp-8 results in the formation of complex IIb via the TNF or Toll-like receptor (TLR) pathway, which ultimately culminates in necroptosis (42). These analogous mechanisms permit us to comprehend the reasons behind the non-standardized structure of the PANoptosome, the potential for

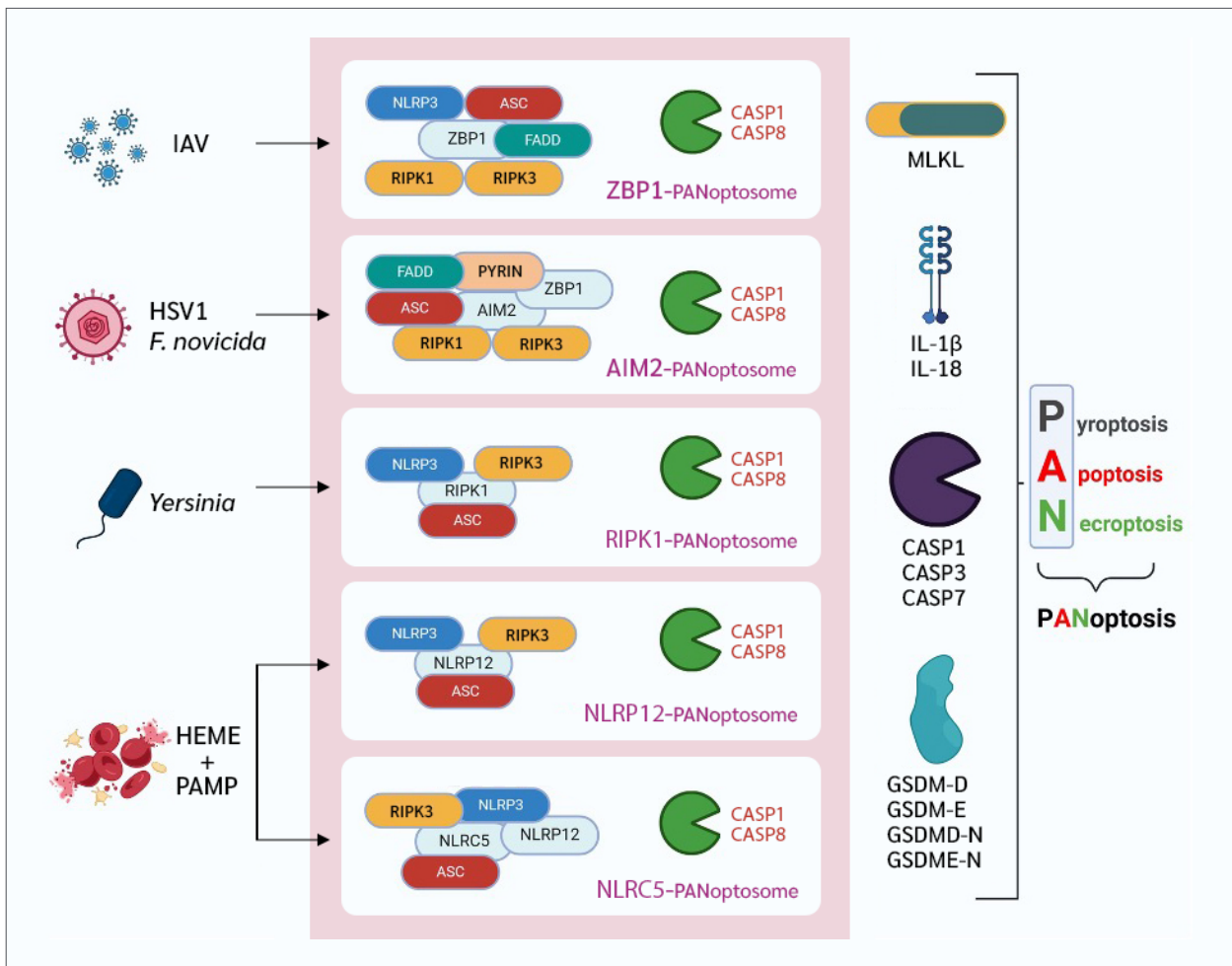


**Figure 4.** Types of PANoptosome defined for different stimuli. (Created with BioRender.com by Karaca, M., 2025)

it to comprise disparate components and the necessity for a PANoptosome in which the three death pathways operate in concert.

The components of the PANoptosome vary between different diseases. Therefore, the main phenotypic members can vary depending on the type of stimulus applied. Single cell analysis of PANoptosome complexes has led to a better understanding of PANoptosomes under specific conditions (30, 43). In addition to the first described PANoptosomes, RIPK1-PANoptosome and NLRP12-PANoptosome were identified (7, 44). Most recently, it was reported that NLR family, CARD domain containing 5 (NLRC5) similarly mediates PANoptosome formation (45).

In the mechanism of PANoptosome formation, the structures that give the aforementioned PANoptosome types their names (ZBP1, AIM2, RIPK1, NLRP12) act as sensors for triggers such as various microbial infections and altered cellular homeostasis. Sensor interactions then initiate the assembly of other components to form the PANoptosome. In necroptosis-associated structures, homotypic actions among receptor-interacting protein homotypic interaction motifs (RHIMs) domains and in the assembly of pyroptotic and apoptotic structures, heterotypic actions between the PYD and the death effector domain are realized (46-49). The PANoptosome is thought to be formed by similar interactions. Furthermore, intrinsically disordered regions (IDRs) have alternatively been reported to be involved in PANoptosome formation (30). The known identified PANoptosome types; ZBP1-PANoptosome (ZBP1, NLRP3, ASC, Casp1, Casp6, Casp8, RIPK1 and RIPK3) (4, 50), AIM2-PANoptosome (AIM2, Pyrin, ZBP1, ASC, Casp1, Casp8, Fas-associated death domain [FADD], RIPK1 and RIPK3) (51), RIPK1-PANoptosome (RIPK1, RIPK3, NLRP3, ASC, Casp1 and Casp8) (44) and NLRP12-PANoptosome (NLRP12, ASC, Casp8 and RIPK3) (7). These PANoptosomes then induce Casp3/7 activation, GSDMD / E cleavage, and phosphorylation of MLKL, leading to membrane pore formation and PANoptosis progression (52). A systematic examination of the established molecular constituents of pyroptosis, apoptosis, and necroptosis, as analyzed through STRING, indicates that these three forms of cell death are not independent processes. This observation supports the hypothesis that they are part of a larger, interconnected PCD network (46, 53).

Furthermore, the formation of PANoptosomes can be regulated by interferon regulatory factor 1 (IRF1) in spe-

cific circumstances (54). This topic has been elaborated in the section on 'Regulatory Factors and Diseases.'

### ZBP1-PANoptosome

ZBP1 is also known as a DNA-dependent activator of interferon-regulatory factors (DAI) or a DNA-dependent activator of DLM1. ZBP1 consists of three parts: N-terminal Z-DNA binding domain (ZBD), RHIM, and C-terminal signal domain (SD) (55-57). The N terminal contains two Z-form nucleic acid binding domains (Z $\alpha$ 1 and Z $\alpha$ 2) and a protein homotypic interaction motif (RHIM1 and RHIM2) in the middle that interacts with two receptors. It is inducible by interferon (IFN) and interacts with the RHIM domain and other proteins. The Z $\alpha$ 2 domain plays a critical role in the activation of PCDs (51, 58).

Activation of ZBP1 results in its interaction with RIPK3 and recruitment of Casp8, thereby forming cell death signaling scaffolds. The resulting ternary complex has the capacity to activate all three death pathways. Furthermore, ZBP1 induces NF- $\kappa$ B signaling during influenza infection (59, 60).

In addition to its ability to recruit cell death elements such as RIPK3 and Casp8, which are required for the formation of PANoptosomes, ZBP1 can activate cell death signals. A lack of Z $\alpha$  domains has been demonstrated to restrict infection-induced ZBP1 mediated inflammatory cell death (55, 56, 58). ZBP1 deletion prevents IAV-induced activation of the NLRP3 inflammasome. Additionally, RIPK1 plays an active role in preventing ZBP1/RIPK3/MLKL-dependent necroptosis during the development of RHIM (61, 62).

Recently, a novel cell death complex known as TRIFosome, which is triggered by TRIF signaling and involves FADD, RIPK1, and Casp8, has been reported. This complex has a critical role in LPS-induced cell death in the context of transforming growth factor- $\beta$  (TGF- $\beta$ )-activated kinase 1 (TAK1) inhibition (63). The regulatory importance of TAK1 for PANoptosis has been mentioned in the "Regulatory Factors and Diseases" section. Despite the absence of evidence indicating a direct interaction between TRIF and other death mediators, it is plausible that TRIF may facilitate the assembly of the PANoptosome complex through its RHIM domain.

PANoptosis caused by ZBP1-PANoptosome is bidirectional. It promotes the elimination of invading pathogens and dysregulated cancer cells, but aberrantly, it

may trigger severe infectious and non-infectious inflammatory responses (64).

### AIM2-PANoptosome

The inflammasome is an oligomeric multiprotein complex located in the cytosol. It is not a fixed cell structure but only forms when stimulated by specific DAMPs and PAMPs. Inflammasomes are classified according to the structure of the sensor molecule (64-68). AIM2 is one of these sensor molecules, characterized by a hematopoietic, interferon-induced, and nuclear localization (HIN) region at the carboxyl site and a PYD at the amino-terminal. The AIM2 inflammasome is activated in response to the presence of dsDNA in the cytoplasm and mediates pyroptosis (69). DNA can be of microbial origin (from pathogens) or host DNA released during cellular stress or damage.

Inflammasome formation is initiated following AIM2 detection of dsDNA produced by pathogens, nucleus, and mitochondria. ASC establishes homotypic domain-based connections with AIM2 and pro-Casp1 through PYD-PYD and CARD-CARD. The components of AIM2-ASC-pro-Casp1 bind to the pseudo-axis of double-stranded DNA, forming a large oligomeric complex. Casp1 is the mature form of pro-Casp1 that converts pro-IL-1 $\beta$ , pro-IL-18, and GSDMD into their active forms. IL-1 $\beta$  and IL-18 elicit a cascade of inflammatory responses, while GSDMD-N binds to the cell membrane and induces pyroptosis (70,71).

The inflammasome is a crucial component in the process of PANoptosis as a part of PANoptosomes (7). The interaction of pyrin and ZBP1 facilitates the formation of the AIM2-PANoptosome. However, current knowledge shows this is limited to infections such as herpes simplex virus 1 and *Francisella novicida* and does not occur upon exposure to pure dsDNA. Z $\alpha$  domains of ZBP1 are activated by detecting nucleic acids. AIM2 can also be controlled by activating the IFN signaling pathway. The AIM2-PANoptosome complex includes AIM2, pyrin and ZBP1 as well as ASC, Casp1, Casp8, RIPK3, RIPK1 and FADD (51). These additional components play an important role in facilitating the PANoptosis process. Targeting AIM2 or other components of the PANoptosome may show therapeutic efficacy in the treatment of inflammatory cell death molecules, as well as various viral and inflammatory diseases.

### RIPK1-PANoptosome

RIPK1 regulation of PANoptosis is crucial for maintaining cell homeostasis and mediating both PCD and inflammatory reactions. The scaffolding role of RIPK1 facilitates

survival signaling by assembling complex I that inhibits cell death, thereby maintaining TNF receptor-1 (TNFR-1) activity (30, 72-76). Complex I activate the NF- $\kappa$ B pro-survival pathway, yet should this signal be disrupted, complex II will then initiate cell death (77, 78). In this context, Casp8 can suppress necroptosis through proteolytic cleavage of RIPK, which are necroptotic mediators. Conversely, the deletion of Casp8 results in the formation of the necrosome (79-82). Deletion of RIPK1 in mice is embryonically lethal and has been shown to cause systemic inflammation through activation of PANoptosis-like cell death regulated by RIPK3, with the involvement of Casp8 and FADD (83-85). PAMPs, via TLRs or death receptor signaling, can promote RIPK1-dependent PANoptosome formation when regulatory proteins such as TAK1 are inhibited (39). Moreover, mutations that inactivate Casp8 catalytic activity can lead to death in embryonic mice by activating RIPK1, RIPK3-MLKL, and Casp1 (86, 87). This situation could be considered as PANoptosis-relation death with the involvement of other effectors. However, it should be noted that MLKL has not been identified in the RIPK1-PANoptosome core scaffold. More specifically, these studies collectively contribute to understanding the regulation of PANoptosis by RIPK1 and Casp8 (30).

### NLRP12-PANoptosome

NLRs belong to a group of cytoplasmic pattern recognition receptors (PRRs) that play a role in detecting pathogens or damage, regulating inflammatory signaling, and controlling the transcription of specific genes. NLRP12 is one of the first members identified in the NLR family to contain an N-terminal PYD, nucleotide-binding domain (NBD), and C-terminal leucine-rich repeat (LRR) domain (88). Furthermore, NLRP12 is the first identified to interact with the adaptor protein ASC, leading to the formation of an active inflammasome capable of releasing IL-1 $\beta$  (89). Following the introduction of the PANoptosis concept, it was recognized that NLRP12 not only activates the inflammasome in response to specific PAMPs or TNF but also drives PANoptosome activation, cell death, and inflammation. TLR2/4-mediated signaling through IRF1 leads to inflammasome formation. NLRP12 acts as an integral component of an NLRP12-PANoptosome that drives inflammatory cell death via Casp8 / RIPK3. PAMPs containing 'heme' groups can trigger cell death (90). Under certain conditions, these heme-containing PAMPs can also activate the NLRP3 inflammasome (91, 92). In addition to the inflammasome, Casp8 has also been shown to play an essential role in directing NLRP12-mediated inflammatory cell death in response to

exposure to PAMP carrying the heme domain. With this, a multiprotein PANoptosome complex is formed that specifically contains ASC, RIPK3, Casp8, and NLRP3. PANoptosomes can form against heme-positive PAMPs even in the absence of NLRP3, demonstrating that NLRP12 is the main actor (7).

PAMPs and DAMPs released as a result of hemolysis-inducing events can induce activation of TLR-2 and TLR4 by a combination of 'heme.' Therefore, Myd88 signaling is also seen with NLRP12 activity. Mitochondrial reactive oxygen species (ROS) also contribute to NLRP12 induction. Activated NLRP12 triggers the formation of an NLRP12-PANoptosome protein complex involving RIPK3, ASC, and Casp8. This complex promotes the well-characterized mechanism of gasdermins (D and E) cleavage in pyroptosis and pore formation in the plasma membrane, leading to PANoptotic cell death (93). During some infections, ZBP1 can be stimulated simultaneously with AIM2. This shows that it is possible to create PANoptosomes containing different sensors (51).

## Molecular Mechanisms and Involvement of the Three Types of Cell Death in PANoptosis

In PANoptosis, the apoptosis, pyroptosis, and necroptosis pathways act together within the same cell, with the components of the three death pathways interacting with each other. This interaction has been described in the literature as cross-talk. The emerging understanding of the connections between cell death pathways has guided the conceptualization of PANoptosis as an inflammatory cell death mechanism. The caspase and RIPK families play the most prominent roles in cross-talk (36).

Caspases are members of the cysteine protease family, proteolytic enzymes that are particularly well characterized in apoptosis. They can be classified according to their role, mechanism of action, and the organism in which they are found. In addition to apoptosis, caspases are also involved in the nonapoptotic cell death processes of necroptosis and autophagy. They also have central roles in pyroptosis (94). In mammals, caspases are classified into three functional groups according to their role: inducers (Casp2, Casp8, Casp9, Casp10), effectors (Casp3, Casp6, Casp7), and inflammatory caspases (Casp1, Casp4, Casp5, Casp11, Casp12, Casp13, Casp14).

Aside from some exceptional caspases, the roles of almost all known caspases in apoptosis, necroptosis, and pyroptosis have been described in detail (95, 96). Casp1, which is known to mediate pyroptosis, can function through the Bid-Casp9-Casp3 axis to initiate apoptosis in cells lacking GSDMD (94). Casp3, which is also involved in apoptosis, can initiate secondary necrosis and pyroptosis after cutting the GSDMD-related protein DFNA5 (97). Furthermore, GSDMD / DFNA5 redirects Casp3-mediated apoptosis to pyroptosis upon stimuli such as TNF or chemotherapy drugs (98, 99).

During PANoptosis, Casp1, Casp8, and Casp3 are activated simultaneously to induce cell death through a complex interaction. Casp8 has emerged as a pioneer regulator that links the apoptotic and necrotic pathways. NLRP3 induces pyroptosis in inflammasome activation. Therefore, Casp8 plays a central role in PANoptosis, regulating the delicate balance between the three pathways and ultimately influencing cell fate by activating specific death signals (100, 101).

Apaf-1, one of the leading players in apoptosis, has been shown to cause Casp4-mediated pyroptosis (102). Looking at the close interaction between apoptosis and necroptosis at the signaling level, the double knockout assays FADD / RIPK3 and FLIP / RIPK3 reveal a complex cross-regulation of apoptosis and necrosis. FLIP (an important modulator of apoptosis) prevents the association of FADD-bound Casp8 homodimers that mediate apoptosis. Instead, Casp8-FLIP heterodimers form, preventing the activation of necrosis-mediating RIPK3. In the absence of this heterocomplex, RIPK3 promotes necrosis; however, when FADD is present without FLIP, Casp8-mediated apoptosis is favored (103). In other words, when RIPK3 expression is high, cells undergo necroptosis, whereas when RIPK3 expression is low, they tend toward apoptosis (104).

The binding of TNF- $\alpha$  to TNFR1 results in the formation of complex II also referred to as the cytosolic death-inducing signaling complex (DISC), which is capable of mediating necroptosis. Polyubiquitination of RIPK1 also affects the transition from complex I to complex II. Casp8 has the capacity to inactivate complex II and RIPK1-3 through proteolytic cleavage, thereby initiating the pro-apoptotic caspase cascade. On the contrary, when Casp8 undergoes deletion, depleted or inhibited complex II does not initiate the apoptotic program, and binding of TNFR1 causes necroptosis (105).

**Table 1.** The key regulators of PANoptosis identified so far in various diseases and conditions.

| Regulator                              | Role   | Condition/Pathogen                            | Mechanisms  |
|--|--|---|---|
| M2, NS1, PB1-F2                        | Regulates ZBP1-NLRP3   | Influenza                                     | Viral proteins act as regulators for PANoptosis   |
| Casp6                                  | Facilitates PANoptosis through the ZBP1-RIPK3 interaction                              | IAV infection<br>Thyroid cancer               | Bridges sensor-effector interaction, diagnostic marker in cancer  |
| RDX                                    | Prognostic marker  | Breast cancer                                 | Associated with molecular clustering in PANoptosis-based survival prediction                              |
| Certain lncRNAs linked to PANoptosis   | Associated with metastasis   | Colon adenocarcinoma                          | Linked to immune infiltration and tumor microenvironment  |
| RIPK1, RIPK3, Casp8, NLRP3, ASC, Casp1 | Forms RIPK-PANoptosome   | <i>Yersinia</i> infection                     | Induces PANoptosis in macrophages independent of ZBP1   |
| TAK1                                   | Inhibits RIPK1 activation, prevents spontaneous PANoptosis                             | <i>Yersinia</i> infection                     | TAK1-RIPK1 phosphorylation restricts PANoptosis; TAK1 inhibitors allow the formation of RIPK-PANoptosomes |
| ADAR1                                  | Negative regulator of ZBP1-mediated PANoptosis   | Cancer  | Tumor suppressor through PANoptosis induction when inhibited  |
| Caspase-1 (Casp1)                      | Inhibits PANoptosis  | <i>E. faecalis</i> infection                  | Suppresses osteoblast PANoptosis through regulation of the NLRP3 inflammasome                             |
| IRF1                                   | It promotes PANoptosome assembly by various mechanisms. (such as the JAK/STAT pathway) | COVID-19<br>Cancer<br>IAV infection           | NLRP12 and RIPK1 activate PANoptosomes and inhibit tumor progression                                      |
| ZBP1                                   | Sensor for PANoptosis  | SLE<br>Fungal infections                      | Activates immune response and links to immune cells through type I interferon signaling                   |
| S100A8/A9 <sup>hi</sup> neutrophils    | ZBP1-mediated PANoptosis inducer   | Lung tissues of septic mice                   | Mitochondrial dysfunctions and mtDNA-mediated PANoptosis  |
| SopF                                   | Regulates PANoptosis in epithelial cells   | <i>Salmonella</i> infection                   | PDK1-RSK phosphorylation downregulates Caspase-8  |
| AIM2                                   | Activates the IL-23 / IL-7 axis, sensor for PANoptosis                                 | Psoriasis                                     | Inflammasome activation increases pro-inflammatory cytokine release                                       |
| NLRC5                                  | Regulates PANoptosome formation  | Colitis<br>Hemophagocytic lymphohistiocytosis | Activated by TLR2/4 signals and NAD <sup>+</sup> levels   |
| Melatonin, Dickkopf-1                  | Inhibits PANoptosis  | Ocular hypertension<br>Diabetic retinopathy   | Suppress cell death and retinal ganglion cell loss  |

**M2:** Matrix protein 2, **NS1:** Nonstructural protein 1, **PB1-F2:** Polymerase basic protein 1-F2, **Casp6:** Caspase-6, **RDX:** Radixin, **RIPK1:** Receptor-interacting protein kinase 1, **RIPK3:** Receptor-interacting protein kinase 3, **Casp8:** Caspase-8, **NLRP3:** NOD-like receptor pyrin domain containing 3, **ASC:** Apoptosis-associated speck-like protein containing a CARD, **Casp1:** Caspase-1, **TAK1:** TGF- $\beta$  activated kinase 1, **ADAR1:** Adenosine deaminase acting on RNA 1, **IRF1:** Interferon regulatory factor 1, **ZBP1:** Z-DNA binding protein 1, **S100A8/A9<sup>hi</sup>:** High expression of S100A8/A9, **SopF:** *Salmonella* outer protein F, **AIM2:** Absent in melanoma 2, **NLRC5:** NLR family, CARD domain containing 5, **TLR2/4:** Toll-like receptor 2/4, **PDK1:** 3-phosphoinositide dependent protein kinase-1, **RSK:** Ribosomal S6 kinase, **IL-23:** Interleukin 23, **IL-7:** Interleukin 7, **SLE:** Systemic lupus erythematosus, **mtDNA:** Mitochondrial DNA, **IAV:** Influenza A virus, **COVID-19:** Coronavirus disease 2019, **SLE:** Systemic lupus erythematosus, **TGF- $\beta$ :** Transforming growth factor-beta, **TLR2/4:** Toll-like receptor 2/4.

The first genetic argument for a relationship between pyroptosis and apoptosis was the ability of Casp1 to dissociate Casp7 from its activation site in macrophages (106).

Casp8 can act on NLRP3 inflammasome-induced pyroptosis interactions, interact with other inflammasomes, and mediate their activation (46).

In the absence of GSDMD, Casp1 has been shown to induce apoptosis by activating Casp3 and Casp7 in monocytes and macrophages. In contrast, during apoptosis, Casp3 and Casp7 can specifically inhibit pyroptosis by interrupting GSDMD at a different point from inflammatory caspases that inactivate the protein (107, 108).

Inflammasome-activated Casp1 can cleave Bid, leading to the release of mitochondrial SMAC (the second mitochondria-derived activator of caspases) and triggering subsequent necrosis (109). In apoptotic Casp3, it cleaves GSDMD at a cytotoxic N-terminal cleavage point, forming an inactive fragment. This may potentially limit GSDMD-mediated pore formation and pyroptosis (46).

Programmed cell death pathways are nonlinear, including interactions not mentioned here. They are interconnected and have complex signaling cascades and interactions. These interactions between death pathways facilitate the fight against pathogenic agents, including preventing some of the escape strategies of cells generated by pathogens. For this reason, PANoptosis is important for the control of infections and host defense.

## PANoptosis and Its Relationship with Different Modes of Cell Death

Available evidence of the relationship between PANoptosis and other pathways of PCD is still limited. Unlike PANoptosis, autophagy was traditionally thought to be regulated primarily through lysosomal pathways rather than caspase enzymes or RIPKs. In time, with the understanding that autophagy and apoptosis are in extensive cross-talk with each other, it is not surprising that many ATGs are recognized and cleaved by caspases (110-114). For instance, hATG3 can be cut down by Casp3, Casp6, and Casp8 (115). While recent research has yet to establish a definitive connection between ER stress, autophagy, and PANoptosis, their involvement in managing cellular stress and orchestrating PCD remains significant. In central gene analyses performed in ulcerative colitis, the TIMP1, TIMP2, TIMP3, IL6, and CCL2 genes were identified as associated with PANoptosis and autophagy (116). Some of the central genes associated with PANoptosis and autophagy have been reported to be correlated with certain immune system cell infiltrations (116). Another study reported that mitochondrial damage mediated by S100A8/A9<sup>hi</sup> (high expression of S100A8/A9) neutrophils in lung tissues of septic mice causes mtDNA-mediated ZBP1 PANoptosome formation. The same study also reported that S100a8/a9 increased the expression of LC3B, a marker of autophagosomes (117). Furthermore, the impaired autophagy mechanism is known to lead to abnormal activation of inflammasomes by cross-talk (118).

In the metabolic-associated fatty liver disease (MAFLD) mice model, it has been reported that the ferroptosis inhibitor LPT1 can act as a PANoptosis blocker and may protect against steatosis (119). Screening for PANoptosis-related genes identified ten genes associated with colorectal adenocarcinoma (120). Among these, CAV1 has regulatory roles for apoptosis, pyroptosis, and ferroptosis (121-123). The GPX3, IGFBP6, and TIMP1 genes, which are known to be associated with ferroptosis, were also identified among these ten genes (124-126). These results raise an important question of whether ferroptosis can be induced simultaneously with PANoptosis and draw attention to the possible relationship between ferroptosis and PANoptosis. It is suggested that anoikis, a type of apoptosis occurring within tissues, may be associated with PANoptosis due to caspase and signaling molecule interactions such as PI3K/Akt and Smad (101).

The elaboration of these interactions and a better understanding of the relationships linking PANoptosis and other types of PCD are still crucial for the development of clinical and therapeutic approaches. Current studies focus on gene analyses for different diseases to understand the relationship between the death complex PANoptosome and PANoptosis, which can differ from disease to disease.

## Regulatory Factors and Diseases

The most important factor affecting PANoptosis and the formation of PANoptosomes with different cellular components is the diversity of the pathogen. Different diseases, such as bacterial, viral, fungal infections, tumors, and autoimmune disorders, can lead to differences in PANoptosome types and regulators. An overview of the summarized regulators is provided in Table 1. For example, influenza viral proteins such as matrix protein 2 (M2), nonstructural protein 1(NS1), and polymerase basic protein 1-F2 (PB1-F2) may play a regulatory role for ZBP1-NLRP (31).

Casp6 also promotes IAV-induced PANoptosis and facilitates the connection between ZBP1 and RIPK3 after infection (32). This is surprising for Casp6, which is characterized as an executioner caspase due to its role as a bridge between a sensor and an effector. Casp6 has also been identified as an important regulator of the cross-talk signaling pathway for PANoptosis in cancer. When

scanning for PANoptosis-related genes as prognostic indicators of thyroid cancer, Casp6 was found to be highly diagnostic and abundant in tumor tissue (127, 128). Casp6 can also promote the differentiation of M2 macrophages and activation of inflammasomes and PANoptosis (32). Despite these, we still have limited knowledge about the role of Casp6 in PANoptosis induced by other pathogens or stimuli (4). Radixin (RDX) was found to be the most relevant gene in investigating the potential of PANoptosis-based molecular profiling and prognostic factors to predict survival in breast cancer patients (129). Nine lncRNAs associated with PANoptosis and colon adenocarcinoma metastasis have been identified and are significantly associated with immune infiltration. This suggests that PANoptosis plays an important role in the tumor immune microenvironment (130).

*Yersinia* infection triggers PANoptosis in macrophages by promoting the formation of a RIPK-PANoptosome complex that includes RIPK1, RIPK3, Casp8, NLRP3, ASC, and Casp1 (independent of ZBP1) (44). TAK1 is pivotal for cell survival and cellular homeostasis in innate immunity (131). This is significant, as it was among the first regulators to identify PANoptosis. The TAK1-RIPK1 relationship is a good demonstration that phosphorylation does not always lead to activation. TAK1 inhibits RIPK1, limiting its activation and preventing spontaneous activation of PANoptosis (3). *Yersinia* can inhibit TAK1 through YopJ mediation, acting as a handbrake for PANoptosis (39, 132, 133). In fact, the effects of TAK1 on cell death were recognized and investigated prior to the identification of PANoptosis (20, 21, 134). Many pathogens produce inhibitors of TAK1 (TAK1i). Inhibition or deletion of TAK1 results in the induction of PANoptosis in the host through the RIPK1-PANoptosome complex. PANoptosis also promotes pathological inflammation. Therefore, it is important to understand the molecular mechanisms that regulate TAK1i-induced cell death. Recently, it was reported that TAK1i-induced RIPK1-mediated activation of PANoptosis requires the phosphatase PP6 complex (131). PTBP1 and RAVER1 are also functional regulators involved in activating TAK1i-induced PANoptosis (135).

Since deletion of components of the linear-ubiquitin assembly complex (LUBAC) associated with cell death signaling and other complex-I molecules such as ubiquitin effector protein A20 can lead to embryonic death and autoinflammatory diseases, it is thought that they may contribute to the regulation of PANoptosis in a similar way to TAK inhibitors (30, 136).

Another regulator of PANoptosis is adenosine deaminase acting on RNA1 (ADAR1). Acting as an RNA regulator to maintain homeostasis, ADAR1 is a negative regulator of ZBP1-mediated PANoptosis. Inhibition of ADAR1 activity triggers ZBP1-mediated PANoptosis to inhibit tumor formation (137).

Casp1 inhibition in macrophages infected with *Enterococcus faecalis* OG1RF prevents PANoptosis formation (138). *E. faecalis* can also induce PANoptosis of osteoblasts, which is detrimental to the regeneration of periapical bone tissue. The regulation is provided by the NLRP3 inflammasome (139).

IRF1 is known to regulate cell death (140-142). TLR2/4 can induce NLRP12 expression through IRF1-mediated signaling, resulting in inflammasome formation to trigger IL-1 $\beta$ /-18 maturation. In addition, the generated inflammasome acts as an integral element of an NLRP12-PANoptosome that drives PANoptosis via Casp8 / RPK3 (94). Studies indicate that pro-inflammatory cytokines are significantly overexpressed during COVID-19 infection (143). However, only the combination of TNF- $\alpha$  and interferon-gamma (IFN- $\gamma$ ) has been reported to trigger PANoptosis. Collectively, TNF- $\alpha$  and IFN- $\gamma$  trigger nitric oxide (NO) formation by activating JAK/STAT1/IRF1 signaling. This is followed by Casp8/FADD-based PANoptosis (144). The synergistic effect of these two cytokines can also inhibit PANoptosis-mediated growth of various types of tumors (145). Although other cytokine associations are not clear for PANoptosis, the signaling of IL6-JAK-STAT3, the IFN- $\gamma$  response, and IL-2-STAT5 signaling in cancer positively correlate with the PANoptosis scoring. This scoring shows that PANoptosis is significantly correlated with the tumor microenvironment and infiltration levels of many types of immune cells, including NK cells, CD4<sup>+</sup> and CD8<sup>+</sup> T cells, and DCs (146). The discovery of gain-of-function mutations in STAT1 and STAT3 has expanded immunological research aimed at understanding both signaling pathways and associated disorders (147). In this respect, their relationship with the realization of PANoptosis is open to further investigation. In a different study, IRF1 was identified as a master regulator of PANoptosis in myeloid and epithelial cells to protect against colorectal cancer formation (148). Furthermore, IRF1 acts as an up-regulator of RIPK1-PANoptosis when co-stimulated with TAK1 and LPS (54). In IAV infection, IRF1 contributes to the formation of the ZBP1-PANoptosome and drives PANoptotic cell death during infection (60).

ZBP1, MEFV, LCN2, IFI27, and HSP90AB1 have been identified as PANoptosis-associated genes in systemic lupus erythematosus (SLE) and are associated with memory B cells, neutrophils, and CD8<sup>+</sup> T cells. These genes play a role in SLE by regulating type I interferon responses and IL-6-JAK-STAT3 signaling-mediated regulation of immune cells (149).

In response to fungus, particularly infections by *Candida albicans* and *Aspergillus fumigatus*, ZBP1 acts as an apical sensor to induce an immune response by activating PANoptosis (150).

*Salmonella* outer protein F (SopF) acts as an effector in *Salmonella* infection, regulating PANoptosis of intestinal epithelial cells to aggravate infection systemically. Phosphoinositide-dependent protein kinase-1 (PDK1) activated by SopF phosphorylates the p90 ribosomal S6 kinase (RSK). Phosphorylation of RSK leads to the downregulation of Casp8. Thus, PANoptosis in intestinal epithelial cells contributes to the severity of systemic infection (10).

The IL-23/IL-7 axis plays an important role in psoriasis and is strongly associated with PANoptosis. AIM2, one of the important sensors of the PANoptosome complex, is elevated in keratinocytes of psoriatic lesions and shows a pro-inflammatory effect by increasing the release of IL-1B and IL-18 and activating the IL-23/IL-7 axis after stimulation (151, 152).

NLRC5, which functions as an innate immune sensor, acts as a regulator for PANoptosome formation by regulating TLR 2/4 signaling and NAD<sup>+</sup> levels. NLRC5 deletion also protects against colitis and hemophagocytic lymphohistiocytosis in mice (45).

PANoptosis is also involved in the death of retinal ganglion cells (RGCs) induced by acute ocular hypertension and diabetic retinopathy. Melatonin and Dickkopf-1 may inhibit PANoptosis and prevent cell death (153, 154).

PANoptosome interactions vary according to the pathogenesis of the disease. Therefore, our molecular understanding of PANoptosis is not yet as well established as that of apoptosis or other cell death mechanisms. Disease- or inducer-specific regulatory mechanisms continue to be investigated. Various PANoptosome components, such as NLRP3 and RIPK3, were known to be associated with different diseases even before PANopto-

sis was identified (30). Reassessing these diseases with PANoptosis mechanisms can contribute to improve our further understanding of PANoptosis regulation.

The classification of many autoimmune diseases, for which there are still no effective treatments, may vary for related reasons, including environmental, biological, and genetic factors (155). The regulatory mechanisms of PANoptosis in autoimmune diseases have been investigated (156). Mechanisms such as the secretion of significant amounts of IFNs by regulating upstream pathways such as GAS/STING influence PANoptosome formation (156).

## Other Interactions of PANoptosis with the Immune System

As a result of the conflict between the host and pathogens, pathogens can develop escape strategies from the immune system and death mechanisms. The innate immune system also has different mechanisms to eliminate pathogens and protect the host. PANoptosis also allows the activation of an innate immune response, giving host cell immunity an advantage as an integrated cell death mechanism that can be particularly effective against invading infectious agents. With different sensors, it can be activated in response to pathogenic triggers ranging from viruses to fungi (157). Cross-talk mechanisms between death pathways are important to overcome bacterial and viral escape strategies. This is because the escape strategies of pathogens are well understood and are generally focused on bypassing a single death pathway; some bacterial species can perform Casp1, Casp4 activations, NLRC4, and NLRP3 inhibition to avoid pyroptosis (158-160).

Furthermore, they can develop different strategies to keep pyrin inactive, such as activating PRK1/2 (161). Both viruses and bacteria carry out this and similar evasion strategies through some specific proteins. For example, HPV from the papillomavirus family can regulate the degradation of the IFI16 inflammasome through the E7 protein (162). Both bacteria and viruses can try to avoid death by similar mechanisms to escape apoptosis and necroptosis (18). PANoptosis offers a strategy to block immune evasion and infections. In addition, it may promote immune activation to combat immune resistance in certain cancer types.

Interactions between innate immune system cells and PANoptosis in cancer studies have been examined according to PAN scoring, a risk-scoring system based on PANoptosis models. M2 macrophage infiltration and cancer-associated fibroblasts were significantly associated with high TGF- $\beta$  expression. A negative correlation exists between M1 macrophages and PAN score (163). Casp6, which plays an important role in inflammasome activation and PANoptosis, promotes differentiation into M2 macrophages. The PAN score is notably correlated with the tumor microenvironment, immune-related genes, and infiltration levels of most immune cells, such as NKs, CD4<sup>+</sup>/CD8<sup>+</sup> lymphocytes, and DCs (146).

A study with specifically created extracellular vesicles (EVs) and ultrasound (US) technique, which has been suggested to improve the efficacy of cancer immunotherapy, showed that immunogenic PANoptotic cell death promotes dendritic cell maturation and macrophage polarization and subsequent presentation of antigens to T cells by activating the STING pathway. STING is an interferon stimulator (164). IFN- $\gamma$  produced by DC cells promotes PANoptosis in mice. IFN- $\gamma$  deficiency affects the activation of the PANoptosis-specific markers Casp3, GSDMD, and MLKL and decreases IL-1 $\beta$  expression. Furthermore, dendritic cells express ZBP1, AIM2, and RIPK1, which are also PANoptosome sensors (165). The role of the STING pathway in immunity against intracellular pathogens and its possible direct effects on T-cells are well known (166). Additional studies are required to understand the contribution of these effects to PANoptosis.

A pro-tumoral group of tumor-associated neutrophils has been identified, with HMGB1 overexpression that reduces anti-tumor immunity and contributes to immune escape through the GATA2 / HMGB1 / TIM-3 axis (167). However, we still have limited knowledge about the direct function of neutrophils, NK cells, and other innate immune system cells in the mechanism of PANoptosis.

## Future perspectives

Our knowledge of the concept of PANoptosis in the literature remains limited. Currently, research conducted primarily by the groups that defined this concept has contributed to its development. In this review, we provide an overview of the basic mechanisms of PANoptosis based on these studies; however, our main goal is to present

the regulators identified in the literature in a comprehensive manner.

The diversity of these regulators across different triggers and disease pathogenesis makes PANoptosomes particularly interesting. Each of the identified sensors mediating the formation of PANoptosomes responds to different pathogens and endogenous danger signals, various PAMPs and DAMPs, to induce PANoptosis. To better understand the mechanisms of PANoptosis and develop therapeutic approaches, it is important to identify downstream molecules and different sensor compositions that activate phenotypic outcomes. The most stunning example of this is that PANoptosis has been implicated in the failure of IFN treatment for SARS-CoV-2 (64). SARS-CoV-2 is able to escape the immune system by inhibiting IFN-I production and reducing its activity (168). IFN therapy can be used to reduce viral load. It was also thought that patients would improve when administered; however, IFN-induced upregulation of ZBP1 activated PANoptosis in response to IFN treatment, compromising therapeutic benefits (64). This suggests that inhibition of ZBP1 may improve the efficacy of IFN-based therapies, suggesting the importance of PANoptosis inhibitors and PANoptosome components in the development of novel therapeutic approaches. Research in this area has shown promising results. A study targeting the inhibition of PANoptosis demonstrated that this approach protects the kidney from reperfusion injury (169).

For therapeutic approaches targeting cancer, infection, and inflammatory diseases, it is important to investigate not only PANoptosome components and regulators but also to consider triggers. For example, as a strategy for escape from bacterial death, *Shigella flexneri* prevents necroptosis by targeting RIPK1 and RIPK3 with the protease effector Ospd3. Similarly, OspC1 can inhibit CASP8 apoptotic signaling (170). *Shigella's* ability to block two death pathways is noteworthy, but its connection to PANoptosis remains unexplored. There are many triggers that have not been investigated in relation to PANoptosis, and this gap is rapidly being filled in the literature. Accumulated knowledge will improve our understanding of the mechanisms, sensors, and regulators of PANoptosis, paving the way for the development of potentially significant new therapeutic strategies.

**Ethics Committee Approval:** N.A

**Informed Consent:** N.A.

**Peer-review:** Externally peer-reviewed

**Author Contributions:** Concept – B.H.O., M.K.; Design – B.H.O., M.K.; Supervision – B.H.O., M.K.; Literature Review – M.K., B.H.O.; Writer – M.K., B.H.O.; Critical Reviews – B.H.O.

**Conflict of Interest:** The authors declare no conflict of interest.

**Financial Disclosure:** The authors declared that this study has received no financial support.

## References

- 1 Bedoui S, Herold MJ, Strasser A. Emerging connectivity of programmed cell death pathways and its physiological implications. *Nat Rev Mol Cell Biol.* 2020;21(11):678-95. [\[CrossRef\]](#)
- 2 Bertheloot D, Latz E, Franklin BS. Necroptosis, pyroptosis and apoptosis: an intricate game of cell death. *Cell Mol Immunol.* 2021;18(5):1106-21. [\[CrossRef\]](#)
- 3 Malireddi RKS, Kesavardhana S, Kanneganti TD. ZBP1 and TAK1: Master regulators of NLRP3 inflammasome/pyroptosis, apoptosis, and necroptosis (PAN-optosis). *Front Cell Infect Microbiol.* 2019;9:406. [\[CrossRef\]](#)
- 4 Christgen S, Zheng M, Kesavardhana S, Karki R, Malireddi RKS, Banoth B, et al. Identification of the PANoptosome: A molecular platform triggering pyroptosis, apoptosis, and necroptosis (PAN-optosis). *Front Cell Infect Microbiol.* 2020;10:237. [\[CrossRef\]](#)
- 5 Zhu P, Ke ZR, Chen JX, Li SJ, Ma TL, Fan XL. Advances in mechanism and regulation of PANoptosis: Prospects in disease treatment. *Front Immunol.* 2023 Feb 9;14:1120034. [\[CrossRef\]](#)
- 6 Christgen S, Tweedell RE, Kanneganti TD. Programming inflammatory cell death for therapy. *Pharmacol Ther.* 2022;232:108010. [\[CrossRef\]](#)
- 7 Sundaram B, Pandian N, Mall R, Wang Y, Sarkar R, Kim HJ, et al. NLRP12-PANoptosome activates PANoptosis and pathology in response to heme and PAMPs. *Cell.* 2023;186(13):2783-801.e20. [\[CrossRef\]](#)
- 8 Xiong Y. The emerging role of PANoptosis in cancer treatment. *Biomed Pharmacother.* 2023;168:115696. [\[CrossRef\]](#)
- 9 Zhou R, Ying J, Qiu X, Yu L, Yue Y, Liu Q, et al. A new cell death program regulated by toll-like receptor 9 through p38 mitogen-activated protein kinase signaling pathway in a neonatal rat model with sepsis associated encephalopathy. *Chin Med J (Engl).* 2022;135(12):1474-85. [\[CrossRef\]](#)
- 10 Yuan H, Zhou L, Chen Y, You J, Hu H, Li Y, et al. *Salmonella* effector SopF regulates PANoptosis of intestinal epithelial cells to aggravate systemic infection. *Gut Microbes.* 2023;15(1):2180315. [\[CrossRef\]](#)
- 11 Vaux DL, Strasser A. The molecular biology of apoptosis. *Proc Natl Acad Sci U S A.* 1996;93(6):2239-44. [\[CrossRef\]](#)
- 12 Zou H, Li Y, Liu X, Wang X. An APAF-1/cytochrome c multimeric complex is a functional apoptosome that activates procaspase-9. *J Biol Chem.* 1999;274(17):11549-56. [\[CrossRef\]](#)
- 13 Singh R, Letai A, Sarosiek K. Regulation of apoptosis in health and disease: the balancing act of BCL-2 family proteins. *Nat Rev Mol Cell Biol.* 2019;20(3):175-93. [\[CrossRef\]](#)
- 14 Galluzzi L, Vitale I, Aaronson SA, Abrams JM, Adam D, Agostinis P, et al. Molecular mechanisms of cell death: recommendations of the Nomenclature Committee on Cell Death 2018. *Cell Death Differ.* 2018;25(3):486-541. [\[CrossRef\]](#)
- 15 Varfolomeev EE, Schuchmann M, Luria V, Chiannikulchai N, Beckmann JS, Mett IL, et al. Targeted disruption of the mouse Caspase 8 gene ablates cell death induction by the TNF receptors, Fas/Apo1, and DR3 and is lethal prenatally. *Immunity.* 1998;9(2):267-76. [\[CrossRef\]](#)
- 16 Sayers TJ. Targeting the extrinsic apoptosis signaling pathway for cancer therapy. *Cancer Immunol Immunother.* 2011;60(8):1173-80. [\[CrossRef\]](#)
- 17 Shi C, Cao P, Wang Y, Zhang Q, Zhang D, Wang Y, et al. PANoptosis: A cell death characterized by pyroptosis, apoptosis, and necroptosis. *J Inflamm Res.* 2023;16:1523-32. [\[CrossRef\]](#)
- 18 Tummers B, Green DR. The evolution of regulated cell death pathways in animals and their evasion by pathogens. *Physiol Rev.* 2022;102(1):411-54. [\[CrossRef\]](#)
- 19 McKenzie BA, Dixit VM, Power C. Fierly cell death: Pyroptosis in the central nervous system. *Trends Neurosci.* 2020;43(1):55-73. [\[CrossRef\]](#)
- 20 Sarhan J, Liu BC, Muendlein HI, Li P, Nilson R, Tang AY, et al. Caspase-8 induces cleavage of gasdermin D to elicit pyroptosis during *Yersinia* infection. *Proc Natl Acad Sci U S A.* 2018;115(46):E10888-97. [\[CrossRef\]](#)
- 21 Orning P, Weng D, Starheim K, Ratner D, Best Z, Lee B, et al. Pathogen blockade of TAK1 triggers caspase-8-dependent cleavage of gasdermin D and cell death. *Science.* 2018;362(6418):1064-9. [\[CrossRef\]](#)
- 22 Man SM, Kanneganti TD. Regulation of inflammasome activation. *Immunol Rev.* 2015;265(1):6-21. [\[CrossRef\]](#)
- 23 Sharma D, Kanneganti TD. The cell biology of inflammasomes: Mechanisms of inflammasome activation and regulation. *J Cell Biol.* 2016;213(6):617-29. [\[CrossRef\]](#)
- 24 Yu P, Zhang X, Liu N, Tang L, Peng C, Chen X. Pyroptosis: mechanisms and diseases. *Signal Transduct Target Ther.* 2021;6(1):128. [\[CrossRef\]](#)

- 25 Vande Walle L, Lamkanfi M. Pyroptosis. *Curr Biol*. 2016;26(13):R568-72. [[CrossRef](#)]
- 26 Feng S, Fox D, Man SM. Mechanisms of gasdermin family members in inflammasome signaling and cell death. *J Mol Biol*. 2018;430(18 Pt B):3068-80. [[CrossRef](#)]
- 27 Newton K, Manning G. Necroptosis and inflammation. *Annu Rev Biochem*. 2016;85:743-63. [[CrossRef](#)]
- 28 Kearney CJ, Martin SJ. An Inflammatory perspective on necroptosis. *Mol Cell*. 2017;65(6):965-73. [[CrossRef](#)]
- 29 Linkermann A, Hackl MJ, Kunzendorf U, Walczak H, Krautwald S, Jevnikar AM. Necroptosis in immunity and ischemia-reperfusion injury. *Am J Transplant*. 2013;13(11):2797-804. [[CrossRef](#)]
- 30 Samir P, Malireddi RKS, Kanneganti TD. The PANoptosome: A deadly protein complex driving pyroptosis, apoptosis, and necroptosis (PANoptosis). *Front Cell Infect Microbiol*. 2020;10:238. [[CrossRef](#)]
- 31 Zheng M, Kanneganti TD. The regulation of the ZBP1-NLRP3 inflammasome and its implications in pyroptosis, apoptosis, and necroptosis (PANoptosis). *Immunol Rev*. 2020;297(1):26-38. [[CrossRef](#)]
- 32 Zheng M, Karki R, Vogel P, Kanneganti TD. Caspase-6 is a key regulator of innate immunity, inflammasome activation, and host defense. *Cell*. 2020;181(3):674-87.e13. [[CrossRef](#)]
- 33 Jiang M, Qi L, Li L, Wu Y, Song D, Li Y. Caspase-8: A key protein of cross-talk signal way in "PANoptosis" in cancer. *Int J Cancer*. 2021;149(7):1408-20. [[CrossRef](#)]
- 34 Nguyen LN, Kanneganti TD. PANoptosis in viral infection: The missing puzzle piece in the cell death field. *J Mol Biol*. 2022;434(4):167249. [[CrossRef](#)]
- 35 Place DE, Lee S, Kanneganti TD. PANoptosis in microbial infection. *Curr Opin Microbiol*. 2021;59:42-9. [[CrossRef](#)]
- 36 Gullett JM, Tweedell RE, Kanneganti TD. It's all in the PAN: Crosstalk, plasticity, redundancies, switches, and interconnectedness encompassed by PANoptosis underlying the totality of cell death-associated biological effects. *Cells*. 2022;11(9):1495. [[CrossRef](#)]
- 37 Liu J, Hong M, Li Y, Chen D, Wu Y, Hu Y. Programmed cell death tunes tumor immunity. *Front Immunol*. 2022;13:847345. [[CrossRef](#)]
- 38 Cai Y, Xiao H, Zhou Q, Lin J, Liang X, Xu W, et al. Comprehensive analyses of PANoptosome with potential implications in cancer prognosis and immunotherapy. *Biochem Genet*. 2025;63(1):331-53. [[CrossRef](#)]
- 39 Malireddi RKS, Gurung P, Kesavardhana S, Samir P, Burton A, Mummareddy H, et al. Innate immune priming in the absence of TAK1 drives RIPK1 kinase activity-independent pyroptosis, apoptosis, necroptosis, and inflammatory disease. *J Exp Med*. 2020;217(3):jem.20191644. [[CrossRef](#)]
- 40 Van Opdenbosch N, Van Gorp H, Verdonck M, Saavedra PHV, de Vasconcelos NM, Gonçalves A, et al. Caspase-1 engagement and TLR-induced c-FLIP expression suppress ASC/caspase-8-dependent apoptosis by inflammasome sensors NLRP1b and NLRC4. *Cell Rep*. 2017;21(12):3427-44. [[CrossRef](#)]
- 41 Gurung P, Burton A, Kanneganti TD. NLRP3 inflammasome plays a redundant role with caspase 8 to promote IL-1 $\beta$ -mediated osteomyelitis. *Proc Natl Acad Sci U S A*. 2016;113(16):4452-7. [[CrossRef](#)]
- 42 Wang L, Zhu Y, Zhang L, Guo L, Wang X, Pan Z, et al. Mechanisms of PANoptosis and relevant small-molecule compounds for fighting diseases. *Cell Death Dis*. 2023;14(12):851. [[CrossRef](#)]
- 43 Wang Y, Pandian N, Han JH, Sundaram B, Lee S, Karki R, et al. Single cell analysis of PANoptosome cell death complexes through an expansion microscopy method. *Cell Mol Life Sci*. 2022;79(10):531. [[CrossRef](#)]
- 44 Malireddi RKS, Kesavardhana S, Karki R, Kancharana B, Burton AR, Kanneganti TD. RIPK1 distinctly regulates *Yersinia*-induced inflammatory cell death, PANoptosis. *Immunohorizons*. 2020;4(12):789-96. [[CrossRef](#)]
- 45 Sundaram B, Pandian N, Kim HJ, Abdelaal HM, Mall R, Indari O, et al. NLRC5 senses NAD<sup>+</sup> depletion, forming a PANoptosome and driving PANoptosis and inflammation. *Cell*. 2024;187(15):4061-77.e17. [[CrossRef](#)]
- 46 Wang Y, Kanneganti TD. From pyroptosis, apoptosis and necroptosis to PANoptosis: A mechanistic compendium of programmed cell death pathways. *Comput Struct Biotechnol J*. 2021;19:4641-57. [[CrossRef](#)]
- 47 Sagulenko V, Thygesen SJ, Sester DP, Idris A, Cridland JA, Vajjhala PR, et al. AIM2 and NLRP3 inflammasomes activate both apoptotic and pyroptotic death pathways via ASC. *Cell Death Differ*. 2013;20(9):1149-60. [[CrossRef](#)]
- 48 Vajjhala PR, Lu A, Brown DL, Pang SW, Sagulenko V, Sester DP, et al. The inflammasome adaptor ASC induces procaspase-8 death effector domain filaments. *J Biol Chem*. 2015;290(49):29217-30. [[CrossRef](#)]
- 49 Sun X, Yin J, Starovasnik MA, Fairbrother WJ, Dixit VM. Identification of a novel homotypic interaction motif required for the phosphorylation of receptor-interacting protein (RIP) by RIP3. *J Biol Chem*. 2002;277(11):9505-11. [[CrossRef](#)]
- 50 Karki R, Kanneganti TD. PANoptosome signaling and therapeutic implications in infection: central role for ZBP1 to activate the inflammasome and PANoptosis. *Curr Opin Immunol*. 2023;83:102348. [[CrossRef](#)]
- 51 Lee S, Karki R, Wang Y, Nguyen LN, Kalathur RC, Kanneganti TD. AIM2 forms a complex with pyrin and ZBP1 to drive PANoptosis and host defence. *Nature*. 2021;597(7876):415-9. [[CrossRef](#)]
- 52 Schwarzer R, Jiao H, Wachsmuth L, Tresch A, Pasparakis M. FADD and caspase-8 regulate gut homeostasis and inflammation by controlling MLKL- and GSDMD-mediated death of intestinal epithelial cells. *Immunity*. 2020;52(6):978-93.e6. [[CrossRef](#)]
- 53 Szklarczyk D, Gable AL, Lyon D, Junge A, Wyder S, Huerta-Cepas J, et al. STRING v11: protein-protein association networks with increased coverage, supporting functional discovery in genome-wide experimental datasets. *Nucleic Acids Res*. 2019;47(D1):D607-13. [[CrossRef](#)]
- 54 Sharma BR, Karki R, Rajesh Y, Kanneganti TD. Immune regulator IRF1 contributes to ZBP1-, AIM2-, RIPK1-, and NLRP12-PANoptosome activation and inflammatory cell death (PANoptosis). *J Biol Chem*. 2023;299(9):105141. [[CrossRef](#)]





- 55 Thapa RJ, Ingram JP, Ragan KB, Nogusa S, Boyd DF, Benitez AA, et al. DAI senses influenza A virus genomic RNA and activates RIPK3-dependent cell death. *Cell Host Microbe*. 2016;20(5):674-81. [\[CrossRef\]](#)
- 56 Oh S, Lee S. Recent advances in ZBP1-derived PANoptosis against viral infections. *Front Immunol*. 2023;14:1148727. [\[CrossRef\]](#)
- 57 Rebsamen M, Heinz LX, Meylan E, Michallet MC, Schroder K, Hofmann K, et al. DAI/ZBP1 recruits RIP1 and RIP3 through RIP homotypic interaction motifs to activate NF- $\kappa$ B. *EMBO Rep*. 2009;10(8):916-22. [\[CrossRef\]](#)
- 58 Kesavardhana S, Malireddi RKS, Burton AR, Porter SN, Vogel P, Pruetz-Miller SM, et al. The Z $\alpha$ 2 domain of ZBP1 is a molecular switch regulating influenza-induced PANoptosis and perinatal lethality during development. *J Biol Chem*. 2020;295(24):8325-30. [\[CrossRef\]](#)
- 59 Kuriakose T, Man SM, Malireddi RK, Karki R, Kesavardhana S, Place DE, et al. ZBP1/DAI is an innate sensor of influenza virus triggering the NLRP3 inflammasome and programmed cell death pathways. *Sci Immunol*. 2016;1(2):aag2045. [\[CrossRef\]](#)
- 60 Kuriakose T, Kanneganti TD. ZBP1: Innate sensor regulating cell death and inflammation. *Trends Immunol*. 2018;39(2):123-34. [\[CrossRef\]](#)
- 61 Lin J, Kumari S, Kim C, Van TM, Wachsmuth L, Polykratis A, Pasparakis M. RIPK1 counteracts ZBP1-mediated necroptosis to inhibit inflammation. *Nature*. 2016;540(7631):124-8. [\[CrossRef\]](#)
- 62 Newton K, Wickliffe KE, Maltzman A, Dugger DL, Strasser A, Pham VC, et al. RIPK1 inhibits ZBP1-driven necroptosis during development. *Nature*. 2016;540(7631):129-33. [\[CrossRef\]](#)
- 63 Muendlein HI, Connolly WM, Magri Z, Smirnova I, Ilyukha V, Gautam A, et al. ZBP1 promotes LPS-induced cell death and IL-1 $\beta$  release via RHIM-mediated interactions with RIPK1. *Nat Commun*. 2021;12(1):86. [\[CrossRef\]](#)
- 64 Karki R, Lee S, Mall R, Pandian N, Wang Y, Sharma BR, et al. ZBP1-dependent inflammatory cell death, PANoptosis, and cytokine storm disrupt IFN therapeutic efficacy during coronavirus infection. *Sci Immunol*. 2022;7(74):eabo6294. [\[CrossRef\]](#)
- 65 Qin Y, Meng X, Wang M, Liang W, Xu R, Chen J, et al. Post-translational ISGylation of NLRP3 by HERC enzymes facilitates inflammasome activation in models of inflammation. *J Clin Invest*. 2023;133(20):e161935. [\[CrossRef\]](#)
- 66 An J, Ouyang L, Yu C, Carr SM, Ramprasath T, Liu Z, et al. Nicotine exacerbates atherosclerosis and plaque instability via NLRP3 inflammasome activation in vascular smooth muscle cells. *Theranostics*. 2023;13(9):2825-42. [\[CrossRef\]](#)
- 67 Kim CU, Jeong YJ, Lee P, Lee MS, Park JH, Kim YS, et al. Extracellular nucleoprotein exacerbates influenza virus pathogenesis by activating Toll-like receptor 4 and the NLRP3 inflammasome. *Cell Mol Immunol*. 2022;19(6):715-25. [\[CrossRef\]](#)
- 68 Zhao M, Zheng Z, Zhang P, Xu Y, Zhang J, Peng S, et al. IL-30 protects against sepsis-induced myocardial dysfunction by inhibiting pro-inflammatory macrophage polarization and pyroptosis. *iScience*. 2023;26(9):107544. [\[CrossRef\]](#)
- 69 Man SM, Karki R, Malireddi RK, Neale G, Vogel P, Yamamoto M, et al. The transcription factor IRF1 and guanylate-binding proteins target activation of the AIM2 inflammasome by *Francisella* infection. *Nat Immunol*. 2015;16(5):467-75. [\[CrossRef\]](#)
- 70 Jiang H, Xie Y, Lu J, Li H, Zeng K, Hu Z, et al. Pristimerin suppresses AIM2 inflammasome by modulating AIM2-PYCARD/ASC stability via selective autophagy to alleviate tendinopathy. *Autophagy*. 2024;20(1):76-93. [\[CrossRef\]](#)
- 71 Lin J, Wang J, Fang J, Li M, Xu S, Little PJ, et al. The cytoplasmic sensor, the AIM2 inflammasome: A precise therapeutic target in vascular and metabolic diseases. *Br J Pharmacol*. 2024;181(12):1695-719. [\[CrossRef\]](#)
- 72 Gerlach B, Cordier SM, Schmukle AC, Emmerich CH, Rieser E, Haas TL, et al. Linear ubiquitination prevents inflammation and regulates immune signalling. *Nature*. 2011;471(7340):591-6. [\[CrossRef\]](#)
- 73 Vince JE, Wong WW, Gentle I, Lawlor KE, Allam R, O'Reilly L, et al. Inhibitor of apoptosis proteins limit RIP3 kinase-dependent interleukin-1 activation. *Immunity*. 2012;36(2):215-27. [\[CrossRef\]](#)
- 74 Dondelinger Y, Aguilera MA, Goossens V, Dubuisson C, Grootjans S, Dejardin E, et al. RIPK3 contributes to TNFR1-mediated RIPK1 kinase-dependent apoptosis in conditions of cIAP1/2 depletion or TAK1 kinase inhibition. *Cell Death Differ*. 2013;20(10):1381-92. [\[CrossRef\]](#)
- 75 Peltzer N, Darding M, Walczak H. Holding RIPK1 on the ubiquitin leash in TNFR1 signaling. *Trends Cell Biol*. 2016;26(6):445-61. [\[CrossRef\]](#)
- 76 Ting AT, Bertrand MJM. More to life than NF- $\kappa$ B in TNFR1 signaling. *Trends Immunol*. 2016;37(8):535-45. [\[CrossRef\]](#)
- 77 Rahighi S, Ikeda F, Kawasaki M, Akutsu M, Suzuki N, Kato R, et al. Specific recognition of linear ubiquitin chains by NEMO is important for NF- $\kappa$ B activation. *Cell*. 2009;136(6):1098-109. [\[CrossRef\]](#)
- 78 Vandenabeele P, Galluzzi L, Vanden Berghe T, Kroemer G. Molecular mechanisms of necroptosis: an ordered cellular explosion. *Nat Rev Mol Cell Biol*. 2010;11(10):700-14. [\[CrossRef\]](#)
- 79 Newton K, Wickliffe KE, Dugger DL, Maltzman A, Roose-Girma M, Dohse M, et al. Cleavage of RIPK1 by caspase-8 is crucial for limiting apoptosis and necroptosis. *Nature*. 2019;574(7778):428-31. [\[CrossRef\]](#)
- 80 O'Donnell MA, Perez-Jimenez E, Oberst A, Ng A, Massoumi R, Xavier R, et al. Caspase 8 inhibits programmed necrosis by processing CYLD. *Nat Cell Biol*. 2011;13(12):1437-42. [\[CrossRef\]](#)
- 81 Feng S, Yang Y, Mei Y, Ma L, Zhu DE, Hoti N, et al. Cleavage of RIP3 inactivates its caspase-independent apoptosis pathway by removal of kinase domain. *Cell Signal*. 2007;19(10):2056-67. [\[CrossRef\]](#)
- 82 Orozco S, Yatim N, Werner MR, Tran H, Gunja SY, Tait SW, et al. RIPK1 both positively and negatively regulates RIPK3 oligomerization and necroptosis. *Cell Death Differ*. 2014;21(10):1511-21. [\[CrossRef\]](#)
- 83 Dillon CP, Weinlich R, Rodriguez DA, Cripps JG, Quarato G, Gurung P, et al. RIPK1 blocks early postnatal lethality me-

- diated by caspase-8 and RIPK3. *Cell*. 2014;157(5):1189-202. [\[CrossRef\]](#)
- 84 Kelliher MA, Grimm S, Ishida Y, Kuo F, Stanger BZ, Leder P. The death domain kinase RIP mediates the TNF-induced NF- $\kappa$ B signal. *Immunity*. 1998;8(3):297-303. [\[CrossRef\]](#)
- 85 Zhang H, Zhou X, McQuade T, Li J, Chan FK, Zhang J. Functional complementation between FADD and RIP1 in embryos and lymphocytes. *Nature*. 2011;471(7338):373-6. Erratum in: *Nature*. 2012 Mar 22;483(7390):498. [\[CrossRef\]](#)
- 86 Fritsch M, Günther SD, Schwarzer R, Albert MC, Schorn F, Werthenbach JP, et al. Caspase-8 is the molecular switch for apoptosis, necroptosis and pyroptosis. *Nature*. 2019;575(7784):683-7. [\[CrossRef\]](#)
- 87 Newton K, Wickliffe KE, Maltzman A, Dugger DL, Reja R, Zhang Y, et al. Activity of caspase-8 determines plasticity between cell death pathways. *Nature*. 2019;575(7784):679-82. [\[Cross-Ref\]](#)
- 88 Tuncer S, Fiorillo MT, Sorrentino R. The multifaceted nature of NLRP12. *J Leukoc Biol*. 2014;96(6):991-1000. [\[CrossRef\]](#)
- 89 Wang L, Manji GA, Grenier JM, Al-Garawi A, Merriam S, Lora JM, et al. PYPAF7, a novel PYRIN-containing Apaf1-like protein that regulates activation of NF- $\kappa$ B and caspase-1-dependent cytokine processing. *J Biol Chem*. 2002;277(33):29874-80. [\[CrossRef\]](#)
- 90 Fortes GB, Alves LS, de Oliveira R, Dutra FF, Rodrigues D, Fernandez PL, et al. Heme induces programmed necrosis on macrophages through autocrine TNF and ROS production. *Blood*. 2012;119(10):2368-75. [\[CrossRef\]](#)
- 91 Li Q, Fu W, Yao J, Ji Z, Wang Y, Zhou Z, et al. Heme induces IL-1 $\beta$  secretion through activating NLRP3 in kidney inflammation. *Cell Biochem Biophys*. 2014;69(3):495-502. [\[CrossRef\]](#)
- 92 Dutra FF, Alves LS, Rodrigues D, Fernandez PL, de Oliveira RB, Golenbock DT, et al. Hemolysis-induced lethality involves inflammasome activation by heme. *Proc Natl Acad Sci U S A*. 2014;111(39):E4110-8. [\[CrossRef\]](#)
- 93 Henkel FDR, O'Neill LAJ. NLRP12 drives PANoptosis in response to heme. *Trends Immunol*. 2023;44(8):574-6. [\[Cross-Ref\]](#)
- 94 Tsuchiya K, Nakajima S, Hosojima S, Thi Nguyen D, Hattori T, Manh Le T, et al. Caspase-1 initiates apoptosis in the absence of gasdermin D. *Nat Commun*. 2019;10(1):2091. [\[CrossRef\]](#)
- 95 Harvey NL, Kumar S. The role of caspases in apoptosis. *Adv Biochem Eng Biotechnol*. 1998;62:107-28. [\[CrossRef\]](#)
- 96 Sahoo G, Samal D, Khandayataray P, Murthy MK. A Review on caspases: Key regulators of biological activities and apoptosis. *Mol Neurobiol*. 2023;60(10):5805-37. [\[CrossRef\]](#)
- 97 Rogers C, Fernandes-Alnemri T, Mayes L, Alnemri D, Cingolani G, Alnemri ES. Cleavage of DFNA5 by caspase-3 during apoptosis mediates progression to secondary necrotic/pyroptotic cell death. *Nat Commun*. 2017;8:14128. [\[CrossRef\]](#)
- 98 Gao J, Xiong A, Liu J, Li X, Wang J, Zhang L, et al. PANoptosis: bridging apoptosis, pyroptosis, and necroptosis in cancer progression and treatment. *Cancer Gene Ther*. 2024;31(7):970-83. [\[CrossRef\]](#)
- 99 Wang Y, Gao W, Shi X, Ding J, Liu W, He H, et al. Chemotherapy drugs induce pyroptosis through caspase-3 cleavage of a gasdermin. *Nature*. 2017;547(7661):99-103. [\[CrossRef\]](#)
- 100 Oberst A, Dillon CP, Weinlich R, McCormick LL, Fitzgerald P, Pop C, et al. Catalytic activity of the caspase-8-FLIP(L) complex inhibits RIPK3-dependent necrosis. *Nature*. 2011;471(7338):363-7. [\[CrossRef\]](#)
- 101 Gao X, Ma C, Liang S, Chen M, He Y, Lei W. PANoptosis: Novel insight into regulated cell death and its potential role in cardiovascular diseases (Review). *Int J Mol Med*. 2024;54(3):74. [\[CrossRef\]](#)
- 102 Xu W, Che Y, Zhang Q, Huang H, Ding C, Wang Y, et al. Apaf-1 pyroptosome senses mitochondrial permeability transition. *Cell Metab*. 2021;33(2):424-36.e10. [\[CrossRef\]](#)
- 103 Dillon CP, Oberst A, Weinlich R, Janke LJ, Kang TB, Ben-Moshe T, et al. Survival function of the FADD-CASPASE-8-cFLIP(L) complex. *Cell Rep*. 2012;1(5):401-7. [\[CrossRef\]](#)
- 104 Zhang DW, Shao J, Lin J, Zhang N, Lu BJ, Lin SC, et al. RIP3, an energy metabolism regulator that switches TNF-induced cell death from apoptosis to necrosis. *Science*. 2009;325(5938):332-6. [\[CrossRef\]](#)
- 105 Nikolettou V, Markaki M, Palikaras K, Tavernarakis N. Crosstalk between apoptosis, necrosis and autophagy. *Biochim Biophys Acta*. 2013;1833(12):3448-59. [\[CrossRef\]](#)
- 106 Lamkanfi M, Kanneganti TD, Van Damme P, Vanden Berghe T, Vanoverberghe I, Vandekerckhove J, et al. Targeted peptidomic proteomics reveals caspase-7 as a substrate of the caspase-1 inflammasomes. *Mol Cell Proteomics*. 2008;7(12):2350-63. [\[CrossRef\]](#)
- 107 Taabazuing CY, Okondo MC, Bachovchin DA. Pyroptosis and apoptosis pathways engage in bidirectional crosstalk in monocytes and macrophages. *Cell Chem Biol*. 2017;24(4):507-14.e4. [\[CrossRef\]](#)
- 108 Rogers C, Erkes DA, Nardone A, Aplin AE, Fernandes-Alnemri T, Alnemri ES. Gasdermin pores permeabilize mitochondria to augment caspase-3 activation during apoptosis and inflammasome activation. *Nat Commun*. 2019;10(1):1689. [\[CrossRef\]](#)
- 109 Heilig R, Dilucca M, Boucher D, Chen KW, Hancz D, Demarco B, et al. Caspase-1 cleaves Bid to release mitochondrial SMAC and drive secondary necrosis in the absence of GSDMD. *Life Sci Alliance*. 2020;3(6):e202000735. [\[CrossRef\]](#)
- 110 Booth LA, Tavallai S, Hamed HA, Cruickshanks N, Dent P. The role of cell signalling in the crosstalk between autophagy and apoptosis. *Cell Signal*. 2014;26(3):549-55. [\[CrossRef\]](#)
- 111 Wu H, Che X, Zheng Q, Wu A, Pan K, Shao A, et al. Caspases: a molecular switch node in the crosstalk between autophagy and apoptosis. *Int J Biol Sci*. 2014;10(9):1072-83. [\[CrossRef\]](#)
- 112 Norman JM, Cohen GM, Bampton ET. The in vitro cleavage of the hAtg proteins by cell death proteases. *Autophagy*. 2010;6(8):1042-56. [\[CrossRef\]](#)
- 113 Djavaheri-Mergny M, Maiuri MC, Kroemer G. Cross talk between apoptosis and autophagy by caspase-mediated cleavage of Beclin 1. *Oncogene*. 2010;29(12):1717-9. [\[CrossRef\]](#)
- 114 Tsapras P, Nezis IP. Caspase involvement in autophagy. *Cell Death Differ*. 2017;24(8):1369-79. [\[CrossRef\]](#)

- 115 Denton D, Nicolson S, Kumar S. Cell death by autophagy: facts and apparent artefacts. *Cell Death Differ.* 2012;19(1):87-95. [\[CrossRef\]](#)
- 116 Lu J, Li F, Ye M. PANoptosis and autophagy-related molecular signature and immune landscape in ulcerative colitis: Integrated analysis and experimental validation. *J Inflamm Res.* 2024;17:3225-45. [\[CrossRef\]](#)
- 117 Wang Y, Shi Y, Shao Y, Lu X, Zhang H, Miao C. S100A8/A9<sup>hi</sup> neutrophils induce mitochondrial dysfunction and PANoptosis in endothelial cells via mitochondrial complex I deficiency during sepsis. *Cell Death Dis.* 2024;15(6):462. [\[CrossRef\]](#)
- 118 Takahama M, Akira S, Saitoh T. Autophagy limits activation of the inflammasomes. *Immunol Rev.* 2018;281(1):62-73. [\[CrossRef\]](#)
- 119 Tong J, Lan XT, Zhang Z, Liu Y, Sun DY, Wang XJ, et al. Ferroptosis inhibitor liproxstatin-1 alleviates metabolic dysfunction-associated fatty liver disease in mice: potential involvement of PANoptosis. *Acta Pharmacol Sin.* 2023;44(5):1014-28. [\[CrossRef\]](#)
- 120 Liu Y, Wang Y, Feng H, Ma L, Liu Y. PANoptosis-related genes function as efficient prognostic biomarkers in colon adenocarcinoma. *Front Endocrinol (Lausanne).* 2024;15:1344058. [\[CrossRef\]](#)
- 121 Jiang X, Li Y, Fu D, You T, Wu S, Xin J, et al. Caveolin-1 ameliorates acetaminophen-aggravated inflammatory damage and lipid deposition in non-alcoholic fatty liver disease via the ROS/TXNIP/NLRP3 pathway. *Int Immunopharmacol.* 2023;114:109558. [\[CrossRef\]](#)
- 122 Gargalovic P, Dory L. Cellular apoptosis is associated with increased caveolin-1 expression in macrophages. *J Lipid Res.* 2003;44(9):1622-32. [\[CrossRef\]](#)
- 123 Ling H, Xiao H, Luo T, Lin H, Deng J. Role of ferroptosis in regulating the epithelial-mesenchymal transition in pulmonary fibrosis. *Biomedicines.* 2023;11(1):163. [\[CrossRef\]](#)
- 124 Nikulin S, Razumovskaya A, Poloznikov A, Zakharova G, Alekseev B, Tonevitsky A. *ELOVL5* and *IGFBP6* genes modulate sensitivity of breast cancer cells to ferroptosis. *Front Mol Biosci.* 2023;10:1075704. [\[CrossRef\]](#)
- 125 Imai H, Matsuoka M, Kumagai T, Sakamoto T, Koumura T. Lipid peroxidation-dependent cell death regulated by GPx4 and ferroptosis. *Curr Top Microbiol Immunol.* 2017;403:143-70. [\[CrossRef\]](#)
- 126 Wang L, Wang J, Chen L. TIMP1 represses sorafenib-triggered ferroptosis in colorectal cancer cells by activating the PI3K/Akt signaling pathway. *Immunopharmacol Immunotoxicol.* 2023;45(4):419-25. [\[CrossRef\]](#)
- 127 Xie D, Huang L, Li C, Wu R, Zheng Z, Liu F, et al. Identification of PANoptosis-related genes as prognostic indicators of thyroid cancer. *Heliyon.* 2024;10(11):e31707. [\[CrossRef\]](#)
- 128 Qi L, Wang L, Jin M, Jiang M, Li L, Li Y. Caspase-6 is a key regulator of cross-talk signal way in PANoptosis in cancer. *Immunology.* 2023;169(3):245-59. [\[CrossRef\]](#)
- 129 He P, Ma Y, Wu Y, Zhou Q, Du H. Exploring PANoptosis in breast cancer based on scRNA-seq and bulk-seq. *Front Endocrinol (Lausanne).* 2023;14:1164930. [\[CrossRef\]](#)
- 130 Huang J, Jiang S, Liang L, He H, Liu Y, Cong L, et al. Analysis of PANoptosis-related LncRNA-miRNA-mRNA network reveals LncRNA SNHG7 involved in chemo-resistance in colon adenocarcinoma. *Front Oncol.* 2022;12:888105. [\[CrossRef\]](#)
- 131 Bynigeri RR, Malireddi RKS, Mall R, Connelly JP, Pruett-Miller SM, Kanneganti TD. The protein phosphatase PP6 promotes RIPK1-dependent PANoptosis. *BMC Biol.* 2024;22(1):122. [\[CrossRef\]](#)
- 132 Sweet CR, Conlon J, Golenbock DT, Goguen J, Silverman N. YopJ targets TRAF proteins to inhibit TLR-mediated NF- $\kappa$ B, MAPK and IRF3 signal transduction. *Cell Microbiol.* 2007;9(11):2700-15. [\[CrossRef\]](#)
- 133 Paquette N, Conlon J, Sweet C, Rus F, Wilson L, Pereira A, et al. Serine/threonine acetylation of TGF $\beta$ -activated kinase (TAK1) by *Yersinia pestis* YopJ inhibits innate immune signaling. *Proc Natl Acad Sci U S A.* 2012;109(31):12710-5. [\[CrossRef\]](#)
- 134 Lamothe B, Lai Y, Hur L, Orozco NM, Wang J, Campos AD, Xie M, et al. Deletion of TAK1 in the myeloid lineage results in the spontaneous development of myelomonocytic leukemia in mice. *PLoS One.* 2012;7(12):e51228. [\[CrossRef\]](#)
- 135 Malireddi RKS, Bynigeri RR, Mall R, Nadendla EK, Connelly JP, Pruett-Miller SM, et al. Whole-genome CRISPR screen identifies RAVER1 as a key regulator of RIPK1-mediated inflammatory cell death, PANoptosis. *iScience.* 2023;26(6):106938. [\[CrossRef\]](#)
- 136 Beck DB, Werner A, Kastner DL, Aksentjevich I. Disorders of ubiquitylation: unchained inflammation. *Nat Rev Rheumatol.* 2022;18(8):435-47. [\[CrossRef\]](#)
- 137 Karki R, Sundaram B, Sharma BR, Lee S, Malireddi RKS, Nguyen LN, et al. ADAR1 restricts ZBP1-mediated immune response and PANoptosis to promote tumorigenesis. *Cell Rep.* 2021;37(3):109858. [\[CrossRef\]](#)
- 138 Chi D, Zhang Y, Lin X, Gong Q, Tong Z. Caspase-1 inhibition reduces occurrence of PANoptosis in macrophages infected by *E. faecalis* OG1RF. *J Clin Med.* 2022;11(20):6204. [\[CrossRef\]](#)
- 139 Ran S, Chu M, Gu S, Wang J, Liang J. *Enterococcus faecalis* induces apoptosis and pyroptosis of human osteoblastic MG63 cells via the NLRP3 inflammasome. *Int Endod J.* 2019;52(1):44-53. [\[CrossRef\]](#)
- 140 Kuriakose T, Zheng M, Neale G, Kanneganti TD. IRF1 is a transcriptional regulator of ZBP1 promoting NLRP3 inflammasome activation and cell death during influenza virus infection. *J Immunol.* 2018;200(4):1489-95. [\[CrossRef\]](#)
- 141 Zander DY, Burkart SS, Wüst S, Magalhães VG, Binder M. Cooperative effects of RIG-I-like receptor signaling and IRF1 on DNA damage-induced cell death. *Cell Death Dis.* 2022;13(4):364. [\[CrossRef\]](#)
- 142 Eckhardt I, Weigert A, Fulda S. Identification of IRF1 as critical dual regulator of Smac mimetic-induced apoptosis and inflammatory cytokine response. *Cell Death Dis.* 2014;5(12):e1562. [\[CrossRef\]](#)
- 143 Chiale C, Greene TT, Zuniga EI. Interferon induction, evasion, and paradoxical roles during SARS-CoV-2 infection. *Immunol Rev.* 2022;309(1):12-24. [\[CrossRef\]](#)

- 144 Sun X, Yang Y, Meng X, Li J, Liu X, Liu H. PANoptosis: Mechanisms, biology, and role in disease. *Immunol Rev*. 2024;321(1):246-62. [\[CrossRef\]](#)
- 145 Malireddi RKS, Karki R, Sundaram B, Kancharana B, Lee S, Samir P, et al. Inflammatory cell death, PANoptosis, mediated by cytokines in diverse cancer lineages inhibits tumor growth. *Immunohorizons*. 2021;5(7):568-80. [\[CrossRef\]](#)
- 146 Zhuang L, Sun Q, Huang S, Hu L, Chen Q. A comprehensive analysis of PANoptosome to prognosis and immunotherapy response in pan-cancer. *Sci Rep*. 2023;13(1):3877. [\[CrossRef\]](#)
- 147 Kiykim A. STAT1/STAT3 gain of function and mechanisms of immune dysregulation. *Turk J Immunol*. 2024;12(Suppl 1):47-52. [\[CrossRef\]](#)
- 148 Karki R, Sharma BR, Lee E, Banoth B, Malireddi RKS, Samir P, et al. Interferon regulatory factor 1 regulates PANoptosis to prevent colorectal cancer. *JCI Insight*. 2020;5(12):e136720. [\[CrossRef\]](#)
- 149 Sun W, Li P, Wang M, Xu Y, Shen D, Zhang X, et al. Molecular characterization of PANoptosis-related genes with features of immune dysregulation in systemic lupus erythematosus. *Clin Immunol*. 2023;253:109660. [\[CrossRef\]](#)
- 150 Banoth B, Tuladhar S, Karki R, Sharma BR, Briard B, Kesavardhana S, et al. ZBP1 promotes fungi-induced inflammasome activation and pyroptosis, apoptosis, and necroptosis (PANoptosis). *J Biol Chem*. 2020;295(52):18276-83. [\[CrossRef\]](#)
- 151 Dombrowski Y, Peric M, Koglin S, Kammerbauer C, Göss C, Anz D, et al. Cytosolic DNA triggers inflammasome activation in keratinocytes in psoriatic lesions. *Sci Transl Med*. 2011;3(82):82ra38. [\[CrossRef\]](#)
- 152 Lu L, Zhang B, Shi M, Liu A. Identification of PANoptosis-related biomarkers and immune infiltration characteristics in psoriasis. *Medicine (Baltimore)*. 2023;102(42):e35627. [\[CrossRef\]](#)
- 153 Ye D, Xu Y, Shi Y, Fan M, Lu P, Bai X, et al. Anti-PANoptosis is involved in neuroprotective effects of melatonin in acute ocular hypertension model. *J Pineal Res*. 2022;73(4):e12828. [\[CrossRef\]](#)
- 154 Xu X, Lan X, Fu S, Zhang Q, Gui F, Jin Q, et al. Dickkopf-1 exerts protective effects by inhibiting PANoptosis and retinal neovascularization in diabetic retinopathy. *Biochem Biophys Res Commun*. 2022;617(Pt 2):69-76. [\[CrossRef\]](#)
- 155 Koppala SN, Guruprasad V. Overview of autoimmunity: Classification, disease mechanisms, and etiology. *Turk J Immunol*. 2023;11(3):93-105. [\[CrossRef\]](#)
- 156 Liu K, Wang M, Li D, Duc Duong NT, Liu Y, Ma J, et al. PANoptosis in autoimmune diseases interplay between apoptosis, necrosis, and pyroptosis. *Front Immunol*. 2024;15:1502855. [\[CrossRef\]](#)
- 157 Pandian N, Kanneganti TD. PANoptosis: A unique innate immune inflammatory cell death modality. *J Immunol*. 2022;209(9):1625-33. [\[CrossRef\]](#)
- 158 Blasche S, Mörtl M, Steuber H, Siszler G, Nisa S, Schwarz F, et al. The *E. coli* effector protein NleF is a caspase inhibitor. *PLoS One*. 2013;8(3):e58937. [\[CrossRef\]](#)
- 159 Stewart MK, Cookson BT. Evasion and interference: intracellular pathogens modulate caspase-dependent inflammatory responses. *Nat Rev Microbiol*. 2016;14(6):346-59. [\[CrossRef\]](#)
- 160 Yang J, Lee KM, Park S, Cho Y, Lee E, Park JH, et al. Bacterial secretant from *Pseudomonas aeruginosa* dampens inflammasome activation in a quorum sensing-dependent manner. *Front Immunol*. 2017;8:333. [\[CrossRef\]](#)
- 161 Chung LK, Park YH, Zheng Y, Brodsky IE, Hearing P, Kastner DL, et al. The *Yersinia* virulence factor YopM hijacks host kinases to inhibit type III effector-triggered activation of the pyrin inflammasome. *Cell Host Microbe*. 2016;20(3):296-306. [\[CrossRef\]](#)
- 162 Song Y, Wu X, Xu Y, Zhu J, Li J, Zou Z, et al. HPV E7 inhibits cell pyroptosis by promoting TRIM21-mediated degradation and ubiquitination of the IFI16 inflammasome. *Int J Biol Sci*. 2020;16(15):2924-37. [\[CrossRef\]](#)
- 163 Pan H, Pan J, Li P, Gao J. Characterization of PANoptosis patterns predicts survival and immunotherapy response in gastric cancer. *Clin Immunol*. 2022;238:109019. [\[CrossRef\]](#)
- 164 Zhou L, Lyu J, Liu F, Su Y, Feng L, Zhang X. Immunogenic PANoptosis-initiated cancer sono-immune reediting nanotherapy by iteratively boosting cancer immunity cycle. *Adv Mater*. 2024;36(2):e2305361. [\[CrossRef\]](#)
- 165 Ocansey DKW, Qian F, Cai P, Ocansey S, Amoah S, Qian Y, et al. Current evidence and therapeutic implication of PANoptosis in cancer. *Theranostics*. 2024;14(2):640-61. [\[CrossRef\]](#)
- 166 Yıldız B, Gürsel İ. Involvement of sting-activating cyclic dinucleotides on T-cell differentiation and function: An unresolved issue. *Turk J Immunol*. 2016;4(3):47-51. [\[CrossRef\]](#)
- 167 Hu Q, Wang R, Zhang J, Xue Q, Ding B. Tumor-associated neutrophils upregulate PANoptosis to foster an immunosuppressive microenvironment of non-small cell lung cancer. *Cancer Immunol Immunother*. 2023;72(12):4293-308. [\[CrossRef\]](#)
- 168 Hidayat M, Handayani D, Nurwidya F, Andarini SL. Hyperinflammation syndrome in COVID-19 disease: Pathogenesis and potential immunomodulatory agents. *Turk J Immunol*. 2021;9(1):1-11. [\[CrossRef\]](#)
- 169 Uysal E, Dokur M, Kucukdurmaz F, Altınay S, Polat S, Batcıoğlu K, et al. Targeting the PANoptosome with 3,4-methylenedioxy- $\beta$ -nitrostyrene, reduces PANoptosis and protects the kidney against renal ischemia-reperfusion injury. *J Invest Surg*. 2022;35(11-12):1824-35. [\[CrossRef\]](#)
- 170 Ashida H, Sasakawa C, Suzuki T. A unique bacterial tactic to circumvent the cell death crosstalk induced by blockade of caspase-8. *EMBO J*. 2020;39(17):e104469. [\[CrossRef\]](#)

# Impact of Genetic Background and Gender on Mouse Susceptibility to H1N1- PR8: Implication of the Host Immune Responses

Dina Nadeem Abd-Elshafy<sup>1,3</sup> , Mohamed Hassan Nasraa<sup>2,3</sup> , Rola Nadeem<sup>2,3</sup> ,  
Mahmoud Mohamed Bahgat<sup>2,3,4</sup> 

<sup>1</sup>The National Research Centre, Institute of Environmental Research and Climate Changes, Department of Water Pollution Research, Environmental Virology Laboratory, Cairo, Egypt; <sup>2</sup>The National Research Centre, Institute of Pharmaceutical and Drug Industries Research, Department of Therapeutic Chemistry, Cairo, Egypt; <sup>3</sup>The National Research Centre, the Center of Excellence for Advanced Sciences, Research Group Immune- and Bio-markers for Infection, Cairo, Egypt; <sup>4</sup>Egypt Center for Research and Regenerative Medicine, Cairo, Egypt

## Abstract

**Objective:** This study aimed to compare the susceptibility of different mouse strains to H1N1-PR8 influenza A virus (IAV) infection.

**Materials and Methods:** The virus was produced in 293T/ Madin-Darby canine kidney (MDCK) cells following a plasmid rescue protocol and then used to infect males of BALB/c, CD1 IGS (CD-1 imprinting control strain), and National Institutes of Health (NIH) Swiss mouse strain as well as both genders of C57BL/6J mice. Both serum virus-specific immunoglobulin M / immunoglobulin G (IgM/IgG) and interferon-gamma (IFN- $\gamma$ ) levels, as well as H1N1-RNA in lungs of infected mouse strains, were investigated.

**Results:** Differential body weight with superior loss was recorded in the C57BL/6J. Differential virus-IgM/IgG levels were recorded with higher IgM in the BALB/c ( $p=0.001$ ) and higher IgG in the CD1 IGS ( $p=0.022$ ). The C57BL/6 males were more susceptible to H1N1 infection and mounted higher IgM compared to females ( $p=0.001$ ), whereas females showed higher IgG than males ( $p=0.034$ ). Differential IFN- $\gamma$  levels were observed among male mice of various strains, with a notable increase in BALB/c mice ( $p=0.071$ ) and a significant decrease in C57BL/6J mice ( $p=0.035$ ). A significant increase in the IFN- $\gamma$  level was recorded in C57BL/6J females compared to males ( $p=0.015$ ). The viral RNA was almost equal in the lungs of the males of various infected mouse strains' and in both genders of the infected C57BL/6J.

**Conclusion:** The studied host factors can be partially implicated in the recorded differential susceptibility of various mouse strains to infection with the H1N1-PR8 IAV. Our results can help in selecting the proper mouse model for vaccine evaluation and can be translated to future human studies to identify the highly susceptible individuals to influenza infection and learn more about the host factors involved in resistance to IAV infection.

**Keywords:** H1N1-PR8 influenza A virus, mice of different genetic backgrounds, IgM/IgG and IFN- $\gamma$  levels

### Correspondence

Mahmoud Mohamed Bahgat

### E-mail

mbahgatriad@yahoo.com

### Received

October 12, 2024

### Accepted

February 14, 2025

### Published

April 29, 2025

### Suggested Citation

Abd-Elshafy DN, Nasraa MH, Nadeem R, Bahgat MM. Impact of genetic background and gender on mouse susceptibility to H1N1- PR8: Implication of the host immune responses. Turk J Immunol. 2025;13(1):22-32.

### DOI

10.36519/tji.2025.565



This work is licensed under the Creative Commons Attribution-NonCommercial-Non-Derivatives 4.0 International License (CC BY-NC-ND 4.0).

## Introduction

Due to feasibility, small size, easiness of handling and maintaining in an animal house, uncomplicated ethical approval to work with, and a high degree of homology to both the human genome and metabolome (1-3), the mouse has always been considered as a very suitable animal model to study virus pathogenesis and understand host susceptibility to virus infection.

Within a given mouse strain, individual animals do not respond similarly to infection (4-7). Also, strains of different genetic backgrounds behave differently in their response to infection (8, 9). Understanding the reasons behind intra- and inter-strain individualized responses might significantly contribute to our understanding of human personalized response to infection. Differential expression of proteases involved in function, cleavage, and activation of virus virulence molecules among mouse strains of different genetic backgrounds could differentially affect infection outcome (10), and their inhibition could block virus infection (11). Also, differential regulation of immune responses in mouse strains of different genetic backgrounds could differentially affect their susceptibility to virus infection (12).

In this study, we compared the susceptibility of BALB/c, C57BL/6J, CD1 IGS (CD-1 imprinting control strain) and National Institutes of Health (NIH) Swiss mouse strains to the H1N1-PR8 influenza A virus (IAV) infection. We also compared the anti-H1N1 immune responses of these mouse strains upon infection to learn how resistant/susceptible mouse strains serologically respond to IAV infection.

## Materials and Methods

### Production of the PR8-H1N1 Virus in Cell Culture

Constructs of the cloned 8 PR8-H1N1 genes in the pHW2000 vector, which encode for the virus hemagglutinin (HA), matrix (M), neuraminidase (NA), nucleoprotein (NP), nonstructural protein (NS), polymerase acidic protein (PA) and polymerase subunits (PB1 and PB2) as well as the empty plasmid, were kindly provided by Prof. Richard Webby at St. Jude Children Hospital, Memphis, the USA through a fully executed material transfer agreement (MTA) with Prof. Mahmoud Mohamed Bahgat. Plasmids encoding individual PR8-H1N1 segments were

used to transfect competent *Escherichia coli* bacterial cells (Invitrogen; Thermo Fisher Scientific Inc., USA) in the presence of ampicillin, as the plasmid contains an ampicillin resistance gene. To prepare stocks of the constructs encoding the individual influenza virus proteins, the growing colonies carrying each construct were subjected to plasmid midi-preparations (Qiagen, Germany), and the concentrations of the purified plasmids were quantified using a NanoDrop 1000 spectrophotometer (Thermo Fisher Scientific Inc., USA). Both their purity and integrity were checked by electrophoresis on 1.1% agarose gel (Promega) followed by visualization using ethidium bromide (EtBr) staining solution, Sigma-Aldrich (Merck KGaA, Germany) in the presence of a molecular weight marker (Promega Corp., USA). The production of the PR8-H1N1 virus in cell culture was done through the plasmid rescue protocol as formerly described (13). Briefly, the equimolar ratio of the individual constructs encoding the PR8-H1N1 8 proteins was mixed and used to co-transfect 293T cells co-cultured with Madin-Darby canine kidney (MDCK) cells (both from the American Type Culture Collection - ATCC) and incubated at 37°C, 5% CO<sub>2</sub>. Control wells where cells were transfected with empty plasmids were included. Cells were assessed daily for the development of cytopathic effect (CPE) in the MDCK sheet as a result of the virus propagation. Once the CPE became obvious, the medium containing the PR8-H1N1 virus was harvested and centrifuged at 1200 g for 5 minutes. The supernatant was collected, divided into aliquots, and subjected to slow deep freezing overnight in Mr. Frosty™ Freezing Container (Thermo Fisher Scientific Inc., USA) (-80°C, cooled with isopropanol).

### Titration of the Generated PR8-H1N1 Virus

The generated virus was propagated in MDCK, as previously reported by us and others (13, 14). Briefly, MDCK cells were co-incubated with the stock PR8-H1N1 virus diluted in infection medium (Dulbecco's modified eagle medium [DMEM]-GlutaMax; 1% penicillin/streptomycin, 1 mM sodium pyruvate, 1% bovine serum albumin, 2 µg/mL tosyl-phenylalanyl-chloromethyl ketone-treated trypsin [TPCK-trypsin]) (Invitrogen; Thermo Fisher Scientific Inc., USA) and with 10-fold dilutions (10<sup>-1</sup> to 10<sup>-6</sup>) for one hour (h) at 37°C, 5% CO<sub>2</sub>. The infection medium was discarded, wells were washed and then coated with agarose overlayer diluted 1:1 with 2X concentrated culture medium (DMEM) to a final concentration of 1%. Then, plates were returned to 37°C, 5% CO<sub>2</sub>, and the formed plaques were monitored within the following 48-72 h. Control wells were included in the same plates;

they were treated with a virus-free infection medium and the agarose overlay to ensure that the observed CPE was because of the virus and not because of any stress caused while manipulating the MDCK cells. For visualization of the growing plaques, wells were first fixed for 1 h in 4% formaldehyde solution, Sigma-Aldrich (Merck KGaA, Germany), stained using 1% crystal violet Staining Solution, Sigma-Aldrich (Merck KGaA, Darmstadt, Germany) diluted in 10% ethanol/acetic acid mixture for 15 minutes, then destained with continuous water flow till appearance of white plaques in blue cells background.

### Mice Infection

BALB/c, C57BL/6J, CD1 IGS, and NIH Swiss mice were bred and maintained at the animal house of the National Research Centre (NRC). Animals were fed on a standard diet and maintained at ambient temperature according to the animal welfare protocols of the NRC in Egypt. Anesthesia procedures complied with the guidelines of the National Institutes of Health in the USA and were approved by the Medical Ethical Committee of the NRC (MREC Registration number: 17-120). Mice infection was carried out according to our previous report (11). Of each strain, five animals received intranasal infection with H1N1-PR8 ( $2 \times 10^3$  plaque-forming units [PFU] in 25  $\mu$ L/mouse) diluted in phosphate-buffered saline (PBS) and five animals received PBS (25  $\mu$ L each) as a control group. Weight loss and survival of infected mice were followed over a period of 11 days. Animals were relaxed by being anesthetized with discontinuous sniffs of diethyl ether vapor before infection and before recording body weight. After 14 days, animals were fully anesthetized with the ketamine-xylazine mixture, Sigma-Aldrich (Merck KGaA, Germany), and blood samples were collected from individual mice by inserting a heparinized capillary tube into the orbital optical venous plexus. Sera were separated by centrifugation of individual blood samples at 10,000 g, divided into multiple aliquots, and frozen at  $-80^\circ\text{C}$  until being used.

### Detection of Virus-Specific Immunoglobulin M / Immunoglobulin G (IgM/IgG) in Sera from the Infected Mouse Strains

Quantification of the immunoglobulin classes in sera of infected and control groups of various mouse strains was performed according to our published protocol with minor modifications (15). Briefly, the ELISA plates were coated (100  $\mu$ L/well) with killed H1N1-PR8 virus ( $10^6$  PFUs/mL) diluted 1:1 in coating buffer (1 M  $\text{Na}_2\text{CO}_3$ ; 1 M  $\text{NaHCO}_3$ , pH 9.6) and incubated at  $37^\circ\text{C}$  for 3 h. Plates

were washed thrice with PBS–0.05% Tween 20 (PBST). None specific binding was blocked by incubating the plates with PBST–5% fetal bovine serum (PBST–FBS; 200  $\mu$ L/well) at  $37^\circ\text{C}$  for 2 h. After washing thrice with PBST, wells were loaded with diluted mice sera in PBST–FBS (1:50; 100  $\mu$ L/well), and plates were incubated at  $37^\circ\text{C}$  for 2 h. Plates were washed thrice and then incubated with 1:2000 (100  $\mu$ L/well) anti-mice IgM/IgG conjugated to horseradish peroxidase (Kirkgaard & Perry Laboratories, Germany) at  $37^\circ\text{C}$  for 2 h, followed by washing plates thrice with PBST. For color development, 100  $\mu$ L/well O-phenylenediamine (OPD) substrate Sigma-Aldrich (Merck KGaA, Germany) was diluted in substrate buffer (0.1 M anhydrous citric acid and 0.2 M dibasic sodium phosphate, pH 5.0) containing 0.06%  $\text{H}_2\text{O}_2$ , and plates were left for 10 minutes at room temperature until color developed. The enzymatic reaction was stopped with 40  $\mu$ L/well 2 M HCl, and the changes in the optical density (OD) in plate wells were recorded at a  $\lambda_{\text{max}}$  of 490 nm using a multi-well SUNRISE plate reader (TECAN Group LTD., Switzerland).

### IFN- $\gamma$ Detection in Sera from the Infected Mouse Strains

IFN- $\gamma$  levels in sera of various infected mouse strains were measured using an indirect ELISA assay. The microtiter plates (SPL Life Sciences Co. Ltd., South Korea) were coated in duplicates with 50  $\mu$ L of individual mouse sera diluted 1:25 in carbonate/bicarbonate coating buffer and incubated at  $37^\circ\text{C}$  overnight. Plate wells were blocked with 100  $\mu$ L blocking buffer containing 5% fetal bovine serum (Serana Europe GmbH, Germany) in phosphate buffer saline–0.05% Tween–20 (LobaChemie PVT, LTD, India) for 1 h. Rat anti-mouse IFN- $\gamma$  antibody (Biolegend, USA) was applied 50  $\mu$ L of 1:1000 dilution (5  $\mu$ g/mL) followed by 2 h incubation at  $37^\circ\text{C}$ . Horseradish peroxidase (HRP)-labeled anti-rat IgG antibody (KPL; USA) was applied 50  $\mu$ L of 1:1000 dilution (5  $\mu$ g/mL) and incubated for 1 h at  $37^\circ\text{C}$ . OPD substrate, Sigma-Aldrich (Merck KGaA, Germany), was used at 0.04% in citrate buffer supplemented with 30%  $\text{H}_2\text{O}_2$ , 50  $\mu$ L was applied to each well and incubated for 10 minutes at  $37^\circ\text{C}$ , and the reaction was stopped using 50  $\mu$ L 2M  $\text{H}_2\text{SO}_4$ . Absorbance was measured at 492 nm, and a reference wavelength at 620 nm filters (Clindiang Systems Co., Ltd., China).

### Quantification of Viral RNA in the Lungs of Infected Mouse Strains

QIAamp viral RNA purification kit was used to extract the nucleic acid of the H1N1-PR8 virus from individual

lung tissues of various mouse strains. RNA concentrations were quantified using a NanoDrop 1000 spectrophotometer (Thermo Fisher Scientific Inc., USA). Specific forward (F) and reverse (R) primers were used to amplify the H1N1-PR8-HA segment by quantitative reverse transcription polymerase chain reaction RT-PCR (qRT-PCR) of the extracted RNA from individual mice (14). The R primer was initially used to reverse transcribe the virus RNA into cDNA using SuperScript III reverse transcriptase (Invitrogen; Thermo Fisher Scientific Inc., USA). The cDNA was quantified using the SYBR Green I Master kit (Roche, Switzerland) in a Rotor-Gene-Q 6000 real-time PCR cyler. The cycling conditions of the conventional PCR included initial denaturation at 94°C for 3 minutes followed by 40 amplification cycles each of denaturation at 94°C for 30 seconds, annealing at 48°C for 1 minute, and extension at 72°C for 1 minute. The program included a final extension at 72°C for 10 minutes.

### Statistical Analysis

Statistical analysis and plots were done using the GraphPad PRISM version 5 software (GraphPad Software Inc., USA). Results were expressed as means  $\pm$  standard deviations (SDs). Statistical significance was calculated by comparing the differences between the means of different studied groups using the Student's t-test. Differences were considered significant when the *p*-value was  $<0.05$ .

## Results

### The H1N1-PR8 Virus Rescue and Analysis of Its Infectivity

Visualizing midi preps of the eight plasmids encoding for influenza virus HA, M, NA, NP, NS, PA, PB1, and PB2 on agarose gel side by side with the empty pHW2000 vector and molecular weight marker revealed both their purity, integrity, and correct relative migration with respect to the molecular weights of the eight inserts. As demonstrated, the eight constructs showed slower migration (higher molecular weight) than the empty vector (EV) (Figure 1A).

Using the supernatant (medium) of co-transfected 293T/MDCK cells with the eight plasmids to infect MDCK cells in a plaque infectivity assay revealed high titer of the produced virus that caused complete damage of the cell monolayer until titer of  $10^{-2}$ , the plaques became

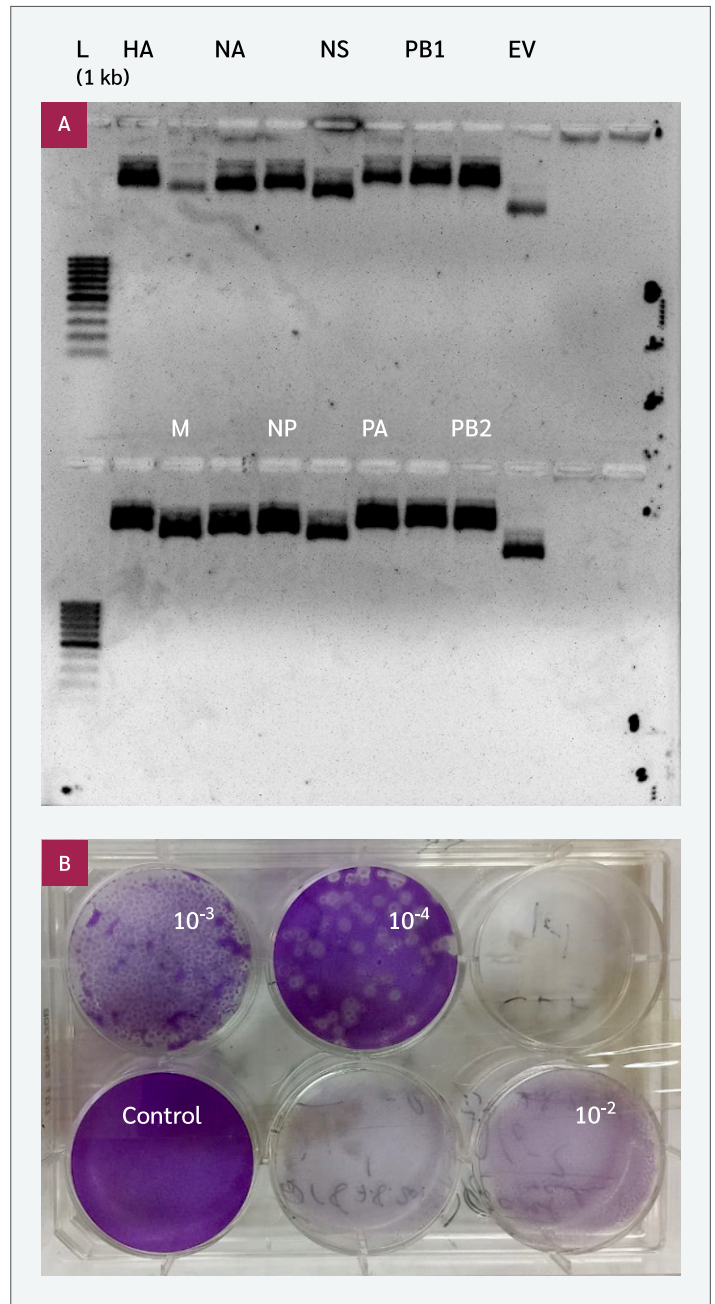


**Figure 1.** The H1N1-PR8 influenza A virus rescue and analysis of its infectivity. **(A)** Visualizing the midi preps of the eight plasmids encoding for the influenza HA, M, NA, NP, NS, PA, PB1 and PB2 on agarose gel side by side with the empty pHW2000 vector and molecular weight ladder (1kb). Both the purity and integrity of the eight inserts were indicated and the eight constructs showed slower migration than the empty vector. The ladder (L), HA, NA, NS, PB1 and EV bands are in the up section while the M, NP, PA and PB2 are in the down section of the gel. **(B)** Plaque infectivity assay for the produced virus. The medium of co-transfected 293T/MDCK cells with the 8 plasmids was used to infect MDCK cells. The results revealed high titer of the produced virus that caused complete damage of the cell monolayer until titer of  $10^{-2}$ , the plaques became visible but uncountable at  $10^{-3}$  and could be counted at  $10^{-4}$ , whereas, the control cells remained intact.

visible but uncountable at  $10^{-3}$  and could be counted at  $10^{-4}$  whereas, the control uninfected cells layer remained totally intact (Figure 1B).

### Susceptibility of the Various Mouse Strains' Males and Both Genders of the C57BL/6 to H1N1-PR8 Infection

The BALB/c, C57BL/6J, CD1 IGS, and NIH Swiss male mice showed differential susceptibilities to the produced H1N1-PR8 IAV as reflected by their differential body-weight loss at different days (d) post-infection (pi) with the top weight loss recorded for C57BL/6J males which reached its peak (25% loss) at d8 pi. In contrast, none of the control, PBS-given male mice of different strains, showed body weight loss (Figure 2A).

Since the C57BL/6J males showed the top body weight loss upon the H1N1-PR8 infection, we decided to compare their susceptibility on the gender level. Of interest, the results showed a gender-specific pattern as recorded by a sharp weight loss in female mice between d1-3 pi, which reached its peak at d3 pi (~20% loss), followed by regaining weight that never reached the starting weight (stayed at 10% loss), whereas, male mice continued to lose weight to reach its peak (25% loss) at d8 pi followed by slight regaining weight thereafter (Figure 2B).

### Serum Levels of Virus-Specific IgM/IgG in Various Mouse Strains' Males and Both Genders of the C57BL/6 Post Infection

The IgM levels were significantly higher in the BALB/c, CD1 IGS, C57BL/6J, and NIH mouse strains' males compared to control ones ( $p=0.001$ ,  $p=0.011$ ,  $p=0.016$ , and  $p=0.007$ , respectively) (Figure 3A). In comparison, only the infected males of the CD1 IGS and NIH strains showed a significant increase in IgG levels than the PBS-given ones ( $p<0.05$ ) (Figure 3B).

Generally, serum IgM and IgG levels were significantly higher in the C57BL/6J infected mice ( $p=0.0003$  and  $p=0.0025$ , respectively, for females;  $p=0.0002$  and  $p=0.0014$ , respectively, for males) compared to the control mice with a significantly higher IgM level recorded for the infected males ( $p=0.001$ ) (Figure 4A), and IgG level for the infected females ( $p=0.034$ ) (Figure 4B).

### Interferon-gamma (IFN- $\gamma$ ) Levels in Various Mouse Strains' Males and Both Genders of the C57BL/6J Post Infection

Obvious strain-specific variations in the IFN- $\gamma$  levels

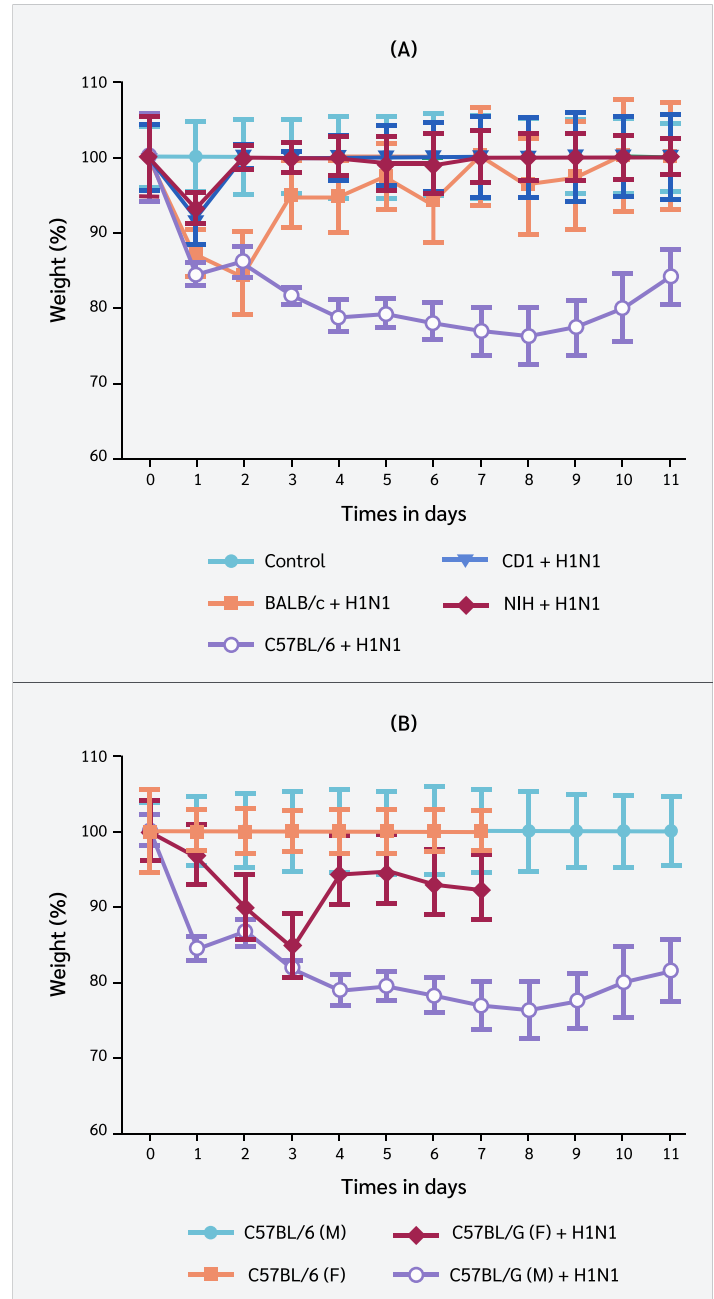


**Figure 2.** Susceptibility of the mouse strains' males (A) and C57BL/6J both genders (B) to the H1N1-PR8 infection. The BALB/c, C57BL/6J, CD1 IGS and NIH Swiss male mice (n=5 each) were either intranasally infected with diluted H1N1-PR8 in PBS ( $2 \times 10^3$  plaque forming units (PFU) in 25  $\mu$ L/ mouse) or received PBS (25  $\mu$ L each) as control group. Weight loss and survival of infected mice was followed over a period of 14 days. Animals were relaxed by being anesthetized with discontinuous sniffs of diethyl ether vapor before infection and before recording bodyweight.

were observed, where both the CD-1IGS and C57BL/6J mouse strain males showed non-significant ( $p=0.142$ ) and significant ( $p=0.035$ ) decreases in the IFN- $\gamma$  levels

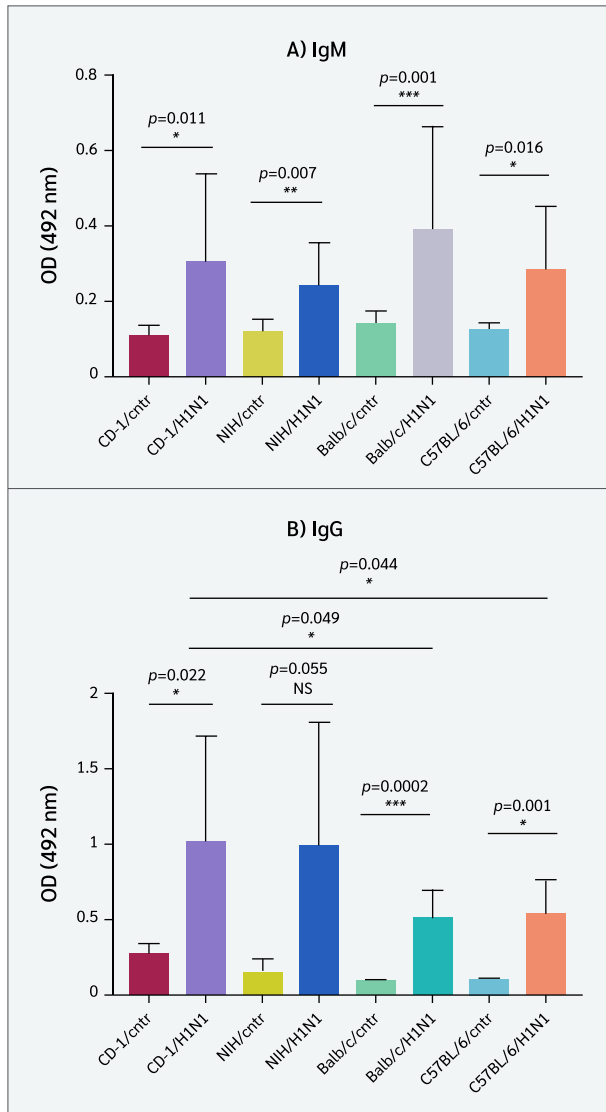


**Figure 3.** Serum levels of virus-specific IgM (A) and IgG (B) in the mouse strains' males post infection. IgM and IgG levels in the infected and control males (n=5 each) from various mouse strains were measured using ELISA.

compared to control mice. Both the NIH and BALB/c mouse strains' males showed non-significant increases in the IFN- $\gamma$  levels ( $p=0.571$  and  $p=0.071$ , respectively) compared to control mice (Figure 5A).

Gender-specific IFN- $\gamma$  levels were noticed in the C57BL/6J mouse strain, where IFN- $\gamma$  level was significantly higher in the infected females ( $p=0.0337$ ) compared to control ones. A non-significant decrease in the IFN- $\gamma$  level was recorded in infected males ( $p=0.111$ ) compared to control mice (Figure 5B).

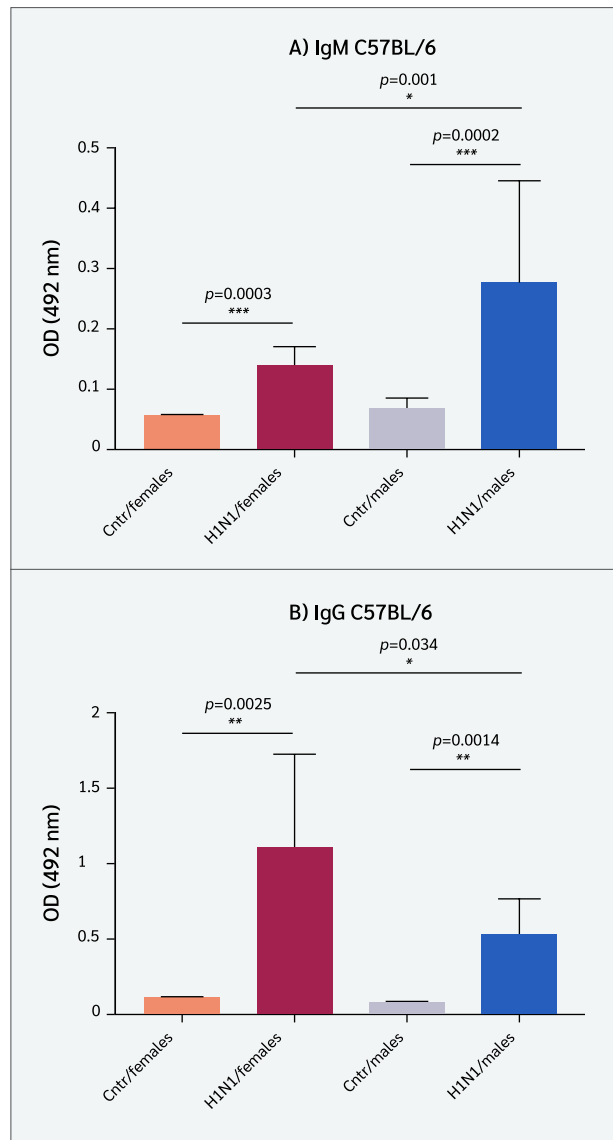


**Figure 4.** Serum levels of virus-specific IgM (A) and IgG (B) in the C57BL/6J both genders post infection. IgM and IgG levels in the infected and control mice from both genders (n=5 each) were measured using ELISA.

The IFN- $\gamma$  means in the PBS-received and H1N1-PR8 infected mouse strain males were 1.203667 and 0.7261, respectively, for the CD1 IGS; 0.6645 and 0.7908, respectively, for the NIH; 0.811667 and 1.1907, respectively, for BALB/c. The gender levels of the C57BL/6J means were 1.3515 and 0.9433, respectively, for females, whereas they were 1.0556 and 1.292125, respectively, for males.

Finally, the IFN- $\gamma$  fold change in the infected mouse strains was 0.60323993 for the CD1 IGS males,

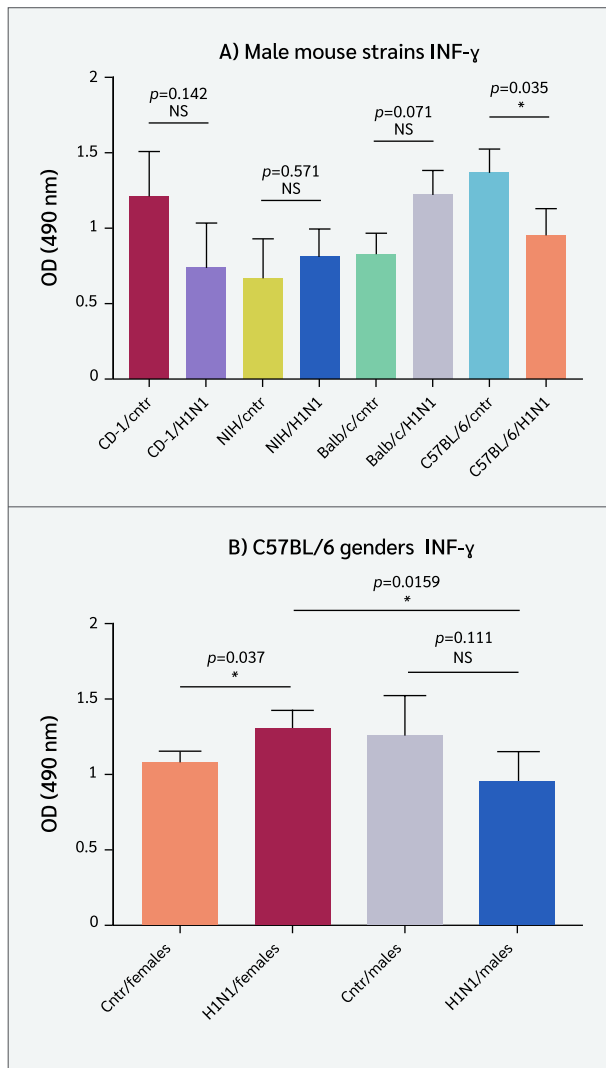


**Figure 5.** Interferon gamma (IFN- $\gamma$ ) levels in the mouse strains' males (A) and C57BL/6J both genders (B) post infection. IFN- $\gamma$  levels in the infected and control mice (n=5 each) from all groups were measured using ELISA.

1.19006772 for the NIH males, 1.46698092 for the BALB/c males, 0.69796522 for the C57BL/6J females, and 1.22406688 for the C57BL/6J males compared to the control mice of the same strain and gender.

### Viral RNA Detection in the Lungs of Mouse Strains' Males and Both Genders of the C57BL/6 Post H1N1 Infection

Although not high, slight differences in the viral RNA levels were recorded in the lungs of infected mouse strains, as revealed by the cycle threshold (Ct) values. The lowest mean Ct values, i.e., the highest virus RNA levels, were recorded in the lungs of C57BL/6J males ( $p=0.227$ ),

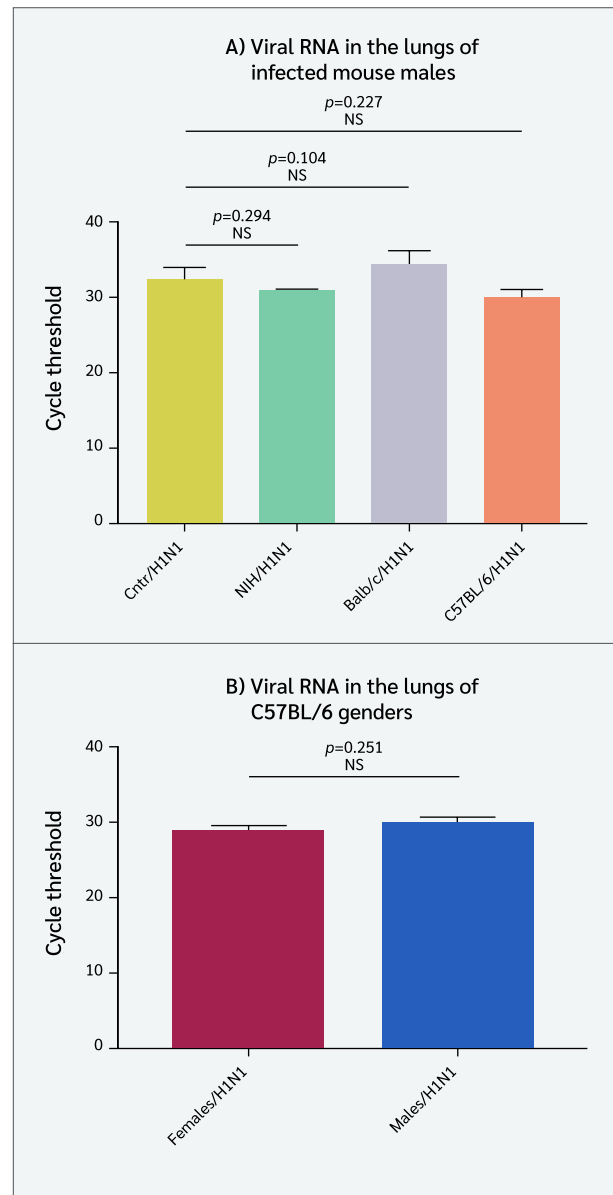


**Figure 6.** Viral RNA detection in the lungs of mouse strains' males (A) and the C57BL/6J both genders (B) post infection. The virus RNA was extracted, The H1N1-PR8 HA was initially transcribed by specific R primer into cDNA using SuperScript III reverse transcriptase. The cycle threshold (Ct) means corresponding to HA virus RNA in the lungs of infected mouse strains and C57BL/6J genders was quantified by quantitative RT-PCR (qRT-PCR) using HA specific forward (F) and reverse (R) primers and the SYBR Green I Master kit in a Rotor-Gene-Q 6000 real-time PCR cyclor.

NIH Swiss males ( $p=0.294$ ), followed by BALB/c males ( $p=0.104$ ) (Figure 6A). On gender levels, the mean viral RNA Ct value was slightly higher in the C57BL/6J males than in females ( $p=0.251$ ) (Figure 6B).

## Discussion

The high titer plaque count of the H1N1-PR8 we produced by the plasmid rescue protocol confirms the infectivity of the generated virus and the validity of the early reported protocol to generate influenza viruses by transfecting mammalian cells with plasmids encoding for the eight IAV proteins (13).

The differential body weight loss and susceptibility of various mouse strains to infection with the generated H1N1-PR8 virus agrees with previous reports on influenza and SARS-CoV2, though using different mouse strains, and may be attributed to differential expression of proteases involved both in the activation and functional cleavage of influenza HA which is mandatory for infecting host cells (8, 9-11). Also, the differential body weight loss of the studied mouse strains upon infection with the H1N1-PR8 can be referred to the previously reported differential regulation of immune responses in mouse strains of various genetic backgrounds, which can differentially influence their susceptibility to infection (12). This finding agrees with the differential anti-H1N1-IgM/IgG levels observed in the mouse strains studied in our study; post-H1N1 infection with the highest IgM levels seen in the BALB/c and the CD1 IGS mice and the highest IgG levels recorded in the CD1 IGS and NIH Swiss mice, which all did not show obvious weight loss upon infection.

BALB/c and C57BL/6J are inbred mouse strains that exhibit Th2- and Th1-biased immune responses, respectively, with C57BL/6J mice known for their higher susceptibility to diet-induced obesity. However, CD1 IGS and NIH Swiss are outbred mouse strains with genetic diversity favoring robust immune responses or displaying high reproductive performance and general adaptability, respectively (16).

Mouse genetic background can greatly impact the immune responses to virus infection (17). Research has demonstrated that BALB/c and C57BL/6J strains have different immune profiles, where BALB/c shows a Th2-biased response, which is linked to increased antibody production, while C57BL/6J mounts a Th1-biased response, which is marked by an increased pro-inflammatory cytokine production (18, 19). These variances might be among the factors leading to variations in the susceptibility and the course of the disease after IAV infection.

Studies comparing the pathogenicity of avian influenza A/H7N9 virus infection in these strains revealed that both showed significant weight loss and lung damage; however, the underlying immune mechanisms varied, indicating that the genetic background is a key factor in regulating the immune responses to influenza viruses (20, 21). On the other hand, we could not find reports concerning infection of the CD1 IGS and NIH Swiss strains with the H1N1-PR8 IAV, but it is known that outbred strains like both have more genetic variability than inbred strains.

The differential mouse gender susceptibility we saw in the present study was reported by others previously, showing that male C57BL/6J mice are more susceptible than females. Specific variants in the Y chromosome were shown to increase susceptibility to IAV infection in males and augment pathogenic immune responses in the lung, including activation of pro-inflammatory IL-17-producing  $\gamma\delta$  T cells, without affecting viral replication (22-25).

Of note, we found that the anti-H1N1-IgM levels were higher among C57BL/6J males than females, while the anti-H1N1-IgG levels were higher among females than males. This finding might indicate that IgG, but not IgM, is the essential immunoglobulin class in neutralizing the IAV infection. The observed heterogeneity in the levels of IFN- $\gamma$  in control, PBS-given, studied mouse strains reflects the influence of genetic background on the regulation of IFN- $\gamma$  production and could support our suggestion of a differential susceptibility of those mouse strains to H1N1 infection as evidenced by both differential bodyweight loss and differential antibody responses to infection.

In agreement with our results, several studies reported a clear impact of genetic backgrounds on IFN- $\gamma$  production in different mouse strains (26, 27). The noticed drop in the IFN- $\gamma$  levels in the infected C57BL/6J mice compared to the PBS-given mice is directly proportional to the drop in the body weight of the same mouse strain upon infection. It points out the partial implication of this cytokine in host susceptibility to influenza infection. Consistent with our findings, several studies proved that H1N1 infection can decrease IFN- $\gamma$  levels in mice, contributing to impaired viral clearance, increased disease severity, and enhanced susceptibility to secondary bacterial infections (26, 28, 29). Unlikely, H1N1 infection induced an increase in the IFN- $\gamma$  levels in the BALB/c

and NIH mice compared to control animals, and this might be partially the reason why these mouse strains did not lose weight upon infection. In agreement with our results, several studies demonstrated that infection of mice with H1N1 induces an increase in IFN- $\gamma$  levels, which is associated with enhanced antiviral immune responses and improved outcomes (26, 30, 31).

The only conflicting result is that although infection caused a drop in the IFN- $\gamma$  levels in CD1 IGS mice, they did not lose weight upon infection, yet, from our particular point of view, this reflects the complexity of the genetic susceptibility of mouse strains to infection which extends beyond interferon regulation and involves many other players. At the gender level, the recorded recovery of the body weight loss in the female C57BL/6J mice between days 3-4 coincides with the observed increase of the IFN- $\gamma$  upon infection of this animal group. Similar results have been previously reported where female mice exhibited higher production of IFN- $\gamma$  level compared to male mice, suggesting that gender influences the immune response to H1N1 infection (32).

In another study, ovariectomized female mice, which lack ovarian hormones such as estrogen, exhibited reduced IFN- $\gamma$  production compared to intact females. This suggests that sex hormones, particularly estrogen, may contribute to the gender differences observed in IFN- $\gamma$  response to H1N1 infection (33). Contrarily, infection of the C57BL/6J male mice resulted in a drop in the IFN- $\gamma$  levels, which might explain why male mice did not regain body weight until day 11.

In contrast to our findings and on the innate immunity level, another report showed that male mice exhibited

higher levels of pro-inflammatory cytokines, including IFN- $\gamma$ , compared to female mice, which suggests gender-related differences in the immune responses corresponding to variations in the innate immune activation (34). While these studies provide evidence for gender-related differences in IFN- $\gamma$  response to H1N1 infection in mice, further research is needed to fully understand the underlying mechanisms and whether similar findings can be extrapolated to humans. Finally, the recorded latest Ct values in the qRT-PCR detection of the virus RNA in lungs of BALB/c, CD1 IGS, NIH Swiss, and the earliest among the C57BL/6J illustrate the differential influenza infectivity of the mice from different genetic backgrounds.

### Study Limitations

First, the sample size of animals per group in the study is relatively low. Second, the live virus in the lungs of infected mouse strains was not titrated by plaque infectivity assay. Therefore, we plan to design a larger-scale study with adequate mice numbers per group and include the missing assays.

## Conclusion

The studied host factors can be partially behind the recorded differential susceptibility of various mouse strains to infection with the H1N1-PR8 IAV. Our findings can help in selecting the proper mouse model for evaluating anti-IAV-vaccines. They can also be translated to future human studies to identify the highly susceptible individuals to influenza infection and learn more about the host factors involved in resistance to IAV infection.

**Ethics Committee Approval:** Animals' maintenance, manipulation and applied anaesthesia procedures are complied with the guidelines of the National Institutes of Health in the USA and are approved by the Medical Ethical Committee of the NRC (MREC Registration number: 17-120).

**Informed Consent:** N.A.

**Peer-review:** Externally peer-reviewed

**Author Contributions:** Concept – M.M.B.; Design – M.M.B., D.N.A.; Supervision – D.N.A.; Fundings – M.M.B.; Materials – D.N.A., R.N., M.H.N.; Data Collection and/or Processing – D.N.A., M.H.N., R.N.; Analysis and/or Interpretation – D.N.A., M.H.N., R.N.; Literature

Review – M.H.N., R.N.; Writer – M.M.B., M.H.N.; Critical Reviews – M.M.B.

**Conflict of Interest:** The authors declare no conflict of interest.

**Financial Disclosure:** This study was funded by grant 12060115 from the National Research Centre of Egypt, awarded to Mahmoud Mohamed Bahgat.





**Acknowledgements:** We acknowledge Prof. Richard Webby from the Department of Infectious Diseases, St. Jude Children's Research Hospital, Memphis, Tennessee, for providing the plasmids used to generate the H1N1-PR8 virus by reverse genetics.

## References

- 1 Fuchs H, Gailus-Durner V, Adler T, Pimentel JA, Becker L, Bolle I, et al. The German Mouse Clinic: a platform for systemic phenotype analysis of mouse models. *Curr Pharm Biotechnol*. 2009;10(2):236-43. [\[CrossRef\]](#)
- 2 Du Y, Zhang W, Qiu H, Xiao C, Shi J, Reid LM, et al. Mouse models of liver parenchyma injuries and regeneration. *Front Cell Dev Biol*. 2022;10:903740. [\[CrossRef\]](#)
- 3 Pap A, Cuaranta-Monroy I, Peloquin M, Nagy L. Is the mouse a good model of human PPAR $\gamma$ -related metabolic diseases? *Int J Mol Sci*. 2016;17(8):1236. [\[CrossRef\]](#)
- 4 Bharucha T, Cleary B, Farmiloe A, Sutton E, Hayati H, Kirkwood P, et al. Mouse models of Japanese encephalitis virus infection: A systematic review and meta-analysis using a meta-regression approach. *PLoS Negl Trop Dis*. 2022;16(2):e0010116. [\[CrossRef\]](#)
- 5 Kamiya T, Greischar MA, Schneider DS, Mideo N. Uncovering drivers of dose-dependence and individual variation in malaria infection outcomes. *PLoS Comput Biol*. 2020;16(10):e1008211. [\[CrossRef\]](#)
- 6 Osbelt L, Thiemann S, Smit N, Lesker TR, Schröter M, Gálvez EJC, et al. Variations in microbiota composition of laboratory mice influence *Citrobacter rodentium* infection via variable short-chain fatty acid production. *PLoS Pathog*. 2020;16(3):e1008448. [\[CrossRef\]](#)
- 7 Contreras C, Newby JM, Hillen T. Personalized virus load curves for acute viral infections. *Viruses*. 2021;13(9):1815. [\[CrossRef\]](#)
- 8 Li K, Shen Y, Miller MA, Stabenow J, Williams RW, Lu L. Differing susceptibility of C57BL/6J and DBA/2J mice-parents of the murine BXD family, to severe acute respiratory syndrome coronavirus infection. *Cell Biosci*. 2021;11(1):137. [\[CrossRef\]](#)
- 9 Srivastava B, Błazejewska P, Hessmann M, Bruder D, Geffers R, Mauer S, et al. Host genetic background strongly influences the response to influenza A virus infections. *PLoS One*. 2009;4(3):e4857. [\[CrossRef\]](#)
- 10 Błazejewska P, Kosciński L, Viegas N, Anhlan D, Ludwig S, Schughart K. Pathogenicity of different PR8 influenza A virus variants in mice is determined by both viral and host factors. *Virology*. 2011;412(1):36-45. Erratum in: *Virology*. 2014;450-451:369-70. [\[CrossRef\]](#)
- 11 Bahgat MM, Błazejewska P, Schughart K. Inhibition of lung serine proteases in mice: a potentially new approach to control influenza infection. *Virology*. 2011;8:27. [\[CrossRef\]](#)
- 12 Alberts R, Srivastava B, Wu H, Viegas N, Geffers R, Klawonn F, et al. Gene expression changes in the host response between resistant and susceptible inbred mouse strains after influenza A infection. *Microbes Infect*. 2010;12(4):309-18. [\[CrossRef\]](#)
- 13 Hoffmann E, Neumann G, Kawaoka Y, Hobom G, Webster RG. A DNA transfection system for generation of influenza A virus from eight plasmids. *Proc Natl Acad Sci U S A*. 2000;97(11):6108-13. [\[CrossRef\]](#)
- 14 Reina J, Fernandez-Baca V, Blanco I, Munar M. Comparison of Madin-Darby canine kidney cells (MDCK) with a green monkey continuous cell line (Vero) and human lung embryonated cells (MRC-5) in the isolation of influenza A virus from nasopharyngeal aspirates by shell vial culture. *J Clin Microbiol*. 1997;35(7):1900-1. [\[CrossRef\]](#)
- 15 Bahgat MM, Kutkat MA, Nasraa MH, Mostafa A, Webby R, Bahgat IM, et al. Characterization of an avian influenza virus H5N1 Egyptian isolate. *J Virol Methods*. 2009;159(2):244-50. [\[CrossRef\]](#)
- 16 Bryda EC. The Mighty Mouse: the impact of rodents on advances in biomedical research. *Mo Med*. 2013;110(3):207-11.
- 17 Zhao G, Liu C, Kou Z, Gao T, Pan T, Wu X, et al. Differences in the pathogenicity and inflammatory responses induced by avian influenza A/H7N9 virus infection in BALB/c and C57BL/6 mouse models. *PLoS One*. 2014;9(3):e92987. [\[CrossRef\]](#)
- 18 Rottmann BG, Singh PK, Singh S, Revankar SG, Chandrasekar PH, Kumar A. Evaluation of susceptibility and innate immune response in C57BL/6 and BALB/c mice during *Candida albicans* endophthalmitis. *Invest Ophthalmol Vis Sci*. 2020;61(11):31. [\[CrossRef\]](#)
- 19 Bleul T, Zhuang X, Hildebrand A, Lange C, Böhringer D, Schlunck G, et al. Different innate immune responses in BALB/c and C57BL/6 strains following corneal transplantation. *J Innate Immun*. 2021;13(1):49-59. [\[CrossRef\]](#)
- 20 Bergersen KV, Barnes A, Worth D, David C, Wilson EH. Targeted transcriptomic analysis of C57BL/6 and BALB/c mice during progressive chronic *Toxoplasma gondii* infection reveals changes in host and parasite gene expression relating to neuropathology and resolution. *Front Cell Infect Microbiol*. 2021;11:645778. [\[CrossRef\]](#)
- 21 Malm Tillgren S, Nieto-Fontarigo JJ, Cerps S, Ramu S, Menzel M, Mahmutovic Persson I, et al. C57BL/6N mice have an attenuated lung inflammatory response to dsRNA compared to C57BL/6J and BALB/c mice. *J Inflamm (Lond)*. 2023;20(1):6. [\[CrossRef\]](#)
- 22 Kremontsov DN, Case LK, Dienz O, Raza A, Fang Q, Ather JL, et al. Genetic variation in chromosome Y regulates susceptibility to influenza A virus infection. *Proc Natl Acad Sci U S A*. 2017;114(13):3491-6. [\[CrossRef\]](#)
- 23 Felgenhauer JL, Brune JE, Long ME, Manicone AM, Chang MY, Brabb TL, et al. Evaluation of nutritional gel supplementation in C57BL/6J mice infected with mouse-adapted influenza A/PR/8/34 virus. *Comp Med*. 2020;70(6):471-86. [\[CrossRef\]](#)
- 24 Honce R, Wohlgemuth N, Meliopoulos VA, Short KR, Schultz-Cherry S. Influenza in high-risk hosts-lessons learned from animal models. *Cold Spring Harb Perspect Med*. 2020;10(12):a038604. [\[CrossRef\]](#)
- 25 Avitsur R, Mays JW, Sheridan JF. Sex differences in the response to influenza virus infection: modulation by stress. *Horm Behav*. 2011;59(2):257-64. [\[CrossRef\]](#)
- 26 McGill J, Van Rooijen N, Legge KL. Protective influenza-specific CD8 T cell responses require interactions with dendritic cells in the lungs. *J Exp Med*. 2008;205(7):1635-46. [\[CrossRef\]](#)

- 27 Bot A, Bot S, Bona CA. Protective role of gamma interferon during the recall response to influenza virus. *J Virol.* 1998;72(8):6637-45. [[CrossRef](#)]
- 28 Brincks EL, Katewa A, Kucaba TA, Griffith TS, Legge KL. CD8 T cells utilize TRAIL to control influenza virus infection. *J Immunol.* 2008;181(7):4918-25. Erratum in: *J Immunol.* 2008;181(10)7428. [[CrossRef](#)]
- 29 Thomas PG, Dash P, Aldridge JR Jr, Ellebedy AH, Reynolds C, Funk AJ, et al. The intracellular sensor NLRP3 mediates key innate and healing responses to influenza A virus via the regulation of caspase-1. *Immunity.* 2009;30(4):566-75. [[CrossRef](#)]
- 30 Sun K, Metzger DW. Inhibition of pulmonary antibacterial defense by interferon-gamma during recovery from influenza infection. *Nat Med.* 2008;14(5):558-64. [[CrossRef](#)]
- 31 Wang X, Li M, Zheng H, Muster T, Palese P, Beg AA, et al. Influenza A virus NS1 protein prevents activation of NF-kappaB and induction of alpha/beta interferon. *J Virol.* 2000;74(24):11566-73. [[CrossRef](#)]
- 32 Robinson CM, Jung JY, Nau GJ. Interferon- $\gamma$ , tumor necrosis factor, and interleukin-18 cooperate to control growth of *Mycobacterium tuberculosis* in human macrophages. *Cytokine.* 2012;60(1):233-41. [[CrossRef](#)]
- 33 Klein SL, Hodgson A, Robinson DP. Mechanisms of sex disparities in influenza pathogenesis. *J Leukoc Biol.* 2012;92(1):67-73. [[CrossRef](#)]
- 34 Huber SA, Sartini D. Roles of tumor necrosis factor alpha (TNF-alpha) and the p55 TNF receptor in CD1d induction and coxsackievirus B3-induced myocarditis. *J Virol.* 2005;79(5):2659-65. [[CrossRef](#)]
-

# Validation and Comparative Analysis of Dihydrorhodamine 123 Oxidative Burst Measurement by Flow Cytometry in Neutrophils: A Study of Two Isolation Techniques and Two Bacterial Strains

Cemil Pehlivanođlu<sup>1,2</sup> , Bařak Aru<sup>2</sup> , Ali Osman Grol<sup>3</sup> , Glderen Yanıkkaya Demirel<sup>2</sup> 

<sup>1</sup>Istanbul University Institute of Graduate Studies in Health Sciences, İstanbul, Trkiye; <sup>2</sup>Yeditepe University Faculty of Medicine, Department of Immunology, İstanbul, Trkiye; <sup>3</sup>Istanbul University Aziz Sançar Institute of Experimental Medicine, Department of Immunology, İstanbul, Trkiye

## Abstract

**Objective:** Dihydrorhodamine (DHR) 123 measurement by flow cytometry is widely used to detect neutrophil phagocytosis and oxidative burst activity. Our study aimed to evaluate the performance characteristics of DHR 123 assay results of neutrophils isolated by two different techniques and stimulated with two bacterial strains according to the validation principles.

**Material and Methods:** The oxidative burst index of neutrophils was measured by flow cytometry using healthy human venous blood samples. Granulocytes were separated by two different density separation methods, Ficoll and dextran sedimentation, and stimulated with two bacterial strains (ATCC 25923 *Staphylococcus aureus* subsp. *aureus* Rosenbach and ATCC 25913 methicillin-resistant *S. aureus*). Flow cytometric measurements were performed at five different time points (0, 10, 20, 30, 60 min). Statistical analysis was performed using GraphPad Prism version 8 software (GraphPad Software, Boston, USA) to assess linearity, precision, and sensitivity and to compare methods, bacterial strains, and incubation times.

**Results:** Our study showed that isolation by the dextran method was more suitable due to low limits of detection and quantification. Both ATCC strains were suitable for use, but ATCC 25923 may be preferred because the dextran isolation method with strain ATCC 25923 had the lowest limit of detection and quantification. Our data also showed that measurement at 0 and 30 min was appropriate.

**Conclusion:** Our study contributes to the standardization of functional methods for neutrophil oxidative burst analysis.

**Keywords:** Flow cytometry, dihydrorhodamine 123, neutrophil, validation study

## Correspondence

Glderen Yanıkkaya Demirel

## E-mail

gulderen.ydemirel@yeditepe.edu.tr

## Received

January 6, 2025

## Accepted

February 12, 2025

## Published

April 29, 2025

## Suggested Citation

Pehlivanođlu C, Aru B, Grol AO, Yanıkkaya Demirel G. Validation and comparative analysis of dihydrorhodamine 123 oxidative burst measurement by flow cytometry in neutrophils: A study of two isolation techniques and two bacterial strains. *Turk J Immunol.* 2025;13(1):33-42.

## DOI

10.36519/tji.2025.574



This work is licensed under the Creative Commons Attribution-NonCommercial-Non-Derivatives 4.0 International License (CC BY-NC-ND 4.0).

## Introduction

Neutrophils are the most abundant cells, accounting for 50-70% of all white blood cells. They are critical in the immune response against bacterial and fungal pathogens. They are characterized by their ability to rapidly migrate to sites of infection or injury to eliminate invading pathogens (1). Neutrophils trigger microbicidal mechanisms by engulfing and digesting foreign particles via phagocytosis, secretion of proteolytic enzymes, and antimicrobial peptides (2, 3). Neutrophils also perform a process called respiratory oxidative burst activity, which leads to an increase in reactive oxygen species (ROS) and oxidative stress (3). ROS are composed of superoxide anions ( $O_2^-$ ) and hydrogen peroxide ( $H_2O_2$ ) and create a highly toxic environment for ingested microorganisms, allowing the bactericidal action of neutrophils (4). Therefore, ROS are ideal targets for investigating neutrophil function.

Defects in neutrophil activity, which can be quantitative or functional, result in weak defense against infection. The functional defect, in which reactive oxidative burst activity fails, is well described in chronic granulomatous disease (CGD) (5). In addition, neutrophil oxidative burst activity may be higher or lower compared to the healthy state during the progression of many diseases, under treatment with certain drugs, or in environmental exposure to certain agents (6-11). The measurement of neutrophil oxidative burst has historically been performed using different techniques to guide clinical practice and research on neutrophil function (12-16). One of these techniques is the widely used flow cytometric dihydrorhodamine (DHR) 123 assay (16). The DHR 123 assay is widely used in clinical immunology to evaluate phagocytic function, particularly for diagnosing CGD and, in some cases, glucose-6-phosphate dehydrogenase (G6PD) deficiency (17, 18). In CGD, the test helps detect nicotinamide adenine dinucleotide phosphate (NADPH) oxidase complex dysfunction by assessing neutrophil oxidative burst capacity. DHR 123 test can also distinguish between the genetic forms of CGD (19, 20). Pathogenic variants in the CYBB gene, which follows an X-linked inheritance pattern, are responsible for about 70% of cases, and carriers can be detected with the DHR 123 test (21). The remaining genetic causes follow an autosomal recessive inheritance pattern and involve mutations in NCF1, NCF2, CYBA, NCF4, or CYBC1 (20). While the DHR 123 test is primarily used for clinical diagnosis, the assay can also be adapted for research purposes to

study neutrophil responses to various stimuli and clinical conditions.

DHR 123, the reduced form of rhodamine 123, is a commonly utilized fluorescent mitochondrial dye (22). DHR 123 itself is non-fluorescent, but it easily enters most cells. It is oxidized by ROS to the fluorescent rhodamine 123, which accumulates in mitochondrial membranes and exhibits green fluorescence (23). Rhodamine 123 emits light at 488 nm, and a right shift in the histogram is observed in flow cytometric analysis due to strong fluorescence excitation (24). Measuring fluorescence intensity by flow cytometry helps us detect the oxidative burst activity of neutrophils (24). Several factors may influence DHR 123 flow cytometric neutrophil oxidative burst assay results, including sample preparation, neutrophil purification technique, storage time and conditions, DHR 123 concentration, type of stimulant used, pre-measurement incubation time, temperature and pH, laser power and filter settings of the flow cytometry (25-32). The validation and optimization of these factors for the experiment are crucial for obtaining the most accurate results.

Before conducting a DHR 123 neutrophil oxidative burst assay, every step must be considered and carefully planned, as neutrophils are sensitive to physical and chemical interventions in *in vitro* studies and have a short lifespan of 4-6 hours when out of circulation (33). At the beginning of the assay, good selection and application of the neutrophil isolation protocol during the sample preparation phase are essential to obtain a cell population with as high survival and purity without monocyte contamination as possible and to avoid de novo activation and false positive signals (34). For this purpose, "gradient separation", called the "Ficoll method", and "dextran sedimentation followed by the density gradient separation", called the "dextran method", are commonly used methods for neutrophil isolation. In addition, the chemical or biological agents used in the stimulation and pre-measurement incubation time are also important parameters affecting the test results' accuracy and sensitivity. Therefore, meticulously identifying and controlling these factors are essential for obtaining accurate and reliable results. Various methods for isolating and stimulating neutrophils have been proposed in the literature; however, there is no consensus on which isolation technique and stimulation type is ideal (27, 35-42). Furthermore, the pre-measurement incubation time, an important part of DHR 123 analysis, may

vary according to different protocols. It is important to optimize and standardize the DHR 123 neutrophil oxidative burst measurement technique between laboratories to achieve accurate results and correctly guide the clinic (43). Validation studies are important stepping stones to this path and help us assess the suitability of different protocols and analysis methods for their intended use (34). To validate an analytical procedure, prior knowledge, data, or experiments are evaluated. According to “ICH Harmonised Guideline: Validation of analytical procedures Q2 (R2)”, in the validation process, analytical procedure objectives should be set in the first step, performance characteristics should be clarified based on the objectives in the second step, and validation tests should be performed in the last step (44). Assay validation is a crucial process in which an assay is rigorously tested against specific criteria to confirm its suitability, reliability, and consistency for its intended use. It is essential for accurate research outputs and ensuring the accuracy of measurement results provided to healthcare providers.

In the framework explained above, in our study, we aimed to detect the performance characteristics of the assay results of the DHR 123 test of healthy human neutrophils isolated by two different techniques and stimulated with two different ATCC strains (ATCC 25923 - *Staphylococcus aureus* subsp. *aureus* Rosenbach and ATCC 25913 - methicillin-resistant *S. aureus* [MRSA]). The results obtained for this purpose were evaluated using validation parameters such as precision (including reproducibility), linearity and analytical sensitivity (limit of detection and limit of quantification). In addition, our research involved comparing two different separation methods, assessing stimulation with two distinct bacterial strains and evaluating incubation and measurement times.

## Materials and Methods

### Blood Samples

For this study, venous blood samples of five healthy volunteers were drawn into 10 mL syringes pre-filled with sodium heparin (40 IU/mL) and immediately subjected to neutrophil isolation. Voluntary informed consent forms were obtained before the utilization of blood samples from healthy individuals. The Yeditepe University Clinical Research Ethics Committee approved the study on October 18, 2024, with the decision number 2024-KAEK-21/1035.

### Bacterial Strains

In this study, two different bacterial strains, *S. aureus* subsp. *aureus* Rosenbach (ATCC® 25923™) and MRSA (ATCC® 25913™), were used to stimulate neutrophils in an oxidative burst assay. Both strains were kindly provided by the Medical Microbiology Department, Faculty of Medicine, Yeditepe University.

### Neutrophil Isolation

Two distinct methods were compared within the context of the study. For the “density gradient separation” method, which we called the “Ficoll method” in the context of the study, 3 mL whole blood samples were layered on the lymphocyte separation medium containing Ficoll (v/v: 1/1) (Lymphocyte Separation Medium, Density 1.077 g/mL, Cat-No: LSM-B; Capricorn Scientific, Germany) and incubated for 40 min at room temperature. Supernatants containing the polymorphonuclear cells were transferred to a clean flow cytometry tube for further analysis. For the “dextran sedimentation followed by the density gradient separation” method, which we called the “dextran method” in the context of the study, whole blood samples were mixed by inverting the tubes with dextran solution (3% in 0.9% NaCl, Cat-No: 31392; Sigma Aldrich, USA). After 40 min of incubation, the tubes were centrifuged at 300 g for 5 min, and the collected supernatants were layered on a lymphocyte separation medium containing Ficoll (v/v: 1/1). The tubes were further incubated for 40 min at room temperature, followed by centrifugation at 300 g for 5 min. The supernatants were discarded, and erythrocytes in the erythrocyte-granulocytes pellet were lysed with VersaLyse Lysing Solution (Cat-No: A09777; Beckman Coulter, USA). After 15 min of incubation, the tubes were centrifuged at 300 g for 5 min. The granulocyte pellets were suspended in Dulbecco’s phosphate-buffered saline (DPBS) and transferred to a clean flow cytometry tube for further analysis.

### Oxidative Burst Measurement in Neutrophils

For stimulating neutrophils, 50 µL of bacterial solution at a concentration of 1 MacFarland was added to 50 µL of neutrophil suspension in each tube. The total volume of the sample was then completed to 500 µL with DPBS, followed by the addition of DHR 123 to tubes (5 µM/test, Cat-No: sc-203027; Santa Cruz Biotechnology, USA). Tubes were incubated at room temperature under dark for 60 min. Mean fluorescence intensity (MFI) values were measured using a DxFLEX flow cytometry system (Beckman Coulter, USA) at 0, 10, 20, 30, and 60 min post-stimulation. The oxidative burst index was cal-

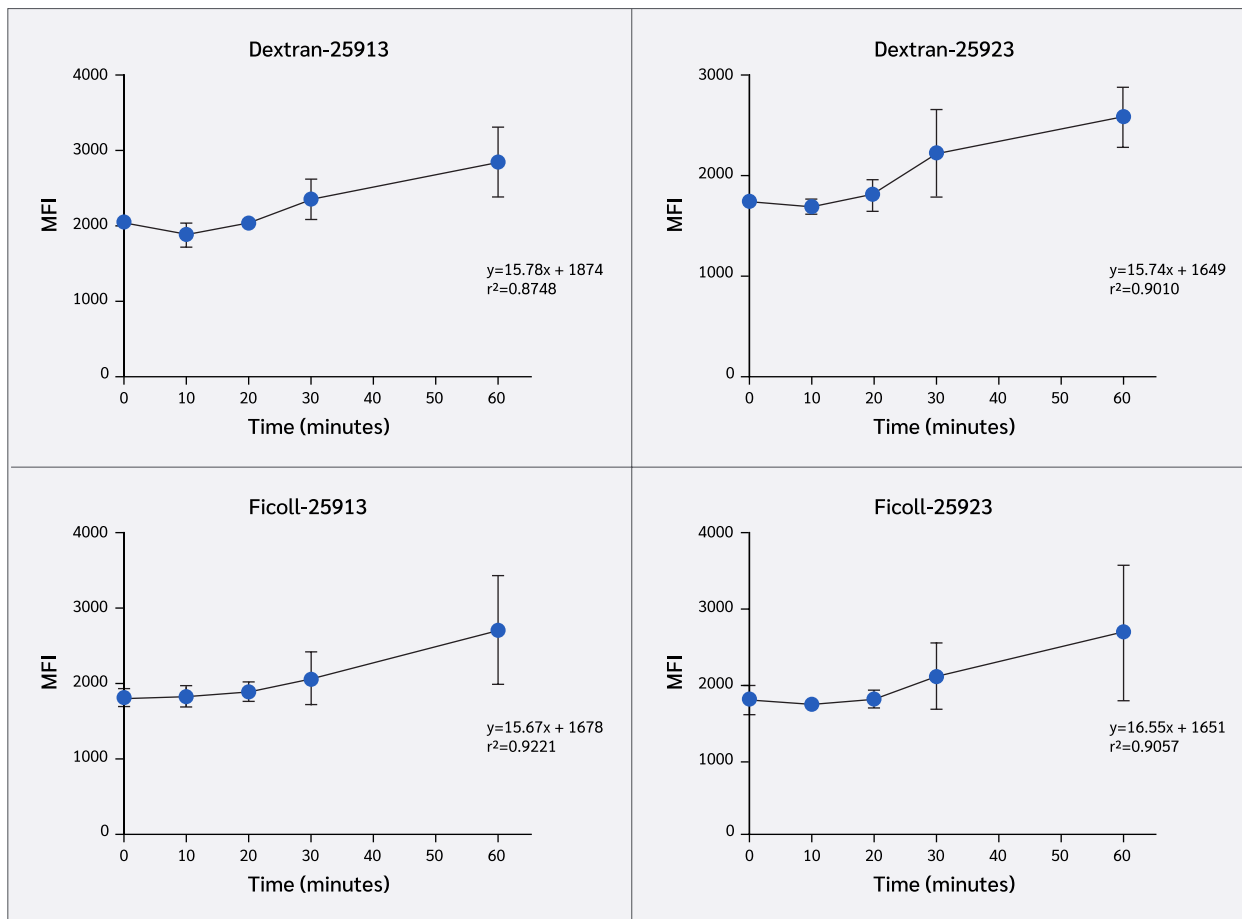


**Figure 1.** Comparative analysis of protocol performances. The coefficient of determination, denoted as  $r^2$ , is computed by squaring the coefficient of correlation ( $r$ ). This metric represents the percentage of variation in the dependent variable ( $y$ ) elucidated by the collective influence of all independent variables ( $x$ ). The higher  $r^2$  value, approaching 1, signifies enhanced linearity in the protocol. The Ficoll isolation method demonstrated the highest level of linearity in the MRSA-25913 protocol.

**MFI:** Mean Fluorescence Intensity.

culated by dividing the MFI measured at each relevant time point by the MFI at minute 0.

### Statistical Analysis and Validation of Analytical Methods

Statistical analyses were conducted using GraphPad Prism version 8 software (GraphPad Software, Boston, USA), incorporating 2-way ANOVA, Pearson correlation, and linear regression methods. The parameters assessed within the framework of this study comprised linearity, analytical sensitivity (including limit of detection [LOD] and limit of quantification [LOQ]), and precision. Two-way ANOVA was performed to compare the efficacy of separation methods and bacterial strains and to determine the optimal incubation duration. Linearity refers to the ability of the method to produce test results that

are directly proportional to analyte concentration. When comparing the performance of different protocols, a higher  $r^2$  value approaching 1 indicates greater protocol linearity. The terms “LOD” and “LOQ” mean the lowest concentration at which the analyte can be detected and reliably quantified, respectively. We calculated the detection and quantification limits using the standard deviation of the blank samples ( $\sigma$ ) and the slope of the standard curve ( $S$ ). However, the precision between laboratories could not be analyzed.

## Results

### Linearity

The Ficoll isolation method used ATCC 25913 MRSA

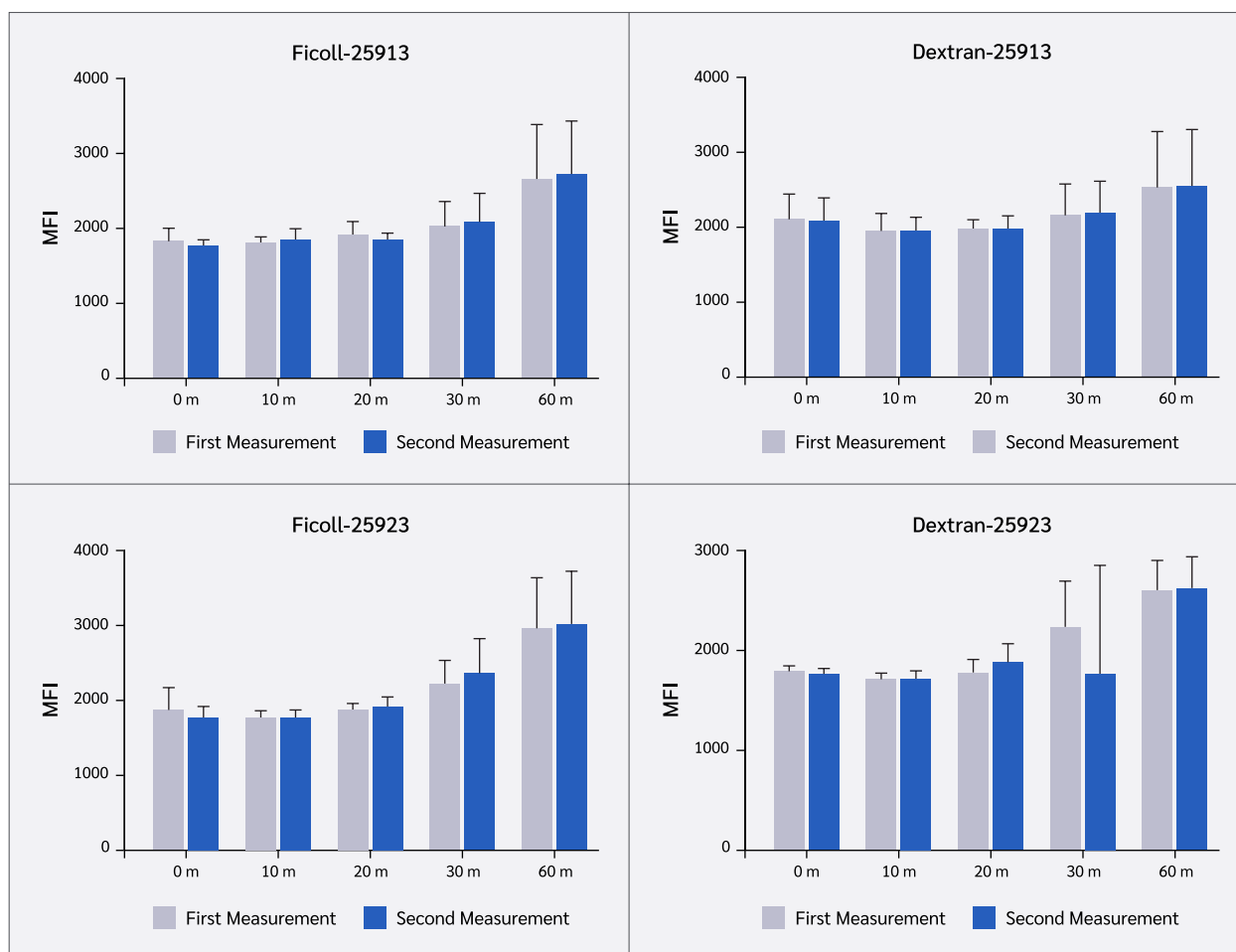


**Figure 2.** Evaluation of measurement repeatability. Measurement repeatability was assessed by conducting the study in duplicate, revealing no significant differences between the first and second measurements ( $p>0.05$ ).

MFI: Mean Fluorescence Intensity.

showed the highest linearity.

In this study, the Ficoll isolation method showed the highest linearity with the MRSA-25913 protocol (Figure 1).

### Precision

The first and second measurements did not show significant differences.

Precision refers to the degree of agreement between individual test results obtained under identical conditions. The study was conducted in duplicate, and no significant differences ( $p>0.05$ ) were observed between the first and second measurements (Figure 2, Table S1).

### Analytical Sensitivity

The dextran isolation method with strain ATCC 25923 had the lowest LOD and LOQ.

The detection limit was determined using the formula

**Table 1.** Comparative analysis of limit of detection (LOD) and limit of quantification (LOQ) across protocols.

| Protocol      | LOD (MFI) | LOQ (MFI) |
|---------------|-----------|-----------|
| Ficoll-25923  | 39.35     | 119.26    |
| Dextran-25923 | 5.51      | 16.68     |
| Ficoll-25913  | 21.66     | 65.64     |
| Dextran-25913 | 60.44     | 183.14    |

LOD and LOQ were determined using the standard deviation of blank samples ( $\sigma$ ) and slope of the standard curve ( $S$ ), with the formulas  $(3.3 \times \sigma) / S$  and  $(10 \times \sigma) / S$ , respectively. The dextran isolation method using bacteria coded 25923 yielded the lowest limits.

LOD: Limit of detection LOQ: Limit of quantification

MFI: Mean fluorescence intensity

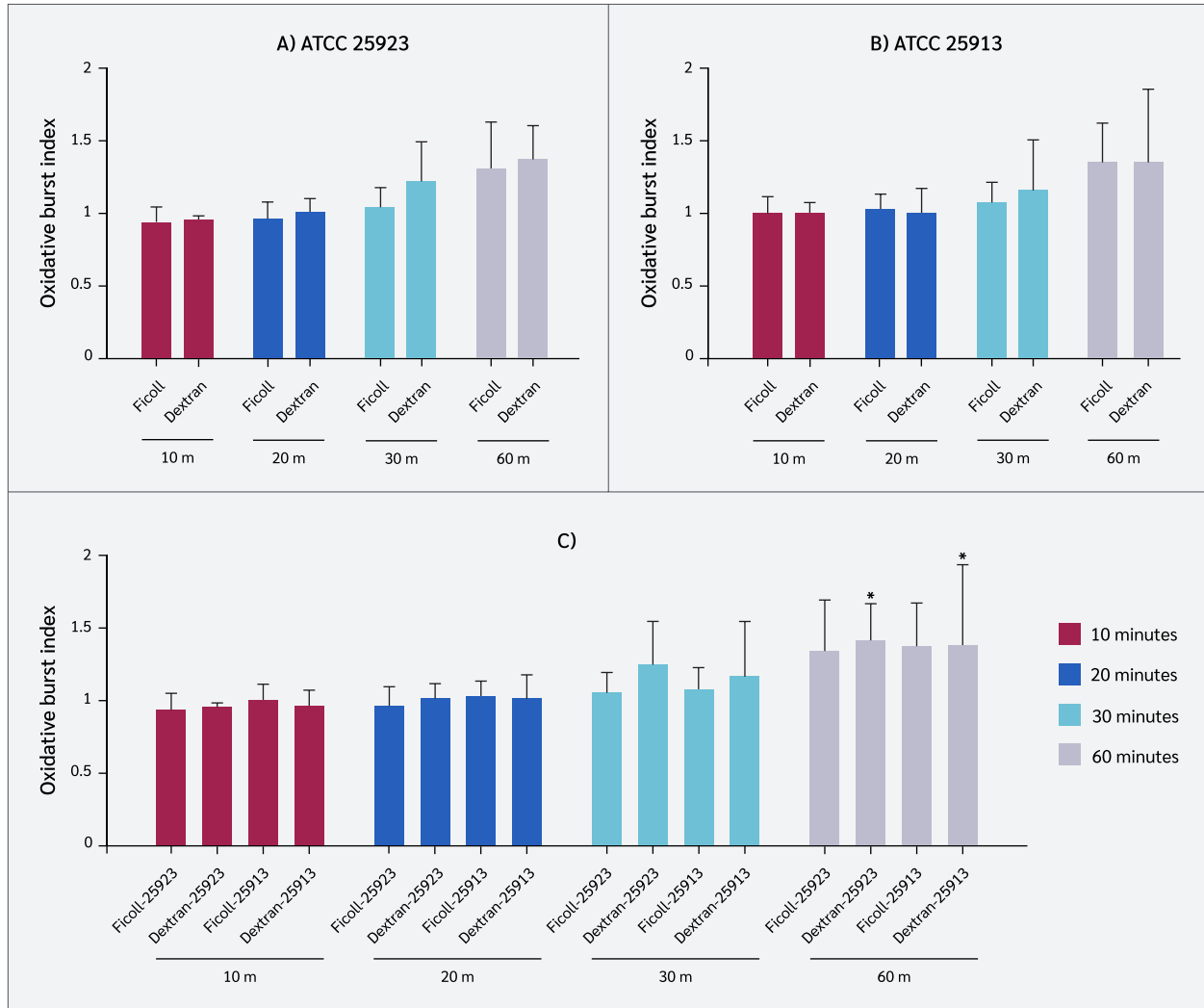


**Figure 3.** Comparative analysis among protocols and bacterial strains. No significant difference was observed among bacterial strains for stimulation between the periods ( $p > 0.05$ ) (A, B). However, a significant difference was identified between the 10th and 60th minutes for both bacterial strains in neutrophils isolated using the dextran method (Dextran-25913: 10 min. vs. 60 min.  $p = 0.04$ ; Dextran-25923 10 min. vs 60 min  $p = 0.02$ ) (C).

“limit of detection =  $(3.3 \times \sigma) / S$ ”, and the lowest detection limit was found using the dextran isolation method and bacteria coded 25923 (Table 1). The quantitative detection limit was calculated using the formula “limit of quantification =  $(10 \times \sigma) / S$ ”, and the lowest limit was obtained using the dextran isolation method with bacteria coded 25923 (Table 1).

### Comparison Among Bacteria Between Periods

In the neutrophil oxidative burst test, the index is obtained by dividing the average fluorescence value obtained in the relevant period by the average fluorescence value at minute zero. No significant difference

was detected between the bacteria between the periods ( $p > 0.05$ ) (Figure 3-A, Figure 3-B, Table S2).

### Pre-Measurement Incubation Time

**Neutrophils isolated using the dextran method showed a notable change in the oxidative burst index between the 10th and 60th minutes for both bacterial strains. However, measurements at 0 and 30 minutes are appropriate.**

A significant difference was found between the 10th and 60th minutes in both bacterial strains in neutrophils isolated by the dextran method (Dextran-25913: 10 min. vs. 60 min.  $p = 0.04$ ; Dextran-25923 10 min. vs 60 min  $p = 0.02$ ) (Figure 3-C). The literature has reported that

the dextran isolation method activates neutrophils, and the stability of DHR 123 in aqueous solutions needs to be investigated to confirm the specificity of the increase in DHR 123 signal in long-term incubation conditions (30, 45). Thus, the data suggests that measurements at 0 and 30 min are appropriate (Figure 1).

## Discussion

The production of ROS is integral to the antimicrobial and physiological functions of phagocytes (1). The precise measurement of this activity is essential, prompting the development of various techniques over the years, each with distinct advantages and limitations (13, 14, 16, 22, 24, 27). Among these, flow cytometric assays have been established to precisely detect oxidative burst activity, traditionally employing nitroblue tetrazolium (NBT) and DHR 123 assays. Emmendörffer et al. (22), in their validation study, identified the DHR 123 method as a highly sensitive alternative to the clinically utilized NBT test for diagnosing chronic granulomatous disease (46). Subsequent studies have established the DHR 123 method as a widely used probe (34, 36, 43). In this study, we used a DHR probe to measure oxidative burst activity.

Purifying human neutrophils for *in vitro* studies is challenging because of their susceptibility to activation during *ex vivo* manipulations (36). Although the DHR 123 test is commonly performed on whole blood in clinical settings, we chose to use isolated neutrophils to ensure a more standardized evaluation of bacterial stimulation effects. This approach minimizes background noise from other blood components, allows more precise gating, and provides better control over the experimental conditions, particularly in assessing bacterial stimulation effects on oxidative burst responses. Quach and Ferrante (45) conducted a comparative analysis of neutrophils purified using the classical 2-step method (dextran sedimentation followed by low-density Ficoll-Hypaque) and the 1-step high-density Ficoll-Hypaque gradient centrifugation. Their findings demonstrated that the 2-step method led to increased CD11b expression, CD62L shedding, adhesion, decreased random migration and chemotaxis, and increased baseline oxidative burst activity. Notably, this effect was not confined to dextran, as Ficoll used for erythrocyte sedimentation also replicated the observed elevation in neutrophil adherence (45). In our study, emphasis was placed on the relative MFI values concerning the zero time point to mitigate the impact

of baseline activation on measurement outcomes. DHR 123 measurements were performed at five separate time points following neutrophil stimulation. Additionally, two distinct isolation procedures were employed, and the purified neutrophils were segregated into groups stimulated by two different bacterial strains. This approach allowed us to assess the relative efficacy of the bacterial strains and determine the isolation technique that yielded optimal results under diverse stimulation conditions. Based on the results obtained by validation methods, the superiority of the dextran method over the Ficoll method with low LOD and LOQ was demonstrated.

Smith and Weidemann (47) examined the oxidative burst in human neutrophils stimulated *in vitro* with opsonized zymosan or phorbol myristate acetate (PMA) at the single-cell level using dichlorofluorescein diacetate and DHR 123 as oxidative probes. DHR was the most sensitive probe, with PMA being the stronger stimulus (47). In the diagnosis of CGD, patients with a stimulation index (SI) below 1.5 are considered to have X-linked CYBB deficiency (48). In our study, SI values in healthy controls were lower than expected compared to previously reported values in studies using PMA stimulation (48). This discrepancy is likely due to the choice of stimulation method, as PMA is a potent activator of the NADPH oxidase complex, leading to a strong oxidative burst response. In contrast, bacterial stimulation may elicit a more variable or lower oxidative response, depending on the bacterial component and strain used, opsonization status, and experimental conditions. Smits et al. (49) suggested that a 20-minute incubation period following *Escherichia coli* stimulation is optimal for testing polymorphonuclear neutrophils (PMN) activity in bovine blood (49). In our study, we found that measurements taken at both the 0th and 30th minutes are adequate and optimal for isolated neutrophils stimulated by either of the two bacterial strains: ATCC 25923 (*S. aureus* subsp. *aureus* Rosenbach) and ATCC 25913 (MRSA). Both ATCC strains are suitable for use, but ATCC 25923 may be preferred because the dextran isolation method with strain 25923 has the lowest LOD and LOQ.

Proper sample preparation, neutrophil purification technique, storage time and conditions, DHR 123 concentration, type of stimulant used, pre-measurement incubation time, temperature and pH, laser power and filter settings of the flow cytometry, and optimization of all these factors for the specific experiment are crucial to obtain the most accurate results. Within the existing

literature, investigations pertaining to neutrophil isolation or stimulation methods commonly emphasize the parameters as viability, purity, cellular yield, pre-activation states of cells, and the expression levels of immunological receptors (26, 27, 29, 34, 37, 40, 41, 44-46). As is different from existing literature, our study focused on the validation parameters, including linearity, analytical sensitivity (LOD, LOQ), and precision.

Recently, Krémer et al. (50) compared different neutrophil isolation methods in terms of their efficacy and impact on neutrophil physiology, and the authors revealed that negative immunomagnetic selection yielded neutrophils resembling those in whole blood in terms of their functions. However, this method is more costly than the methods evaluated in our study. Herein, although the dextran method with 30 min stimulation provided similar data compared to the Ficoll method with 60 min stimulation, it is widely accepted that the dextran method yields high-purity neutrophils (40, 45). Additionally, prolonged incubation with DHR 123 may result in non-specific signals (51). Shorter incubation durations with DHR 123 may increase assay sensitivity, but this should be confirmed in future studies.

### Study Limitations

The main limitations of this study were the use of only two standard bacterial strains, the limited number of healthy samples, and the use of a single measurement method and device. Evaluating more bacterial strains for clinical trials, increasing the sample size, and comparing the DHR 123 test with other tests based on fluorescence emission detection, such as fluorimetry, would increase

the accuracy and reliability of the study. Additionally, analyzing the inter-instrument validity of the test by measuring the samples of the same individuals in another flow cytometry device is recommended. Future studies should address these limitations and compare data from a more comprehensive sample.

## Conclusion

Our study revealed that the dextran isolation method was optimal, given its lower LOD and LOQ. ATCC 25923-*S. aureus* subsp. *aureus* Rosenbach was the preferred strain because of its lowest LOD and LOQ using this method, whereas ATCC 25913 MRSA remained suitable. Furthermore, our data suggested that measuring at 0 and 30 min was appropriate.

Our study provided a detailed overview of the DHR 123 flow cytometric assay for measuring neutrophil oxidative burst, the critical role of isolation methodologies, stimulation protocols, and temporal considerations in ensuring the accuracy of the results. By addressing key technical questions, our research significantly contributes to the ongoing efforts to identify ideal methods for studying neutrophil oxidative bursts, benefiting both research and clinical applications. In future studies, exploring alternative methods to isolate neutrophils, examining additional bacterial strains, testing different stimulants, conducting more extensive validation studies, and exploring potential diagnostic applications will further enhance our understanding and application of these assays.

**Ethics Committee Approval:** The study was approved by the Yeditepe University Clinical Research Ethics Committee on October 18, 2024, with the decision number 2024-KAEK-21/1035.

**Informed Consent:** Informed consent was obtained from all participants.

**Peer-review:** : Externally peer-reviewed

**Author Contributions:** Concept – CP, BA, AOG, GYD; Design – CP, BA, AOG, GYD; Supervision – AOG, GYD; Fundings – GYD; Materials – CP, BA, AOG, GYD; Data Collection and/

or Processing – CP, BA, AOG, GYD; Analysis and/or Interpretation – CP, BA, AOG, GYD; Literature Review – CP, BA, AOG, GYD; Writer – CP, BA, AOG, GYD; Critical Reviews –CP, BA, AOG, GYD.

**Conflict of Interest:** The authors declare no conflict of interest.




**Financial Disclosure:** All the materials required for the study were provided by the Flow Cytometry Laboratory, Immunology Department, Faculty of Medicine, Yeditepe University.

## References

- 1 Humbert JR. Neutrophil physiology and pathology. Introduction. *Semin Hematol*. 1975;12(1):3-5.
- 2 Del Fabbro M, Francetti L, Pizzoni L, Rozza R, Weinstein RL. [Neutrophil physiology: role and mechanism of action in the immune response at gingival level]. *Minerva Stomatol*. 2000;49(5):227-48. Italian.
- 3 Freebern WJ, Bigwarfe TJ, Price KD, Haggerty HG. Methods: implementation of *in vitro* and *ex vivo* phagocytosis and respiratory burst function assessments in safety testing. *J Immunotoxicol*. 2013;10(1):106-17. [\[CrossRef\]](#)
- 4 Kampen AH, Tollersrud T, Lund A. Flow cytometric measurement of neutrophil respiratory burst in whole bovine blood using live *Staphylococcus aureus*. *J Immunol Methods*. 2004;289(1-2):47-55. Erratum in: *J Immunol Methods*. 2004;294(1-2):211. [\[CrossRef\]](#)
- 5 Volpp BD, Nauseef WM, Clark RA. Two cytosolic neutrophil oxidase components absent in autosomal chronic granulomatous disease. *Science*. 1988;242(4883):1295-7. [\[CrossRef\]](#)
- 6 Toller-Kawahisa JE, Canicoba NC, Venancio VP, Kawahisa R, Antunes LM, Cunha TM, et al. Systemic lupus erythematosus onset in lupus-prone B6.MRL/lpr mice is influenced by weight gain and is preceded by an increase in neutrophil oxidative burst activity. *Free Radic Biol Med*. 2015;86:362-73. [\[CrossRef\]](#)
- 7 Ramasamy R, Maqbool M, Mohamed AL, Noah RM. Elevated neutrophil respiratory burst activity in essential hypertensive patients. *Cell Immunol*. 2010;263(2):230-4. [\[CrossRef\]](#)
- 8 Parodi JC, Ferreira LM, Fornari MC, Berardi VE, Diez RA. Neutrophil respiratory burst activity and pro- and anti-inflammatory cytokines in AAA surgery: conventional versus endoluminal treatment. *J Endovasc Ther*. 2001;8(2):114-24. [\[CrossRef\]](#)
- 9 Lyapina M, Zhelezova G, Petrova E, Boev M. Flow cytometric determination of neutrophil respiratory burst activity in workers exposed to formaldehyde. *Int Arch Occup Environ Health*. 2004;77(5):335-40. [\[CrossRef\]](#)
- 10 Kojima K, Inoue Y, Katayama Y, Kataoka M, Sunami K, Fukuda S, et al. Improvement with disodium cromoglycate of neutrophil phagocytosis and respiratory burst activity in a patient with hyperimmunoglobulin E syndrome. *Allergy*. 1998;53(11):1101-3. [\[CrossRef\]](#)
- 11 Houston N, Stewart N, Smith DS, Bell SC, Champion AC, Reid DW. Sputum neutrophils in cystic fibrosis patients display a reduced respiratory burst. *J Cyst Fibros*. 2013;12(4):352-62. [\[CrossRef\]](#)
- 12 Yusof N, Yasin NM, Yousuf R, Wahab AA, Aziz SA. Comparison of neutrophil respiratory oxidative burst activity between flow cytometry using dihydrorhodamine (DHR) 123 and conventional nitroblue tetrazolium test (NBT). *Bangladesh Journal of Medical Science*. 2022;21(3):626-33. [\[CrossRef\]](#)
- 13 Wardle EN. Assessment of neutrophil function--I. *Postgrad Med J*. 1986;62(733):997-1000. [\[CrossRef\]](#)
- 14 Wardle EN. Assessment of neutrophil function--II. Laboratory tests of neutrophil function. *Postgrad Med J*. 1986;62(734):1089-92. [\[CrossRef\]](#)
- 15 Lord R. Assessment of neutrophil function: an introduction. *Med Lab Sci*. 1989;46(4):347-56.
- 16 Rothe G, Oser A, Valet G. Dihydrorhodamine 123: a new flow cytometric indicator for respiratory burst activity in neutrophil granulocytes. *Naturwissenschaften*. 1988;75(7):354-5. [\[CrossRef\]](#)
- 17 Siler U, Romao S, Tejera E, Pastukhov O, Kuzmenko E, Valencia RG, et al. Severe glucose-6-phosphate dehydrogenase deficiency leads to susceptibility to infection and absent NETosis. *J Allergy Clin Immunol*. 2017;139(1):212-19.e3. [\[CrossRef\]](#)
- 18 Baris HE, Ogulur I, Akcam B, Kiykim A, Karagoz D, Saraymen B, et al. Diagnostic modalities based on flow cytometry for chronic granulomatous disease: A multicenter study in a well-defined cohort. *J Allergy Clin Immunol Pract*. 2020;8(10):3525-34.e1. [\[CrossRef\]](#)
- 19 Vowells SJ, Fleisher TA, Sekhsaria S, Alling DW, Maguire TE, Malech HL. Genotype-dependent variability in flow cytometric evaluation of reduced nicotinamide adenine dinucleotide phosphate oxidase function in patients with chronic granulomatous disease. *J Pediatr*. 1996;128(1):104-7. [\[CrossRef\]](#)
- 20 Aygun D, Koker MY, Nepesov S, Koker N, van Leeuwen K, de Boer M, et al. Genetic characteristics, infectious, and noninfectious manifestations of 32 patients with chronic granulomatous disease. *Int Arch Allergy Immunol*. 2020;181(7):540-50. [\[CrossRef\]](#)
- 21 Arnadottir GA, Norddahl GL, Gudmundsdottir S, Agustsdottir AB, Sigurdsson S, Jensson BO, et al. A homozygous loss-of-function mutation leading to CYBC1 deficiency causes chronic granulomatous disease. *Nat Commun*. 2018;9(1):4447. [\[CrossRef\]](#)
- 22 Emmendorffer A, Hecht M, Lohmann-Matthes ML, Roesler J. A fast and easy method to determine the production of reactive oxygen intermediates by human and murine phagocytes using dihydrorhodamine 123. *J Immunol Methods*. 1990;131(2):269-75. [\[CrossRef\]](#)
- 23 Köker MY. The evaluation of dihydrorhodamine 123 assay in chronic granulomatous disease. *Pediatr Infect Dis J*. 2010;29(2):190-1; author reply 191. [\[CrossRef\]](#)
- 24 Richardson MP, Ayliffe MJ, Helbert M, Davies EG. A simple flow cytometry assay using dihydrorhodamine for the measurement of the neutrophil respiratory burst in whole blood: comparison with the quantitative nitrobluetetrazolium test. *J Immunol Methods*. 1998;219(1-2):187-93. [\[CrossRef\]](#)
- 25 Krabbe J, Beilmann V, Alamzad-Krabbe H, Böll S, Seifert A, Ruske N, et al. Blood collection technique, anticoagulants and storing temperature have minor effects on the isolation of polymorphonuclear neutrophils. *Sci Rep*. 2020;10(1):14646. [\[CrossRef\]](#)
- 26 Mosca T, Forte WC. Comparative efficiency and impact on the activity of blood neutrophils isolated by Percoll, Ficoll

- and spontaneous sedimentation methods. *Immunol Invest.* 2016;45(1):29-37. [\[CrossRef\]](#)
- 27 Marchi LF, Sesti-Costa R, Chedraoui-Silva S, Mantovani B. Comparison of four methods for the isolation of murine blood neutrophils with respect to the release of reactive oxygen and nitrogen species and the expression of immunological receptors. *Comp Clin Pathol.* 2014;23:1469-76. [\[CrossRef\]](#)
  - 28 Quach A, Glowik S, Putty T, Ferrante A. Delayed blood processing leads to rapid deterioration in the measurement of the neutrophil respiratory burst by the dihydrorhodamine-123 reduction assay. *Cytometry B Clin Cytom.* 2019;96(5):389-96. [\[CrossRef\]](#)
  - 29 Zahler S, Kowalski C, Brosig A, Kupatt C, Becker BF, Gerlach E. The function of neutrophils isolated by a magnetic antibody cell separation technique is not altered in comparison to a density gradient centrifugation method. *J Immunol Methods.* 1997;200(1-2):173-9. [\[CrossRef\]](#)
  - 30 van Pelt LJ, van Zwieten R, Weening RS, Roos D, Verhoeven AJ, Bolscher BG. Limitations on the use of dihydrorhodamine 123 for flow cytometric analysis of the neutrophil respiratory burst. *J Immunol Methods.* 1996;191(2):187-96. [\[CrossRef\]](#)
  - 31 Haslett C, Guthrie LA, Kopaniak MM, Johnston RB Jr, Henson PM. Modulation of multiple neutrophil functions by preparative methods or trace concentrations of bacterial lipopolysaccharide. *Am J Pathol.* 1985;119(1):101-10.
  - 32 Djiadeu P, Azzouz D, Khan MA, Kotra LP, Sweezey N, Palaniyar N. Ultraviolet irradiation increases green fluorescence of dihydrorhodamine (DHR) 123: false-positive results for reactive oxygen species generation. *Pharmacol Res Perspect.* 2017;5(2):e00303. [\[CrossRef\]](#)
  - 33 Mahendran AJ, Gupta N. Dihydrorhodamine test from a clinical point of view. *Chest.* 2022;161(5):e327. [\[CrossRef\]](#)
  - 34 Pioch J, Blomgran R. Optimized flow cytometry protocol for dihydrorhodamine 123-based detection of reactive oxygen species in leukocyte subpopulations in whole blood. *J Immunol Methods.* 2022;507:113308. [\[CrossRef\]](#)
  - 35 Russo-Carbolante EMS, Azzolini A, Polizello A, Lucisano-Valim YM. Comparative study of four isolation procedures to obtain rat neutrophils. *Comp Clin Path.* 2002;11(2):71-6. [\[CrossRef\]](#)
  - 36 Kuhns DB, Priel DAL, Chu J, Zarembler KA. Isolation and functional analysis of human neutrophils. *Curr Protoc Immunol.* 2015;111:7.23.1-16. [\[CrossRef\]](#)
  - 37 Soltys J, Swain SD, Sipes KM, Nelson LK, Hanson AJ, Kantele JM, et al. Isolation of bovine neutrophils with biomagnetic beads: comparison with standard Percoll density gradient isolation methods. *J Immunol Methods.* 1999;226(1-2):71-84. [\[CrossRef\]](#)
  - 38 Kremserova S, Nauseef WM. Isolation of human neutrophils from venous blood. *Methods Mol Biol.* 2020;2087:33-42. [\[CrossRef\]](#)
  - 39 Böyum A. Isolation of mononuclear cells and granulocytes from human blood. Isolation of mononuclear cells by one centrifugation, and of granulocytes by combining centrifugation and sedimentation at 1 g. *Scand J Clin Lab Invest Suppl.* 1968;97:77-89.
  - 40 Avcı E, Akkaya-Ulum Y, Yoyen-Ermis D, Esendagli G, Balci-Peynircioğlu B. A method for high-purity isolation of neutrophil granulocytes for functional cell migration assays. *Turkish Journal of Biochemistry.* 2019;44(6):810-21. [\[CrossRef\]](#)
  - 41 Eggleton P, Gargan R, Fisher D. Rapid method for the isolation of neutrophils in high yield without the use of dextran or density gradient polymers. *J Immunol Methods.* 1989;121(1):105-13. [\[CrossRef\]](#)
  - 42 Kalmar JR, Arnold RR, Warbington ML, Gardner MK. Superior leukocyte separation with a discontinuous one-step Ficoll-Hypaque gradient for the isolation of human neutrophils. *J Immunol Methods.* 1988;110(2):275-81. [\[CrossRef\]](#)
  - 43 Çiçekkökü D, Ögüller İ, Karakoç-Aydiner E, Barış S, Kıyıkım A, Özen A, et al. Oxidative burst with dihydrorhodamine test: Reference values in healthy controls. *Turk J Immunol.* 2015;3(2):49-53. [\[CrossRef\]](#)
  - 44 ICH Harmonised Guideline: Validation of analytical procedures Q2 (R2) [Internet]. Amsterdam: European Medicines Agency (EMA); March 31, 2022. [cited December 01, 2024]. Available from: [https://www.ema.europa.eu/en/documents/scientific-guideline/ich-guideline-q2r2-validation-analytical-procedures-step-2b\\_en.pdf](https://www.ema.europa.eu/en/documents/scientific-guideline/ich-guideline-q2r2-validation-analytical-procedures-step-2b_en.pdf)
  - 45 Quach A, Ferrante A. The Application of dextran sedimentation as an initial step in neutrophil purification promotes their stimulation, due to the presence of monocytes. *J Immunol Res.* 2017;2017:1254792. [\[CrossRef\]](#)
  - 46 Filiz S, Kocacı Uygün DF, Yeğın O. Chronic granulomatous disease. *Turk J Immunol.* 2013;1(1):22-31. [\[CrossRef\]](#)
  - 47 Smith JA, Weidemann MJ. Further characterization of the neutrophil oxidative burst by flow cytometry. *J Immunol Methods.* 1993;162(2):261-8. [\[CrossRef\]](#)
  - 48 Köker MY, Camcıoğlu Y, van Leeuwen K, Kılıç SŞ, Barlan I, Yılmaz M, et al. Clinical, functional, and genetic characterization of chronic granulomatous disease in 89 Turkish patients. *J Allergy Clin Immunol.* 2013;132(5):1156-63.e5. [\[CrossRef\]](#)
  - 49 Smits E, Burvenich C, Heyneman R. Simultaneous flow cytometric measurement of phagocytotic and oxidative burst activity of polymorphonuclear leukocytes in whole bovine blood. *Vet Immunol Immunopathol.* 1997;56(3-4):259-69. [\[CrossRef\]](#)
  - 50 Krémer V, Godon O, Bruhns P, Jönsson F, de Chaisemartin L. Isolation methods determine human neutrophil responses after stimulation. *Front Immunol.* 2023;14:1301183. [\[CrossRef\]](#)
  - 51 Bylund J, Brown KL, Movitz C, Dahlgren C, Karlsson A. Intracellular generation of superoxide by the phagocyte NADPH oxidase: how, where, and what for? *Free Radic Biol Med.* 2010;49(12):1834-45. [\[CrossRef\]](#)

# Fc Receptor-Like 3 Gene Polymorphism and the Risk of Lupus Nephritis in Systemic Lupus Erythematosus Patients

Amany Gamal Thabit<sup>1</sup>, Michael Nazmi Agban<sup>1</sup> , Rania Mohamed Gamal<sup>2</sup> , Ahmed Mahmoud Rayan<sup>3</sup>, Mona Sallam Embarek Mohamed<sup>1</sup> 

<sup>1</sup>Assiut University Faculty of Medicine, Department of Medical Microbiology and Immunology, Assiut, Egypt; <sup>2</sup>Assiut University Faculty of Medicine, Department of Rheumatology and Rehabilitation, Assiut, Egypt; <sup>3</sup>Pharmacist, Minya University Hospital, 61519 Minya, Egypt

## Abstract

**Objective:** Fc receptor-like 3 (*FCRL3*) is a novel autoimmune activator with an immunoregulatory role in several autoimmune disorders, including systemic lupus erythematosus (SLE). We aimed to assess *FCRL3* gene polymorphism in the risk of nephritis and different clinical and laboratory parameters in Egyptian SLE patients.

**Materials and Methods:** The study categorized SLE patients into two groups with and without lupus nephritis (LN) and compared them with healthy controls. SLE patients underwent clinical and laboratory assessment. Single nucleotide polymorphism of the *FCRL3* gene was done at positions –169A/G rs7528684 and –110C/T rs11264799.

**Results:** The study included 47 SLE patients divided into patients with and without lupus nephritis (LN) and 40 healthy controls. SLE patients with LN had higher disease activity, were positive for anti-DNA, and had disturbed kidney and liver functions, disturbed hematological parameters, higher inflammatory markers, and lower immunological markers (complement 3 and 4) levels than patients without nephritis. Statistical analysis showed no deviation of genotype frequencies of rs7528648 and rs11264799 of *FCRL3* gene from Hardy–Weinberg equilibrium, neither in SLE patients compared to controls nor in SLE patients with nephritis compared to patients without nephritis.

**Conclusion:** For the rs7528648 single nucleotide polymorphism (SNP), the C allele and the CC genotype were non-significantly higher in SLE patients than in patients without nephritis. The rs11264799 SNP showed that the frequency of the G allele and the GG genotype was non-significantly higher in LN patients, while the frequency of the A allele was higher among patients without nephritis.

**Keywords:** *FCRL3*, lupus nephritis, rs7528684, rs11264799, SLE

## Correspondence

Mona Sallam Embarek Mohamed

## E-mail

monaembarek@aun.edu.eg

## Received

December 28, 2024

## Accepted

April 14, 2025

## Published

April 29, 2025

## Suggested Citation

Thabit AG, Agban MN, Gamal RM, Rayan AM, Mohamed MSE. Fc receptor-like 3 gene polymorphism and the risk of lupus nephritis in systemic lupus erythematosus patients. *Turk J Immunol.* 2025;13(1):43-53.

## DOI

10.36519/tji.2025.569



This work is licensed under the Creative Commons Attribution-NonCommercial-Non-Derivatives 4.0 International License (CC BY-NC-ND 4.0).

## Introduction

Systemic lupus erythematosus (SLE) is a chronic autoimmune disease that affects multiple organs. Its prevalence is higher in women, but its course is more critical in men with bad prognosis expeditious (1). The exact etiology of SLE is unclear. However, an interaction that includes genetic and environmental issues triggers the immune system to produce autoantibodies and cytokine dysregulation, resulting in tissue injury (2). SLE is distinguished by the presence of antinuclear and anticytoplasmic antibodies, and other autoantibodies can be found as well (3).

Lupus nephritis (LN) is a severe complication of SLE. Most SLE patients develop kidney affection during the disease course (4). Fc receptor-like (*FCRL*) proteins are groups of six molecules (*FCRL1-FCRL6*) that belong to the immunoglobulin superfamily (5). *FCRL3* is particularly highly valued because it is a significant marker for B lymphocytes and responsible for the maturation and reaction of these cells (6). Other cells that express *FCRL3* include natural killer (NK) and regulatory T (Treg) cells (7). Single nucleotide polymorphism (SNP) in the *FCRL3* has been identified in previous reports (polymorphisms at rs7528684 and rs11264799), and it is associated with the occurrence of autoimmune diseases like rheumatoid arthritis, Behçet's disease, and multiple sclerosis (MS) (8).

Previous data had found an association between the SNP of rs7528684 of the *FCRL3* gene and the occurrence of SLE in Japan (9). The expression of the *FCRL3* gene on various immune cells could be affected by SNP of the gene, which may lead to modulation of the B and T cell activation and function and alter the signaling pathways in these cells (10). Reports about SNP of rs7528684 and rs11264799 in SLE and LN are globally few and lacking for Egyptian SLE patients. Therefore, in this study, we aimed to assess the potential association of common polymorphism of *FCRL3* gene in SLE Egyptian patients with and without nephritis and to correlate *FCRL3* gene polymorphism with different clinical and laboratory data.

## Materials and Methods

### Study Design and Participants

This hospital-based case-control study included patients with SLE who met the criteria approved by the European League Against Rheumatism (EULAR) Executive Committee and the Board of the American College of Rheuma-

tology (ACR). They were divided into two groups (based on the results of histopathological examination of renal biopsy): a group of SLE patients without LN and another group included SLE patients with LN. Controls comprised healthy age- and sex-matched individuals. Patients aged <18 years old or >60 years old, coexistence of other autoimmune diseases, viral infections (including viral hepatitis B or C), malignancies, and pregnant or lactating females were excluded.

The Institutional Review Board of the Faculty of Medicine, Assiut University, approved the study with the number 04-2023-200089. Written consent was obtained from all participants. Each participant was coded by number to ensure confidentiality.

### Clinical and Laboratory Assessment

Controls and SLE patients underwent a full medical history and clinical assessment, including chest, cardiovascular, gastrointestinal, eye, genitourinary, neuropsychiatric, and associated comorbidities. Additionally, they underwent an assessment of disease activity (using the SLE disease activity index; SLEDAI) and disease-induced damage (using the SLEDAI-2K index). Laboratory investigations included complete blood count, liver function tests, kidney function tests, complete urine analysis, C-reactive protein (CRP) levels, erythrocyte sedimentation rate (ESR), antinuclear antibody (ANA), anti-double stranded DNA (anti-ds-DNA), complement 3 (C3), and complement 4 (C4). Renal biopsy for histopathological grading of LN was collected from SLE patients suspected to have LN.

### Determination of *FCRL3* Gene Polymorphism (SNP Genotyping)

For the SNP genotyping assay of *FCRL3*, 3 mL of peripheral venous blood was collected from SLE patients and controls in labeled EDTA tubes. Genomic DNA (gDNA) extraction from whole blood was done using QIAamp DNA Blood Mini Kit (Qiagen N.V., Germany; Catalog no: 51104) according to the manufacturer's instructions. NanoDrop® Spectrophotometer (*ThermoFisher Scientific, USA*) was used to quantify and assess the purity of DNA in samples. Determination of *FCRL3* gene polymorphism of two studied SNPs was performed using TaqMan™ SNP Genotyping Assay (*ThermoFisher Scientific, USA*) at positions -169A/G rs7528684 (primer sequences were F:5'GAAAATAATACAAATGTACAGATTA3' and R:5'GGCTTTAAAAACGGTGGTAC3') and -110C/T rs11264799 (primer sequences were F:5'CTCAATCCGGTAGTGATACA3' and R:5'CTCATAAACAACTTATGTGA-GA3') as recommended previously (11). The total reaction

volume of the allele discrimination reaction mix was 20  $\mu$ L. The reaction mix was composed of 10  $\mu$ L Applied Biosystems™ TaqMan™ Universal PCR Master Mix (ThermoFisher Scientific, USA), 0.5  $\mu$ L of 40XSNP genotyping assay, and 9.5  $\mu$ L of 20 ng purified gDNA diluted in nuclease-free water.

The reaction was conducted on a 7500 Real-Time PCR system (ThermoFisher Scientific, USA). The following protocol was used: denaturation at 95°C for 10 min, followed by 40 cycles of denaturation at 92°C for 15 seconds and annealing and extension at 60°C for 1 min. The plate's post-PCR fluorescence measurement was evaluated by real-time PCR software (ThermoFisher Scientific, USA).

### Statistical Analysis

All statistical calculations were done using SPSS version 22. Data were statistically described as mean  $\pm$  standard deviation, or median and range as appropriate, frequencies (number of cases), and relative frequencies (percentages) when appropriate. Student-t test, Mann-Whitney U test, and chi-square test were used. Significance was considered when the *p*-value was  $\leq$  0.05.

## Results

### Demographic, Clinical Data, And Treatment Regimens of SLE Patients

The study included 47 SLE patients and 40 healthy controls. SLE patients were 46 (98%) females and one (2%) male and aged  $33.2 \pm 7.9$  years (childbearing age). The mean age at onset of SLE disease in patients was  $27.6 \pm 7.6$  (range 18–40.5) years, with a mean disease duration of  $5.3 \pm 4.5$  (range 0.25–21) years. Healthy controls were age- and sex-matched with SLE patients. Histopathological examination of renal biopsies of SLE patients revealed that 22 (47%) patients had no LN; on the other hand, 25 (53%) patients had LN categorized as class 4 in 24 patients and class 5 in one patient. The mean age of LN patients was significantly younger than those without nephritis ( $30.3 \pm 6.9$  years vs.  $36.4 \pm 8$  years; *p*=0.008). The mean disease duration in LN patients was significantly shorter than patients without nephritis ( $4.4 \pm 2.7$  years vs  $6.3 \pm 5.85$  years; *p*=0.034). Body mass index (BMI) was lower for LN patients than patients without nephritis ( $24.7 \pm 2.9$  vs.  $25.2 \pm 4.5$ ), but differences were not significant (*p*=0.161). Clinical manifestations of LN patients showed that they significantly had frothy urine and suffered nephrotic syndrome and nasal ulcers more

than patients without nephritis. Clinical data, including chest, cardiovascular, gastrointestinal, and associated comorbidities, did not show significant differences between the groups. Arthralgia and arthritis affected LN patients more than others, but such differences did not reach significant levels (Table 1). Treatment medication for SLE patients is shown in Table 2. Significantly, a higher number of LN patients were treated with methotrexate, azathioprine, mycophenolate, and methylprednisolone. No significant differences were shown between the two groups regarding other regimens.

### Disease-Induced Damage Among SLE with and without LN according to SLICC/ACR Damage Index and SLEADI-2K

Out of the 25 SLE patients complicated with nephritis, 10 cases (40%) suffered from disease-induced damage as assessed by the Systemic Lupus International Collaborating Clinics (SLICC)/ACR Damage Index; on the other hand, this number was 2 (9%) among patients without nephritis (*p*=0.02). Furthermore, patients with LN suffered significantly higher SLEADI-2K compared to patients without nephritis (*p* $\leq$ 0.001), including 19 (76%) patients who suffered severe disease activity and 6 (24%) who suffered very severe activity. Among non-LN patients, 12 (54.5%) had moderate activity, 6 (27%) had mild activity, and 4 (18.2%) had no flare.

### Laboratory Findings

Kidney function tests of SLE patients showed that LN patients had significantly higher blood urea, higher serum creatinine, elevated 24-hour protein in urine, and lower creatinine clearance compared to patients without nephritis. LN patients showed significant proteinuria, increased number of casts, red blood cells (RBCs), and pus cells in urine compared to patients without nephritis. Complete blood count findings showed that LN patients were significantly anemic compared to non-LN patients, and RBC count, white blood cell (WBC) count, and platelet count showed no significant differences between both groups (*p*>0.05). In addition, patients with LN had significantly higher neutrophils, lower lymphocytes, lower eosinophils, and lower basophils than patients without nephritis. Liver function tests showed that LN patients had significantly lower serum protein levels, albumin levels, total bilirubin levels, and alkaline phosphatase enzyme levels compared to patients without nephritis (*p*<0.05). Meanwhile, aspartate transaminase (AST) and alanine transaminase (ALT) levels show no significant differences between patients with and without

**Table 1.** Clinical data of SLE patients with and without lupus nephritis (LN).

| Variables                       | Without LN (n=22) | With LN (n=25) | p-value* |
|---------------------------------|-------------------|----------------|----------|
|                                 | n (%)             |                |          |
| <b>Clinical Presentation</b>    |                   |                |          |
| Fatigue                         | 11 (50)           | 13 (52)        | 1.00     |
| Morning stiffness               | 4 (18)            | 7 (28)         | 0.500    |
| Fever                           | 2 (9)             | 2 (8)          | 1.00     |
| Raynaud's phenomenon            | 1 (4.5)           | 0 (0)          | 0.468    |
| Delirium                        | 1 (4.5)           | 0 (0)          | 0.468    |
| Headache                        | 2 (9)             | 0 (0)          | 0.214    |
| Frothy urine                    | 3 (13.6)          | 22 (88)        | <0.001*  |
| Nephrotic syndrome              | 0 (0)             | 5 (20)         | 0.050*   |
| Alopecia                        | 19 (86.4)         | 21 (84)        | 1.00     |
| Vascular purpura                | 1 (4.5)           | 1 (4)          | 1.00     |
| Urticaria                       | 0 (0)             | 1 (4)          | 1.00     |
| Malar rash                      | 12 (54.5)         | 15 (60)        | 0.773    |
| Oral ulcers                     | 17 (77)           | 22 (88)        | 0.446    |
| Nasal ulcers                    | 1 (4.5)           | 7 (28)         | 0.050*   |
| Genitourinary manifestations    | 0 (00)            | 1 (4)          | 1.00     |
| Photosensitivity                | 15 (68)           | 21 (84)        | 0.300    |
| <b>Chest Manifestations</b>     |                   |                |          |
| Dyspnea on exertion             | 2 (9)             | 4 (16)         | 0.530    |
| Cough                           | 1 (4.5)           | 0 (0)          |          |
| Arthralgia                      | 12 (54.5)         | 14 (56)        | 1.00     |
| Arthritis                       | 6 (27)            | 10 (40)        | 0.540    |
| <b>Cardiovascular</b>           |                   |                |          |
| Palpitation                     | 0 (0.0)           | 1 (3.4)        | 1.00     |
| History of angina               | 1 (3.2)           | 0 (0)          |          |
| <b>Gastrointestinal</b>         |                   |                |          |
| Constipation                    | 1 (4.5)           | 0 (0)          | 0.214    |
| Epigastric pain                 | 1 (4.5)           | 0 (0)          |          |
| <b>Associated Comorbidities</b> |                   |                |          |
| Diabetes mellitus               | 1 (4.5)           | 2 (8)          | 1.00     |
| Hypertension                    | 1 (4.5)           | 1 (4)          |          |
| Positive Family History         | 1 (4.5)           | 0 (0)          | 1.00     |

\*Significance defined by  $p < 0.05$

**Table 2.** Treatment history of SLE patients with and without nephritis.

| Treatment               | Without LN (n=22) | With LN (n=25) | p-value*     |
|-------------------------|-------------------|----------------|--------------|
|                         | n (%)             |                |              |
| Methotrexate            | 11 (50)           | 21 (84)        | <b>0.026</b> |
| Hydroquinone            | 2 (9)             | 1 (4)          | 0.590        |
| Sulfasalazine           | 0 (0)             | 4 (16)         | 0.110        |
| Azathioprine            | 1 (4.5)           | 9 (36)         | <b>0.012</b> |
| Cyclophosphamide        | 12 (54.5)         | 18 (72)        | 0.240        |
| Steroids                | 15 (68)           | 22 (88)        | 0.150        |
| NSAIDS                  | 2 (9)             | 5 (20)         | 0.420        |
| Others                  |                   |                |              |
| Mycophenolate           | 0 (0)             | 4 (16)         | <b>0.014</b> |
| Methylprednisolone      | 0 (0)             | 2 (8)          |              |
| ACEI                    | 0 (0)             | 1 (4)          |              |
| Calcium channel blocker | 0 (0)             | 1 (4)          |              |
| Marivan                 | 0 (0)             | 1 (4)          |              |

ACEI: Angiotensin converting enzyme inhibitors, NSAIDS: Non-steroidal anti-inflammatory drugs, SLE: Systemic lupus erythematosus.

\*Significance defined by  $p < 0.05$ .

nephritis. SLE patients with LN have significantly higher inflammatory markers (ESR & CRP) and significantly lower immunological markers (C3 & C4) compared to those without nephritis ( $p < 0.05$ ). All SLE patients were ANA positive ( $p = 1.00$ ), while all LN patients were anti-DNA positive compared to patients without nephritis (were negative for anti-DNA) (chi-square;  $p \leq 0.001$ ) (Table 3).

### FCRL3 Gene Polymorphism and Risk of LN

Table 4 demonstrates the frequencies of genotypes and alleles of rs7528648 and rs11264799 FCRL3 in SLE patients and controls. There were no significant genotype differences between patients and controls ( $p > 0.05$ ). For rs7528648, we found that SLE patients had a higher predominance of the homozygous CC and TT genotypes vs controls. LN patients had a higher CC genotype than patients without nephritis. The frequencies of C and T alleles were higher in SLE patients than in controls. LN patients had a higher C allele than patients without nephritis. Concerning the rs11264799 SNP, there were no significant differences between patients and controls ( $p > 0.05$ ). Nevertheless, SLE patients had a higher predominance of the heterozygous AG genotype and higher G and A alleles than the control group.

LN patients had higher GG and AG genotype frequencies than patients without nephritis. The frequency of the G allele was higher in LN patients than in patients without nephritis, while the frequency of the A allele was higher among patients without nephritis. The genotype and allelic frequencies of rs7528684 and rs11264799 genes in SLE patients regarding different clinical data are shown in Table 5. According to renal biopsy grades of 4 and 5, SLICC/ACR Damage Index, and SLEDAI-2K, the predominance of the TC genotype and C allele for the rs7528684 gene, and the GG genotype and the G allele for the rs11264799 gene was observed. However, this predominance was not significant. The genotype and allelic frequencies of rs7528684 and rs11264799 genes in SLE patients regarding different laboratory data are shown in Table 6. For the rs7528684 gene, predominance of the CC genotype was observed with higher levels of 24h protein, significantly higher levels of C4 in serum, and higher levels of CRP.

On the other hand, the TT genotype was predominant, with higher creatinine clearance and higher C3 levels. The heterozygous TC genotype was predominant in higher ESR levels and among patients with positive anti-DNA.

**Table 3.** Laboratory and immunologic markers of SLE patients with and without nephritis.

| Laboratory Tests                            | without LN (n=22) | with LN (n=25) | p-value*          |
|---|-------------------|----------------|-------------------|
| <b>Kidney Function</b>                      |                   |                |                   |
| Serum urea (mmol/L)                         | 6.7 ± 6           | 12.43 ± 12.1   | <b>0.012*</b>     |
| Serum creatinine (µmol/L)                   | 72.6 ± 38.2       | 104 ± 107.6    | <b>0.033*</b>     |
| Serum uric acid (mg/dL)                     | 3.9 ± 1.4         | 4 ± 1.6        | 0.567             |
| 24h protein in urine (mg/day)               | 286 ± 142.5       | 2880 ± 1956    | <b>&lt;0.001*</b> |
| Creatinine clearance (mL/min)               | 104.7 ± 38.2      | 80.4 ± 42      | <b>0.043*</b>     |
| <b>Liver Function Tests</b>                 |                   |                |                   |
| Total protein (g/L)                         | 72.5 ± 14.4       | 58.2 ± 15.8    | <b>0.002*</b>     |
| Serum albumin (g/L)                         | 43.2 ± 3.4        | 33.3 ± 7.6     | <b>&lt;0.001*</b> |
| Total bilirubin (µmol/L)                    | 10.4 ± 10.9       | 5.3 ± 3.8      | <b>0.033*</b>     |
| Aspartate transaminase (U/L)                | 18.9 ± 10.2       | 24.6 ± 11.16   | 0.072             |
| Alanine transaminase (U/L)                  | 25.4 ± 15.9       | 22.7 ± 16.1    | 0.566             |
| Alkaline phosphatase (U/L)                  | 60.8 ± 22.3       | 46 ± 22        | <b>0.029*</b>     |
| <b>Urine Examination, n (%)</b>             |                   |                |                   |
| Proteinuria                                 | 4 (18)            | 25 (100)       | <b>&lt;0.001*</b> |
| <b>Casts in Urine</b>                       |                   |                |                   |
| None  | 22 (100)          | 13 (52)        | <b>&lt;0.001*</b> |
| Hyaline casts                               | 0 (0)             | 7 (28)         |                   |
| Granular casts                              | 0 (0)             | 5 (20)         |                   |
| <b>Hematuria (RBCs in urine)</b>            | 3 (9.7)           | 12 (41.4)      | <b>0.002*</b>     |
| <b>Pyuria (pus in urine)</b>                | 2 (90)            | 20 (80)        | <b>&lt;0.001*</b> |
| Low (6-10 pus cells/HPF)                    | 2 (9)             | 2 (8)          |                   |
| Moderate (11-20 pus cells/HPF)              | 0 (0)             | 3 (12)         |                   |
| High (>20 pus cells/HPF)                    | 0 (0)             | 15 (60)        |                   |
| <b>Complete Blood Count</b>                 |                   |                |                   |
| Hemoglobin level (g/dL)                     | 12.3 ± 1.0        | 10.8 ± 2.3     | <b>0.008*</b>     |
| RBC (10 <sup>6</sup> /µL)                   | 4.2 ± 0.54        | 4.0 ± 0.71     | 0.216             |
| WBC (10 <sup>3</sup> /µL)                   | 6.6 ± 2.6         | 6.9 ± 3.8      | 0.735             |
| Neutrophils (%)                             | 59 ± 15           | 74 ± 10        | <b>&lt;0.001*</b> |
| Lymphocytes (%)                             | 27.5 ± 11         | 18 ± 12.5      | <b>0.008*</b>     |
| Eosinophils (%)                             | 1.8 ± 1.78        | 0.96 ± 1.0     | <b>0.007*</b>     |
| Basophils (%)                               | 0.45 ± 0.32       | 0.28 ± 0.31    | <b>0.050*</b>     |
| Platelets (10 <sup>3</sup> /µL)             | 250.4 ± 75.5      | 272.2 ± 85.5   | 0.358             |
| <b>Inflammatory and Immunologic Markers</b> |                   |                |                   |
| ESR (mm/h)                                  | 29.8 ± 25.7       | 48.8 ± 30      | <b>0.024*</b>     |
| CRP (mg/L)                                  | 9 ± 7.2           | 13.6 ± 7.6     | <b>0.046*</b>     |
| C3 (g/L)                                    | 1.53 ± 0.27       | 0.12 ± 0.25    | <b>&lt;0.001*</b> |
| C4 (g/L)                                    | 1.1 ± 0.66        | 0.084 ± 0.14   | <b>&lt;0.001*</b> |
| ANA: Positive, n (%)                        | 22 (100)          | 25 (100)       | 1.00              |
| Anti-DNA: Positive, n (%)                   | 0 (0)             | 25 (100)       | <b>&lt;0.001*</b> |

ANA: Antinuclear antibody, C3: Complement 3, C4: Complement 4, CRP: C-reactive protein; ESR: Erythrocyte sedimentation rate, LN: Lupus nephritis, RBC: Red blood cells, WBC: White blood cells. \*Significance defined by p<0.05.

**Table 4.** Genotype & allelic frequencies of the studied cohort (SLE patients vs controls) of rs7528684 (T/C) and rs11264799 (A/G) SNPs of FCRL3 gene.

| SNPs (genotype/allele)   | Controls (n=40) | SLE patients (n=47) | p-value* | Patients without nephritis (n=22) | LN patients (n=25) | p-value* |
|--------------------------|-----------------|---------------------|----------|-----------------------------------|--------------------|----------|
| <b>rs7528684, n (%)</b>  |                 |                     |          |                                   |                    |          |
| CC                       | 8 (20)          | 12 (25.5)           | 0.60     | 5 (23)                            | 7 (28)             | 0.643    |
| TT                       | 3 (7.5)         | 6 (12.8)            |          | 4 (18)                            | 2 (8)              |          |
| TC                       | 29 (72.5)       | 29 (61.7)           |          | 13 (59)                           | 16 (64)            |          |
| C                        | 45 (56)         | 53 (56.4)           |          | 23 (52)                           | 30 (60)            |          |
| T                        | 35 (44)         | 41 (43.6)           |          | 21 (48)                           | 20 (40)            |          |
| <b>rs11264799, n (%)</b> |                 |                     |          |                                   |                    |          |
| GG                       | 26 (65)         | 26 (55.3)           | 0.241    | 11 (50)                           | 15 (60)            | 0.567    |
| AA                       | 6 (15)          | 4 (8.5)             |          | 3 (13.6)                          | 1 (4)              |          |
| AG                       | 8 (20)          | 17 (36.2)           |          | 8 (36.4)                          | 9 (36)             |          |
| G                        | 60 (75)         | 69 (73.4)           |          | 30 (68)                           | 39 (78)            |          |
| A                        | 20 (25)         | 25 (26.6)           |          | 14 (32)                           | 11 (22)            |          |

\*Significance defined by  $p < 0.05$ .

For the rs11264799 gene, predominance of the AA genotype was observed in higher C3, higher C4, higher ESR, and higher CRP serum levels. At the same time, the homozygous GG genotype was predominant in patients with positive anti-DNA.

## Discussion

This study aimed to assess the common polymorphism in the *FCRL3* gene in SLE Egyptian patients with and without nephritis, compare them with healthy controls, and evaluate such polymorphisms with clinical and laboratory data in SLE patients. Our SLE patients were mostly females. It is consistent with Narani (12) and Jolly et al. (13), who concluded that SLE is more common in the female sex, especially at childbearing age. The mean age of our patients complicated with nephritis was younger than that of the patients without nephritis. This finding aligned with previous data that declared that the development of LN in SLE patients occurs at an earlier age than in patients with no nephritis. In addition, LN develops early during the disease, within six to 36 months,

and may be present at initial diagnosis (14, 15). Clinical evaluation for SLE patients included in the study revealed that frothy urine, nephrotic syndrome, and laboratory evaluation of proteinuria were significantly higher among patients complicated with LN. Parikh et al. (16) concluded that proteinuria must be present to diagnose LN and nephrotic-range proteinuria clinically, which was found in more than half of the cases in their study.

A considerable number of our LN patients suffered from disease-induced damage as assessed by the SLICC/ACR Damage Index vs patients without nephritis. Also, our LN patients suffered significantly higher disease activity compared to patients without nephritis. Previous data revealed that LN is considered a serious organ involvement in SLE that increases the risk of mortality in those patients. Mortality rate ranges from 5% to 25% in LN patients within 5 years of onset.

Moreover, about a third of LN patients may proceed to renal failure that requires renal replacement treatment (17, 18). In the current study, patients with LN had significantly higher serum urea and creatinine levels and

**Table 5.** Relation between rs7528684 and rs11264799 genes polymorphism and clinical data in SLE patients (n=47).

| Variables                     | rs7528684 |          |         |         |         |         | rs11264799 |       |        |         |         |         |
|-------------------------------|-----------|----------|---------|---------|---------|---------|------------|-------|--------|---------|---------|---------|
|                               | CC        | TT       | TC      | C       | T       | p-value | GG         | AA    | AG     | G       | A       | p-value |
| <b>Renal Biopsy, n (%)</b>    |           |          |         |         |         |         |            |       |        |         |         |         |
| Class 4 (n=24)                | 7 (29)    | 2 (8)    | 15 (63) | 29 (60) | 19 (40) | 0.78    | 14 (58)    | 1 (4) | 9 (38) | 37 (77) | 11 (23) | 0.721   |
| Class 5 (n=1)                 | 0 (0)     | 0 (0)    | 1 (100) | 1 (50)  | 1 (50)  |         | 1 (100)    | 0 (0) | 0 (0)  | 2 (100) | 0 (0)   |         |
| <b>SLIC/ACR Damage, n (%)</b> |           |          |         |         |         |         |            |       |        |         |         |         |
| Yes (n=12)                    | 4 (33)    | 1 (8)    | 7 (53)  | 15 (63) | 9 (37)  | 0.793   | 7 (58)     | 1 (8) | 4 (33) | 18 (75) | 6 (25)  | 0.858   |
| <b>SLEDAI-2K, n (%)</b>       |           |          |         |         |         |         |            |       |        |         |         |         |
| Mild activity (n=6)           | 2 (33)    | 1 (17)   | 3 (50)  | 7 (58)  | 5 (42)  | 0.956   | 3 (50)     | 2(33) | 1 (17) | 7 (58)  | 5 (42)  | 0.429   |
| Moderate activity (n=12)      | 2 (17)    | 2 (17)   | 8 (67)  | 12 (50) | 12 (50) |         | 6 (50)     | 1 (8) | 5 (42) | 17 (71) | 7 (29)  |         |
| Severe activity (n=19)        | 5 (26)    | 2 (10.5) | 12 (63) | 22 (58) | 16 (42) |         | 10 (53)    | 1 (5) | 8 (42) | 28 (74) | 10 (26) |         |
| Very severe activity (n=6)    | 2 (33)    | 0 (0)    | 4 (67)  | 8 (67)  | 4 (33)  |         | 5 (83)     | 0 (0) | 1 (17) | 11 (92) | 1 (8)   |         |

**Table 6.** Relation between rs7528684 and rs11264799 genes polymorphism and some laboratory data in SLE patients (n=47).

| Variables                        | rs7528684   |            |             |         | rs11264799  |             |             |              |
|----------------------------------|-------------|------------|-------------|---------|-------------|-------------|-------------|--------------|
|                                  | CC          | TT         | TC          | p-value | GG          | AA          | AG          | p-value      |
| 24 h protein (mg/day)            | 2381 ± 2778 | 897±1186   | 1529 ± 1568 | 0.257   | 1714 ± 1885 | 1414 ± 2036 | 1652 ± 2083 | 0.960        |
| Urea (mg/dL)                     | 7.2 ± 5.8   | 12.3±15.2  | 10.3 ± 10.4 | 0.55    | 11 ± 12     | 10.7 ± 12   | 7 ± 5       | 0.269        |
| Creatinine (mg/dL)               | 74.8 ± 52   | 99 ± 45    | 93 ± 99.4   | 0.78    | 100 ± 106   | 104 ± 85    | 70 ± 23     | 0.495        |
| Creatinine clearance (mL/min)    | 94 ± 36     | 104 ± 39   | 88.2 ± 45   | 0.68    | 89.3 ± 47   | 93 ± 54     | 95 ± 32     | 0.899        |
| C3 (g/L)                         | 0.75 ± 0.76 | 1 ± 0.84   | 0.73 ± 0.76 | 0.643   | 0.7 ± 0.76  | 1.43 ± 0.23 | 0.74 ± 0.78 | 0.198        |
| C4 (g/L)                         | 0.65 ± 0.8  | 0.5 ± 0.56 | 0.53 ± 0.67 | 0.852   | 0.43 ± 0.55 | 1.4 ± 0.8   | 0.54 ± 0.44 | <b>0.026</b> |
| ESR (mm/h)                       | 36 ± 24     | 37 ± 27    | 42 ± 32     | 0.81    | 42.3 ± 32   | 48 ± 33     | 34 ± 24     | 0.573        |
| CRP (mg/L)                       | 15.7 ± 7.8  | 9.3 ± 8.9  | 10.2 ± 6.7  | 0.086   | 11.1 ± 8.6  | 15.8 ± 4.3  | 11 ± 6.7    | 0.517        |
| Anti-DNA: positive (n=25), n (%) | 7 (28)      | 2 (8)      | 16 (64)     | 0.643   | 15 (60)     | 1 (4)       | 9 (36)      | 0.567        |

significantly lower creatinine clearance compared to SLE patients without nephritis. Also, patients with LN have significantly higher 24-hour protein in the urine, higher hematuria, pyuria, and increased urinary casts compared to patients without nephritis. Previous reports revealed that abnormal laboratory findings of kidney function tests raise the possibility of LN and necessitate renal biopsy for proper diagnosis and grading (16). Also, Pons-Estel et al. (17) declared that LN is a type of glomerulonephritis and represents an important organ manifestation

of SLE associated with disturbed renal functions and may lead to end-stage renal failure.

In our study, analysis of liver function tests showed that patients complicated with LN had significantly lower total protein, lower serum albumin levels, and lower total bilirubin levels compared to patients without nephritis. González-Regueiro et al. (19) correlated the degree of hypoalbuminemia and lower total protein level in patients with LN to the degree of proteinuria. Also, intensive

drug therapy for high-class LN can explain the disturbed liver function tests (14). Previous data determined the antioxidant and immunomodulator role of bilirubin, thus acting as a protector against autoimmune diseases (20). In a meta-analysis conducted in 2023, the authors found that levels of bilirubin were significantly elevated in SLE patients without nephritis than in patients with nephritis, as revealed in our study (21).

Our LN patients were significantly anemic compared to those without nephritis. Previous studies clarified that decreased erythropoietin production and erythropoietin resistance in LN contribute to anemia in SLE (22). Additionally, in this study, patients with LN suffered significantly higher neutrophils, lower lymphocytes, lower eosinophils, and lower basophils when compared to patients without nephritis. Abdalhadi et al. (23) explained that high neutrophil counts in SLE patients with nephritis are due to the inability of the complement pathway to get rid of the lupus neutrophils, thus leading to their accumulation. Wanitpongpun et al. (24) declared that the low lymphocytes, eosinophils, and basophils counts in patients with LN were explained based on intensive myelosuppressive drugs used for these patients.

Patients with LN included in this study had significantly higher inflammatory markers (ESR & CRP) and significantly lower immunological markers (C3 & C4) compared to those without nephritis. Our findings are consistent with previous data that declared LN to be a form of glomerulonephritis (inflammation of renal parenchyma) that is markedly associated with elevated inflammatory markers (i.e., ESR & CRP) (17). Complement proteins are engaged in the pathogenesis of LN; any decline in complement levels in serum or the complement deposition/activation in kidney tissues are related to LN and can be used as a diagnostic label for LN (25).

All patients with LN in our study had positive anti-DNA in contrast to patients without nephritis, who were all negative for anti-DNA. Rekvig (26) assumed that the pathogenic potential of anti-DNA interactions is to stir up LN, which could be related to a common pathogenic sequela. Previous reports on genetic polymorphism in the *FCRL3* gene and its relation to SLE are scarce. We evaluated the genotype frequency for rs7528648 and rs11264799 genes of *FCRL3*. Statistical analysis showed no deviation of genotype frequencies of rs7528648 and rs11264799 of *FCRL3* neither in SLE patients in comparison to controls nor LN patients in comparison to non-LN

patients. However, certain genotypes and certain alleles were associated with some clinical or laboratory data in SLE patients, such as the predominance of the TC, GG genotypes, and C and G alleles in patients with severe kidney affection, SLICC/ACR damage, and degree of disease activity. Meanwhile, the TT genotype was associated with improved creatinine clearance and elevated C3 levels. The AA genotype was associated with elevated C3 and C4 levels but also with elevated levels of inflammatory markers. Although such associations did not reach significant values, they are still promising. With large-scale studies, results could reveal significant values.

In contrast to our findings, SNP at rs7528684 was found to be related to SLE in Japanese patients but not in African Americans or European Americans (9). Ikari et al. (27) studies, including rheumatoid arthritis patients in Japanese, Dutch Caucasian, and several autoimmune thyroiditis cohorts in the United Kingdom (UK) and Caucasian populations, reported an association between *FCRL3* variants and these autoimmune diseases. Also, they reported its association with autoimmune pancreatitis in Japan. So, findings reveal that *FCRL3* SNP relations with disease susceptibility are common in variable autoimmune diseases and ethnic populations. The polymorphism in the promoter region of *FCRL3* increases its expression in the disease-risk allele. The preferred expression of *FCRL3* in B-cell's germinal center can influence B cell maturation and reactivity, which may enhance autoimmune responses by B cells. Furthermore, previous clinical data stated that the production of autoantibodies that are elevated in patients with the disease-susceptibility genotype reveals the important role of *FCRL3* in B cell-driven autoimmunity (28).

### Study Limitations

The study was limited by the small number of participants, and only a limited number of SNPs were tested.

### Conclusion

SLE patients with nephritis suffered higher grades of disease activity than patients without nephritis. For the rs7528648 SNP, the C allele and the CC genotype were non-significantly higher in LN patients than in patients without nephritis. The rs11264799 SNP showed that the frequency of the G allele and the GG genotype was non-significantly higher in LN patients, while the frequency of the A allele was higher among patients with-

out nephritis. Although these differences did not reach significant levels, larger-scale studies, different ethnic groups, and different SNPs have to be performed to de-

cide whether *FCRL3* gene polymorphism is related to the occurrence of SLE or a risk factor for LN, relation to the disease activity index and patient outcome.

**Ethics Committee Approval:** The study was approved by the Institutional Review Board of the Faculty of Medicine, Assiut University in April 2023 with the decision number 04-2023-200089.

**Informed Consent:** Written informed consent was obtained from all participants, including information about the aim of the study and their right to withdraw at any time. Each participant was assigned a numerical code to ensure confidentiality.

**Peer-review:** : Externally peer-reviewed

**Author Contributions:** Concept – A.G.T., M.S.E.M.; Design – A.G.T., M.N.A.; Supervision – A.G.T., M.N.A.; Fundings – A.M.R.; Materials –

R.M.G., A.M.R.; Data Collection and/or Processing – A.M.R., M.S.E.M.; Analysis and/or Interpretation – R.M.G., M.N.A., M.S.E.M.; Literature Review – A.G.T., M.S.E.M.; Writer – M.S.E.M., A.M.R.; Critical Reviews – A.G.T., M.N.A., R.M.G., M.S.E.M.

**Conflict of Interest:** The authors declare no conflict of interest.

**Financial Disclosure:** The authors declared that this study has received no financial support.

## References

- 1 Ameer MA, Chaudhry H, Mushtaq J, Khan OS, Babar M, Hashim T, et al. An overview of systemic lupus erythematosus (SLE) pathogenesis, classification, and management. *Cureus*. 2022;14(10):e30330. [\[CrossRef\]](#)
- 2 Karrar S, Cunningham Graham DS. Abnormal B Cell Development in Systemic Lupus Erythematosus: What the Genetics Tell Us. *Arthritis Rheumatol*. 2018;70(4):496-507. [\[CrossRef\]](#)
- 3 Didier K, Bolko L, Giusti D, Toquet S, Robbins A, Antonicelli F, et al. Autoantibodies associated with connective tissue diseases: What meaning for clinicians? *Front Immunol*. 2018;9:541. [\[CrossRef\]](#)
- 4 Yo JH, Barbour TD, Nicholls K. Management of refractory lupus nephritis: challenges and solutions. *Open Access Rheumatol*. 2019;11:179-88. [\[CrossRef\]](#)
- 5 Rostamzadeh D, Kazemi T, Amirghofran Z, Shabani M. Update on Fc receptor-like (FCRL) family: new immunoregulatory players in health and diseases. *Expert Opin Ther Targets*. 2018;22(6):487-502. [\[CrossRef\]](#)
- 6 Ehrhardt GR, Leu CM, Zhang S, Aksu G, Jackson T, Haga C, et al. Fc receptor-like proteins (FCRL): immunomodulators of B cell function. *Adv Exp Med Biol*. 2007;596:155-62. [\[Cross-Ref\]](#)
- 7 Bajpai UD, Swainson LA, Mold JE, Graf JD, Imboden JB, McCune JM. A functional variant in FCRL3 is associated with higher Fc receptor-like 3 expression on T cell subsets and rheumatoid arthritis disease activity. *Arthritis Rheum*. 2012;64(8):2451-9. [\[CrossRef\]](#)
- 8 Martínez A, Mas A, de Las Heras V, Bartolomé M, Arroyo R, Fernández-Arquero M, et al. FcRL3 and multiple sclerosis pathogenesis: role in autoimmunity? *J Neuroimmunol*. 2007;189(1-2):132-6. [\[CrossRef\]](#)
- 9 Gibson AW, Li FJ, Wu J, Edberg JC, Su K, Cafardi J, et al. The FCRL3-169CT promoter single-nucleotide polymorphism, which is associated with systemic lupus erythematosus in a Japanese population, predicts expression of receptor protein on CD19+ B cells. *Arthritis Rheum*. 2009;60(11):3510-2. [\[CrossRef\]](#)
- 10 Salles JI, Lopes LR, Duarte MEL, Morrissey D, Martins MB, Machado DE, et al. Fc receptor-like 3 (-169T>C) polymorphism increases the risk of tendinopathy in volleyball athletes: a case control study. *BMC Med Genet*. 2018;19(1):119. [\[CrossRef\]](#)
- 11 Shahram F, Kazemi J, Mahmoudi M, Jadali Z. Single nucleotide polymorphisms of FCRL3 in Iranian patients with Behcet's disease. *Iran J Public Health*. 2019;48(6):1133-9.
- 12 Narani A. Systemic lupus erythematosus (SLE)-a review of clinical approach for diagnosis and current treatment strategies. *Jaffna Medical Journal*. 2019;31(2):9-13. [\[CrossRef\]](#)
- 13 Jolly M, Sequeira W, Block JA, Toloza S, Bertoli A, Blazevic I, et al. Sex differences in quality of life in patients with systemic lupus erythematosus. *Arthritis Care Res (Hoboken)*. 2019;71(12):1647-52. [\[CrossRef\]](#)
- 14 Al-Gahtani SN. A review of systemic lupus erythematosus (SLE): symptoms, risk factors, treatment, and health related quality of life issues. *Open J Rheumatol Autoimmune Dis*. 2021;11(4):115-43. [\[CrossRef\]](#)
- 15 Kosatka-Węgiel J, Dziedzic R, Siwiec-Koźlik A, Spałkowska M, Milewski M, Żuk-Kuwik J, et al. Clinical and laboratory characteristics of early-onset and delayed-onset lupus nephritis patients: A single-center retrospective study. *Rheumatol Int*. 2024;44(7):1283-94. [\[CrossRef\]](#)
- 16 Parikh SV, Almaani S, Brodsky S, Rovin BH. Update on lupus nephritis: Core curriculum 2020. *Am J Kidney Dis*. 2020;76(2):265-81. [\[CrossRef\]](#)

- 17 Pons-Estel GJ, Serrano R, Plasín MA, Espinosa G, Cervera R. Epidemiology and management of refractory lupus nephritis. *Autoimmun Rev.* 2011;10(11):655-63. [\[CrossRef\]](#)
- 18 Borchers AT, Leibushor N, Naguwa SM, Cheema GS, Shoenfeld Y, Gershwin ME. Lupus nephritis: a critical review. *Autoimmun Rev.* 2012;12(2):174-94. [\[CrossRef\]](#)
- 19 González-Regueiro JA, Cruz-Contreras M, Merayo-Chalico J, Barrera-Vargas A, Ruiz-Margáin A, Campos-Murguía A, et al. Hepatic manifestations in systemic lupus erythematosus. *Lupus.* 2020;29(8):813-24. [\[CrossRef\]](#)
- 20 Filipyuk AL, Bek NS, Sklyarova VO, Filipyuk IT, Huk-Leshnevskaya ZO, Zhakun IB. Low serum bilirubin levels in women with the antiphospholipid syndrome. *Wiad Lek.* 2022;75(1 pt 2):203-8.
- 21 Yu Y, Wang Q, Zhang D, Wu W, Jiang Z. Relationship between bilirubin and systemic lupus erythematosus: A systematic review and meta-analysis. *Immun Inflamm Dis.* 2023;11(12):e1115. [\[CrossRef\]](#)
- 22 Ardalan MR. Anemia in lupus nephritis; etiological profile. *J Renal Inj Prev.* 2013;2(3):103-4. [\[CrossRef\]](#)
- 23 Abdalhadi S, Khalayli N, Al-Ghotani B, Kudsi M. Systemic lupus erythematosus disease activity and neutrophil-to-lymphocyte ratio and platelet-to-lymphocyte ratio: a cross-sectional case-control study. *Ann Med Surg (Lond).* 2023;85(5):1448-53. [\[CrossRef\]](#)
- 24 Wanitpongpun C, Teawtrakul N, Mahakkanukrauh A, Siritunyaporn S, Sirijerachai C, Chansung K. Bone marrow abnormalities in systemic lupus erythematosus with peripheral cytopenia. *Clin Exp Rheumatol.* 2012;30(6):825-9.
- 25 Gandino IJ, Scolnik M, Bertiller E, Scaglioni V, Catoggio LJ, Soriano ER. Complement levels and risk of organ involvement in patients with systemic lupus erythematosus. *Lupus Sci Med.* 2017;4(1):e000209. [\[CrossRef\]](#)
- 26 Rekvig OP. The dsDNA, Anti-dsDNA antibody, and lupus nephritis: What we agree on, what must be done, and what the best strategy forward could be. *Front Immunol.* 2019;10:1104. [\[CrossRef\]](#)
- 27 Ikari K, Momohara S, Nakamura T, Hara M, Yamanaka H, Tomatsu T, et al. Supportive evidence for a genetic association of the FCRL3 promoter polymorphism with rheumatoid arthritis. *Ann Rheum Dis.* 2006;65(5):671-3. [\[CrossRef\]](#)
- 28 Kochi Y, Myouzen K, Yamada R, Suzuki A, Kurosaki T, Nakamura Y, Yamamoto K. FCRL3, an autoimmune susceptibility gene, has inhibitory potential on B-cell receptor-mediated signaling. *J Immunol.* 2009;183(9):5502-10. [\[CrossRef\]](#)

# Soluble HLA-G as a Novel Biomarker for the Diagnosis of Acute Lymphoblastic Leukemia

Sura M.Y. Al-Tae<sup>1</sup> , Rojan G.M. Al-Allaff<sup>1</sup> 

<sup>1</sup>University of Mosul, College of Sciences, Department of Biology, Mosul, Iraq

## Abstract

**Objective:** Acute lymphoblastic leukemia (ALL) is a malignant proliferation of immature lymphocytes in the bone marrow and blood. Cancer cells utilize soluble human leukocyte antigen G (sHLA-G) as a key component of their immune evasion strategy. This study aimed to assess sHLA-G levels in patients with ALL, as it may serve as a diagnostic marker for tumors.

**Materials and Methods:** Children diagnosed with ALL were compared with healthy children in a control group. Participants in both groups were between 1 and 14 years of age. Patient samples were categorized into three subgroups based on disease duration and treatment. Serum sHLA-G levels were measured using enzyme-linked immunosorbent assay (ELISA).

**Results:** The patient group consisted of 80 participants, while the control group included 40 individuals. The findings indicated that sHLA-G levels were significantly higher in patients (mean  $\pm$  standard deviation [SD]= 42.08  $\pm$  21.62 ng/mL) in contrast to control subjects (mean  $\pm$  SD=23.20  $\pm$  21.54 ng/mL;  $p=0.001$ ). While no significant differences were found in sHLA-G levels across the three patient subgroups compared with Duncan's test ( $p=0.213$ ), all patient groups had a considerable elevation in sHLA-G levels compared to the control group.

**Conclusions:** sHLA-G acts as an immune checkpoint used by tumor cells to spread and evade immunity. Therefore, it can be used as an indicator for diagnosing and monitoring tumor development and treatment response.

**Keywords:** Acute lymphoblastic leukemia, biomarker, cancer, children, diagnosis, sHLA-G

## Introduction

Acute lymphoblastic leukemia (ALL) is an uncontrolled proliferation of immature lymphocytes that are precursors to either B-cells or T-cells, and their rapid proliferation leads to their collection in the blood, bone marrow, and other organs (1). ALL is one of the most common types of tumors among children, and the incidence rate peaks between the ages of 1-4 years (2, 3). It also constitutes

### Correspondence

Rojan G.M. AL-Allaff

### E-mail

rojsbio57@uomosul.edu.iq

### Received

December 25, 2024

### Accepted

April 14, 2025

### Published

April 29, 2025

### Suggested Citation

Al-Tae SMY, Al-Allaff RGM. Soluble HLA-G as a novel biomarker for the diagnosis of acute lymphoblastic leukemia. Turk J Immunol. 2025;13(1):54-61.

### DOI

10.36519/tji.2025.567



This work is licensed under the Creative Commons Attribution-NonCommercial-Non-Derivatives 4.0 International License (CC BY-NC-ND 4.0).

about 20% of leukemia among adults (4, 5). Following the bone marrow, leukemia cells spread to the brain, spinal cord, and other extramedullary locations, such as the spleen, liver, mediastinum, and lymph nodes. In pediatric ALL patients, B cells constitute 85%, and T cells account for 15% (5-7).

Human leukocyte antigen G (HLA-G) is primarily derived from the non-classical major histocompatibility complex class I molecule. It is a molecule associated with autoimmune illnesses and susceptibility to viral infections, resulting in an imbalanced and pathological environment (8). First identified in fetal cytotrophoblasts through gestation, HLA is believed to contribute to a phenomenon known as fetal-maternal tolerance, which shields the fetus from immune system destruction (9). Also, HLA-G is observed in tumors (10). In both normal and abnormal circumstances, HLA-G is located on the membrane of various cell types, and it can also be found in soluble form in cerebrospinal fluid, bodily plasma, and even extracellular vesicles (11).

sHLA-G serves as an immune checkpoint and is a promising candidate for disease monitoring and cancer outcome prediction due to (i) its restricted expression pattern in physiological tissues, (ii) minimal polymorphism in the coding region, and (iii) diverse immunomodulatory properties. Under pathological circumstances, Nonetheless, HLA-G is present in several primary tumor types and metastases with differing frequencies, and it is significantly associated with elevated tumor grade and a bad prognosis for cancer patients (12).

sHLA-G plays a critical role in the clinical context of ALL, particularly regarding prognosis and immunological response, as a biomarker for forecasting outcomes in ALL patients. sHLA-G expression in ALL facilitates immune evasion by down-regulating natural killer (NK) cells and compromising both innate and adaptive immunological responses (13). The engagement of sHLA-G with immune cells results in a suppressive tumor microenvironment, hence facilitating tumor survival and growth (14).

Functioning through its receptors on immune cells, such as immunoglobulin-like transcript receptor 4 (ILT-4), immunoglobulin-like transcript receptor 2 (ILT-2), killer inhibitory receptor (KIR), CD160 receptor, and CD8 receptor, sHLA-G functionally impacts both non-specific and specific immune by compromising anti-tumor immune responses (15-17).

This study aimed to quantify sHLA-G concentrations in patients with ALL since it serves as a significant and promising immunological marker for diagnosis and disease progression while assessing its use in monitoring tumor growth.

## Materials and Methods

### Study Area

ALL patient samples were collected under the supervision of a haematology specialist from the Al-Hadbaa Specialized Hospital in Mosul, Iraq, from March to July 2024. The samples of ALL patients were collected under the supervision of a hematology specialist. The study was approved by the Iraqi Ministry of Health and the ethical and scientific board of Mosul University in Mosul, Iraq. All procedures followed the Declaration of Helsinki. Informed consent was obtained from all participants. Participants were assured confidentiality and received blood testing free of charge.

### Study Subject

Blood samples were collected from children diagnosed with ALL and healthy controls. All participants were aged 1 and 14 years. Demographic information, including age, sex, disease duration, treatment type, and family medical history, was recorded. The samples of ALL patients were divided into three subgroups based on disease duration and treatment type:

Group 1: <1 year

Group 2: 1–2 years

Group 3: >2 years

Clinical features of the patients are summarized in Table 1, and the FAB (French-American-British) classification is presented in Table 2. Chemotherapy regimens included vincristine, methotrexate, and prednisone, following international pediatric oncology protocols. The response to chemotherapy was complete and within the standard risk category.

### Serum Collection

A 3 mL venous blood sample was collected from each participant and placed in a gel tube. Samples were centrifuged at 3000 rpm for 15 minutes. The separated serum was transferred to Eppendorf tubes to prepare for analysis and stored at -20°C.

**Table 1.** The clinical characteristics of ALL patients.

| Clinical characteristics of ALL patients |
|--|
| Fever                                    |
| Extreme fatigue                          |
| Feeling of exhaustion                    |
| Anaemia                                  |
| Bone pain                                |
| Easy bruising                            |

**Table 2.** The FAB (French-American-British) classification of ALL patients.

| Subtype of ALL | Description  | %  |
|----------------|--|----|
| L1             | Blast cells that are uniformly tiny and have a high nuclear-to-cytoplasm ratio             | 90 |
| L2             | Larger blasts that have nucleoli, a more-varied cytoplasm, and an uneven nuclear structure | 10 |

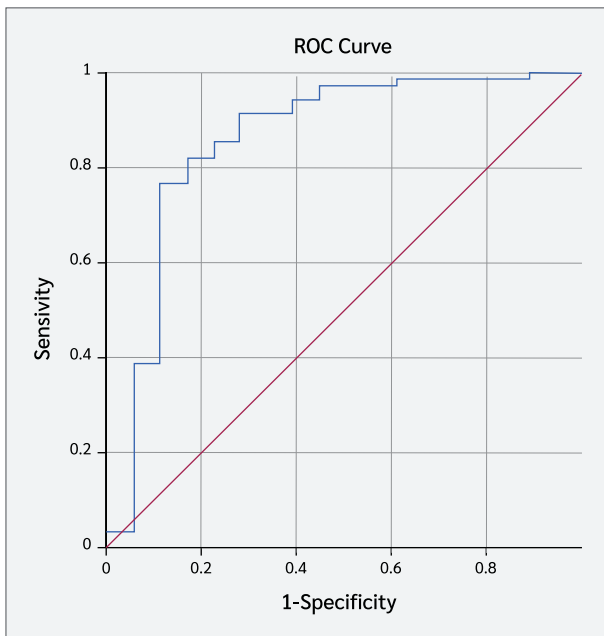


**Figure 5.** ROC curve of the variable sHLA-G.

### Complete Blood Count (CBC)

Hematological parameters were measured using the Mythic™ 18 automated hematology analyzer (Orphée S.A., Switzerland).

### Measurement of sHLA-G Concentration by ELISA

The principle of the assay is based on the reaction of sHLA-G present in serum samples with antibodies previously fixed on the surface of a polystyrene plate. A biotin-labeled antibody is added, which binds to the Ag-AB complex. After incubation, washing is done, streptavidin-horseradish peroxidase (HRP) enzyme and substrate solution are added in order, and the color develops according to the amount of sHLA-G. After stopping the reaction with an acid-stop solution, the absorbance is read at 450 nm.

### Procedure

1. The ELISA kit (Fine Test Company, China) was used. 100 µL of the standard solution was added to the first twelve wells, and 100 µL of the sample was introduced to the remaining wells; the plate was covered and incubated at 37°C for 90 minutes. Subsequent to incubation, the plate was rinsed three times and immersed in the wash solution for one minute.
2. Added 100 µL of biotin-labeled antibody to each well and incubated the plate at 37°C for 60 minutes. After incubation, the plate was washed twice with wash solution.
3. Added 100 µL of HRP-streptavidin conjugate solution to each well and incubated at 37°C for 30 minutes.
4. Added 90 µL of TMB solution to each well. Incubation was carried out at 37°C for 10-20 minutes in the dark.
5. 50µL of stop solution was added to each well, and the optical density was read at 450 nm within 10 minutes using a microplate reader model Rt-2100c.

### Statistical Analysis

Duncan’s test was used to compare the means, and the probability level was set as  $p \leq 0.05$ . Statistical analyses, including the receiver operating characteristic (ROC) curve, were performed using the Statistical Package for the Social Sciences (SPSS), version 24.0.

### Results

A total of 80 blood samples from the patient group were compared to 40 samples from the control group. The patient group consisted of 60 males and 20 females; while the control group included 20 males and 20 females. The results of Duncan’s test for paired comparisons and

**Table 3.** Duncan's test for pairs of comparisons and to test the significance level of the variable WBC count.

| Variable             | Groups            | n  | Mean ± SD         | Duncan test             |         |
|----------------------|-------------------|----|-------------------|-------------------------|---------|
|                      |                   |    |                   | Subset for alpha = 0.05 |         |
|                      |                   |    |                   | 1                       | 2       |
| WBC<br>cell/ $\mu$ L | 1-2 years         | 25 | 3211.50 ± 1948.29 | 3211.50                 |         |
|                      | Less than 1 year  | 30 | 3482.52 ± 2095.82 | 3482.52                 |         |
|                      | More than 2 years | 25 | 3705.50 ± 1772.09 | 3705.50                 |         |
|                      | Control           | 40 | 8013.22 ± 2165.74 |                         | 8013.22 |
| <i>p</i> -value      |                   |    |                   | 0.460                   | 1.000   |

WBC: White blood cell count, SD: Standard deviation.

**Table 4.** Comparison of sHLA-G concentrations in ALL patients and control group.

| Parameter       | Groups   | Number | Mean ± SD     | Extreme value | T-test | <i>p</i> -value |
|-----------------|----------|--------|---------------|---------------|--------|-----------------|
| sHLA-G<br>ng/mL | Patients | 80     | 42.08 ± 21.62 | 10.85-132.09  | 3.292  | 0.001*          |
|                 | Control  | 40     | 23.20 ± 21.54 | 6.16-102.55   |        |                 |

sHLA-G: Soluble human leukocyte antigen-G, SD: Standard deviation.

**Table 5.** Duncan's test for pairs of comparisons and to test the significance level of the variable sHLA-G.

| Variable        | Groups            | Number | Mean ± SD     | Duncan's test         |       |
|-----------------|-------------------|--------|---------------|-----------------------|-------|
|                 |                   |        |               | Subset for alpha=0.05 |       |
|                 |                   |        |               | 1                     | 2     |
| sHLA-G<br>ng/mL | Less than 1 year  | 30     | 45.99 ± 28.95 |                       | 45.99 |
|                 | 1-2 years         | 25     | 37.05 ± 13.16 |                       | 37.05 |
|                 | More than 2 years | 25     | 41.82 ± 15.99 |                       | 41.82 |
|                 | Control           | 40     | 23.20 ± 21.54 | 23.20                 |       |
| <i>p</i> -value |                   |        |               | 1.000                 | 0.213 |

sHLA-G: Soluble human leukocyte antigen-G, SD: Standard deviation.

significance level test for white blood cell (WBC) count showed no significant differences between the three subgroups of the patients ( $p=0.460$ ). However, all patient groups showed significantly lower WBC counts than the control group (Table 3).

sHLA-G concentrations were significantly elevated in patients with ALL compared to controls ( $p=0.001$ ) (Table 4). However, sHLA-G demonstrated no significant difference among the subgroups of the patients ( $p=0.213$ ) (Table 5).

**Table 6.** ROC curve of the variable sHLA-G.

| ROC curve            |       |                   |             | Max.              | Cut-off value |
|----------------------|-------|-------------------|-------------|-------------------|---------------|
| Test result variable | Area  | Asymptotic 95% CI |             |                   |               |
|                      |       | Lower bound       | Upper bound |                   |               |
| sHLA-G               | 0.858 | 0.739             | 0.978       | Sensitivity=0.821 | 27.4885       |
|                      |       |                   |             | Specificity=0.833 |               |

sHLA-G: Soluble human leukocyte antigen-G, ROC: Receiver operating characteristic, CI: Confidence interval.

The results of the ROC curve analysis showed the sensitivity as 0.821 and the specificity as 0.833 (Table 6) (Figure 1), indicating that sHLA-G is a valuable tool for diagnosing ALL patients.

## Discussion

The total WBC count is a measure of the presence of extramedullary cells in ALL (17). Alghamdi et al. (18) indicated that a decrease in WBC count in patients with ALL undergoing chemotherapy is a common and expected outcome. This decrease is primarily due to the effects of chemotherapeutic agents, which target rapidly dividing cells, including leukemic and normal hematopoietic cells.

The reason for the decrease in the total WBC counts and the absolute number of WBC types in ALL patients compared to the control in Table 3 is that all patients were undergoing chemotherapy. Chemotherapy is designed to target rapidly dividing cells, including cancer cells. It also affects other rapidly dividing cells in the body, such as those in the bone marrow, which produces blood cells. The drugs damage the DNA of dividing cells, leading to cell death. This results in a decrease in the absolute number of cells, which can serve as a prognostic indicator of treatment effectiveness and patient outcomes.

One important immunological checkpoint protein in cancer is sHLA-G (19), a vital biomarker for invasion and metastasis of cancer cells, as it inhibits all stages of the anti-tumor response (12, 21). Elevated sHLA-G in cancer can alter the immune surveillance system and cause tumor escape from the immunity in a number of hematologic malignancies, including acute and chronic leukemia (12).

Excessive levels of sHLA-G in children with ALL are connected to leukemia cells' capacity to elude the immune system, which may result in worse clinical outcomes. sHLA-G often acts as a "disappearance cloak" for tumor cells by inhibiting immune responses, including those from NK and T cells. Consequently, HLA-G appears as a potential tumor biomarker of clinical results, as shown in Table 1 (13, 22).

Our findings support the study by Ribeiro et al. (13), who reported increased sHLA-G levels in patients with leukemia and lymphoma but not in healthy individuals. Moreover, we found sHLA-G levels considerably higher in ALL patients than healthy controls, suggesting it is usable as a prognostic marker. Also, Almeida et al. found that elevated sHLA-G levels in bone marrow were linked to increased blood cell counts in juvenile T-cell ALL, a metric linked to a bad prognosis (24). High HLA-G levels are generally related to adverse outcomes in ALL. As reported by Xu et al. (20), high sHLA-G levels in cancer are connected with poor survival in ALL. Chemotherapy in ALL targets leukemia cells, which may indirectly affect sHLA-G by reducing tumor burden.

Ribeiro et al. (13) indicated that sHLA-G levels decreased after chemotherapy and were associated with improved clinical outcomes. Chemotherapy targets tumor cells, which indirectly affects sHLA-G by reducing tumor burden, in addition to causing significant changes in the cellular metabolism of tumor cells, which may indirectly affect the secretion of sHLA-G, although this has not been directly measured in studies (25). This situation explains what is shown in Table 2. The protein concentration was higher in Group 1 because they were at the beginning of the disease and the beginning of chemotherapy, and the expression of the protein was at its highest levels for use as a means of cancer cell proliferation. Then, the protein

concentration began to decrease somewhat in Group 2 and Group 3 as a result of undergoing chemotherapy for long periods. Therefore, sHLA-G can serve as a prognostic marker for treatment response in ALL.

Physiological tissues have a limited pattern of sHLA-G expression, while a wide range of primary and malignant tumors has shown positivity. There is a significant correlation between elevated tumor grade and worse prognosis in cancer patients (12). This is also attributable to its immunosuppressive properties, which tumor cells use to circumvent the host immune system. Consequently, in recent decades, the expression of sHLA-G and its immunosuppressive effects have emerged as a significant subject of investigation, particularly in cancer research. Multiple studies suggest that sHLA-G may pave the way for its consideration as a novel immune checkpoint in tumor diagnosis, acting as a natural immune signal that prevents the development of an immune response (26, 27).

The interaction of sHLA-G with its receptors causes inhibition of cytotoxic T cells, inhibition of CD4<sup>+</sup> T cell proliferation (28) and may also lead to reduced expression of pro-inflammatory cytokines generated by T helper 1 (Th1) cells and enhanced production of anti-inflammatory cytokines produced by T helper 2 (Th2) cells. Therefore, it is believed that abnormal HLA-G/sHLA-G expression enables tumor cells to evade immune responses (29).

Expression of this protein in hematological malignancies, such as leukemia, is linked to immune cell-mediated

cytotoxicity resistance and the development of an immunological milieu that supports tumors, including the activation of regulatory T cells and interleukin 10 (IL-10)-producing dendritic cells (13).

Additionally, distinct micro RNAs that differ depending on the leukemia subtype affect the control of sHLA-G expression in leukemia, suggesting a complicated regulatory mechanism that could aid in the course of the disease and immune evasion (21). Therefore, it is possible to view the presence of sHLA-G in leukemic cells as a means of evading immune monitoring, which could result in treatment resistance and lower survival rates in afflicted children (13, 22).

Leukemia patients receiving hematopoietic stem cell transplantation have experienced unfavorable results because of genetic variations in the sHLA-G gene in the 3' untranslated region (3'-UTR) and 5' upstream regulatory region (5'-URR). This suggests a genetic vulnerability to immunological regulation by sHLA-G (30)

## Conclusion

We concluded that increased sHLA-G is an immune mechanism that tumor cells utilize to eliminate the immune system response. sHLA-G is one of the most significant contemporary indicators that should be used as a marker for the onset and progression of the tumor condition in patients with lymphocytic leukemia.

**Ethics Committee Approval:** Prior to the initiation of the clinical study, ethical approval was obtained from the Scientific and Ethical Committee of Mosul University, Mosul, Iraq (Approval No. 476, dated January 21, 2024), and further authorization was granted by the Iraqi Ministry of Health (Approval No. 6428, dated February 12, 2024).

**Informed Consent:** Ethical approvals for patient data were obtained under the supervision of the Department of Health and the Scientific Committee of the Department of Biology, Faculty of Science, University of Mosul, in accordance with the Declaration of Helsinki.

**Peer-review:** : Externally peer-reviewed

**Author Contributions:** Concept – S.M.Y.A., R.G.M.A.; Design – S.M.Y.A., R.G.M.A.; Supervision – S.M.Y.A., R.G.M.A.; Fundings –

S.M.Y.A., R.G.M.A.; Materials – S.M.Y.A., R.G.M.A.; Data Collection and/or Processing – S.M.Y.A., R.G.M.A.; Analysis and/or Interpretation – S.M.Y.A., R.G.M.A.; Literature Review – S.M.Y.A., R.G.M.A.; Writer – S.M.Y.A., R.G.M.A.; Critical Reviews – S.M.Y.A., R.G.M.A.

**Conflict of Interest:** The authors declare no conflict of interest.

**Financial Disclosure:** The authors declared that this study has no financial support.


**Acknowledgment:** We would like to thank the Department of Biology, College of Science, University of Mosul, for their contribution and unwavering support in completing this manuscript.

## References

- 1 Al-Qadi SH, Al-Dulamey QK, Abed MA, Mehuaiden AK. Effect the static magnetic field on some hematological parameters of human AML leukemia: *in vitro*. Rafidain J Sci. 2023;32(3):32-40. [\[CrossRef\]](#)
- 2 Al-Tae SMY, AL-Allaff RGM. A new strategy to evaluate emerging tumour-associated antigens as biomarkers of acute lymphocytic leukaemia development. J Appl Nat Sci. 2025;17(1):179-85. [\[CrossRef\]](#)
- 3 Ibrahim RM, Idrees NH, Younis NM. Epidemiology of leukemia among children in Nineveh Province, Iraq. Rawal Med J. 2023; 48(1):137.
- 4 Inaba H, Mullighan CG. Pediatric acute lymphoblastic leukemia. Haematologica. 2020;105(11):2524-39. [\[CrossRef\]](#)
- 5 Al-Helaly LA, Younes SH. Role of glutaredoxin-1 and some oxidative stress enzymes in acute lymphocytic leukemia patients. Rafidain J Sci. 2024;33(4):90-8. [\[CrossRef\]](#)
- 6 Ajaj MM, Mikael MH. Estimation of some biochemical variables in women with breast cancer after chemotherapy treatment in Nineveh Governorate. Rafidain J Sci. 2024;33(2A):1-11.
- 7 Hameed MA, Hamed OM. Detection of P53 suppressor gene mutation in women with breast cancer in Mosul City. AIP Conf Proc. 2023;2834(1):020007. [\[CrossRef\]](#)
- 8 Contini P, Murdaca G, Puppo F, Negrini S. HLA-G expressing immune cells in immune mediated diseases. Front Immunol. 2020;11:1613. [\[CrossRef\]](#)
- 9 Wedenoja S, Yoshihara M, Teder H, Sariola H, Gissler M, Kayama S, et al. Fetal HLA-G mediated immune tolerance and interferon response in preeclampsia. EBioMedicine. 2020;59:102872. [\[CrossRef\]](#)
- 10 Loustau M, Anna F, Dréan R, Lecomte M, Langlade-Demoyen P, Caumartin J. HLA-G neo-expression on tumors. Front Immunol. 2020;11:1685. [\[CrossRef\]](#)
- 11 Rebmann V, König L, Nardi Fda S, Wagner B, Manvailer LF, Horn PA. The Potential of HLA-G-bearing extracellular vesicles as a future element in HLA-G immune biology. Front Immunol. 2016;7:173. [\[CrossRef\]](#)
- 12 Lin A, Yan WH. Heterogeneity of HLA-G expression in cancers: Facing the challenges. Front Immunol. 2018;9:2164. [\[CrossRef\]](#)
- 13 Ribeiro T, Nogueira GM, Souza-Barros M, Pereira DS, Santos V, Neto J, Costa H. Human leukocyte antigen (HLA)-G: as an invisibility cloak for tumour cells in hematological malignancies. Hematology, Transfusion and Cell Therapy. 2023;45:S184. [\[CrossRef\]](#)
- 14 Anna F, Bole-Richard E, LeMaoult J, Escande M, Lecomte M, Certoux JM, et al. First immunotherapeutic CAR-T cells against the immune checkpoint protein HLA-G. J Immunother Cancer. 2021;9(3):e001998. [\[CrossRef\]](#)
- 15 Wu CL, Caumartin J, Amodio G, Anna F, Loustau M, Gregori S, et al. Inhibition of iNKT cells by the HLA-G-ILT2 checkpoint and poor stimulation by HLA-G-expressing tolerogenic DC. Front Immunol. 2021;11:608614. [\[CrossRef\]](#)
- 16 Bai Y, Liang J, Liu W, Wang F, Li C. Possible roles of HLA-G regulating immune cells in pregnancy and endometrial diseases via KIR2DL4. J Reprod Immunol. 2020;142:103176. [\[CrossRef\]](#)
- 17 Helenius M, Vaitkeviciene G, Abrahamsson J, Jonsson ÖG, Lund B, Harila-Saari A, et al. Characteristics of white blood cell count in acute lymphoblastic leukemia: A COST LEG-END phenotype-genotype study. Pediatr Blood Cancer. 2022;69(6):e29582. [\[CrossRef\]](#)
- 18 Alghamdi AT, Alead JE, Darwish EG, Matasif ST, Qari MH. Prognostics and clinical outcomes in patients diagnosed with acute lymphoblastic leukemia in King Abdulaziz University Hospital, Jeddah, Saudi Arabia. Cureus. 2022;14(3):e22952. [\[CrossRef\]](#)
- 19 Wang Q, Song H, Cheng H, Qi J, Nam G, Tan S, et al. Structures of the four Ig-like domain LILRB2 and the four-domain LILRB1 and HLA-G1 complex. Cell Mol Immunol. 2020;17(9):966-75. [\[CrossRef\]](#)
- 20 Xu HH, Gan J, Xu DP, Li L, Yan WH. Comprehensive transcriptomic analysis reveals the role of the immune checkpoint HLA-G molecule in cancers. Front Immunol. 2021;12:614773. [\[CrossRef\]](#)
- 21 Carosella ED, Rouas-Freiss N, Tronik-Le Roux D, Moreau P, LeMaoult J. HLA-G: An immune checkpoint molecule. Adv Immunol. 2015;127:33-144. [\[CrossRef\]](#)
- 22 Martín-Villa JM, Vaquero-Yuste C, Molina-Alejandre M, Juárez I, Suárez-Trujillo F, López-Nares A, et al. HLA-G: Too much or too little? Role in cancer and autoimmune disease. Front Immunol. 2022;13:796054. [\[CrossRef\]](#)
- 23 Motawi TM, Zakhary NI, Salman TM, Tadros SA. Serum human leukocyte antigen-G and soluble interleukin 2 receptor levels in acute lymphoblastic leukemic pediatric patients. Asian Pac J Cancer Prev. 2012;13(11):5399-403. [\[CrossRef\]](#)
- 24 Almeida RS, Gomes TT, Araújo FS, de Oliveira SAV, Santos JF, Donadi EA, et al. Differentially expressed bone marrow microRNAs are associated with soluble HLA-G bone marrow levels in childhood leukemia. Front Genet. 2022;13:871972. [\[CrossRef\]](#)
- 25 Saito T, Wei Y, Wen L, Srinivasan C, Wolthers BO, Tsai CY, et al. Impact of acute lymphoblastic leukemia induction therapy: findings from metabolomics on non-fasted plasma samples from a biorepository. Metabolomics. 2021;17(7):64. [\[CrossRef\]](#)
- 26 Dumont C, Jacquier A, Verine J, Noel F, Goujon A, Wu CL, et al. CD8+PD-1-ILT2+ T cells are an intratumoral cytotoxic population selectively inhibited by the immune-checkpoint HLA-G. Cancer Immunol Res. 2019;7(10):1619-32. [\[CrossRef\]](#)
- 27 Kuroki K, Matsubara H, Kanda R, Miyashita N, Shiroishi M, Fukunaga Y, et al. Structural and functional basis for LILRB immune checkpoint receptor recognition of HLA-G isoforms. J Immunol. 2019;203(12):3386-94. [\[CrossRef\]](#)
- 28 Naji A, Menier C, Maki G, Carosella ED, Rouas-Freiss N. Neoplastic B-cell growth is impaired by HLA-G/ILT2 interaction. Leukemia. 2012;26(8):1889-92. [\[CrossRef\]](#)

- 29 Rohn H, Lang C, Schramm S, Heinemann FM, Trilling M, Gäckler A, et al. Effect of HLA-G5 immune checkpoint molecule on the expression of ILT-2, CD27, and CD38 in splenic B cells. *J Immunol Res.* 2022;2022:4829227. [\[CrossRef\]](#)
- 30 Chen DP, Wang PN, Hour AL, Lin WT, Hsu FP, Wang WT, et al. The association between genetic variants at 3'-UTR and 5'-UTR of HLA-G gene and the clinical outcomes of patients with leukemia receiving hematopoietic stem cell transplantation. *Front Immunol.* 2023;14:1093514. [\[CrossRef\]](#)
-

# Symbiotic Life is a Success of Immunity

Şefik Ş. Alkan<sup>1</sup> 

<sup>1</sup>Retired Microbiologist and Immunologist, Basel, Switzerland

*“If you shut the door to all errors, truth will be shut out.”*

R. Tagore

## Abstract

Microorganisms (including viruses) have shaped the evolution of all living creatures since the beginning of life on Earth 3.8 billion years ago. They still put pressure on all living organisms. Because life is symbiotic (i.e., all life depends on other lives), the initial primitive border protection of single cells had to be developed against transgressive microorganisms. Thus, all organisms needed to discriminate self from non-self. With time, this simple recognition system developed into highly complex immunological mechanisms. In the symbiotic relationship, all animals take in and feed trillions of microorganisms in their body, mainly in the gut, to help digest food but also to train their immune system. We need to understand that microorganisms are neither our enemies nor friends. Survival of all life forms depends on maintaining a delicate balance between self and non-self, i.e., microorganisms. Understanding the symbiotic nature of life on Earth might help prevent further destruction of nature.

**Keywords:** Microorganisms, symbiosis, immune system, evolution, microbiota, environmental balance

## Introduction

Not so long ago, a tiny virus has turned our lives upside down. We witnessed how our civilization can fall to its knees so easily. After infecting 770 million individuals and killing over 7 million people across the globe, COVID-19 is still with us. Previously, I shortly examined the coronavirus pandemic from an evolutionary perspective (1, 2). It looks like SARS-CoV-2 is going to stay with us longer (3, 4).

In this “opinion” article, I wish to examine not just coronaviruses but the co-evolution of all organisms and the pivotal role immune systems play. I will first remind you of some basics of the evolution of life, then will go into obligatory partnership and deal with the immune system, which keeps all life in balance. By understanding the begin-

### Correspondence

Şefik Ş. Alkan

### E-mail

sefik.alkan@gmail.com

### Received

February 24, 2025

### Accepted

March 24, 2025

### Published

April 29, 2025

### Suggested Citation

Alkan ŞŞ. Symbiotic life is a success of immunity. Turk J Immunol. 2025;13(1):63-8.

### DOI

10.36519/tji.2025.591



This work is licensed under the Creative Commons Attribution-NonCommercial-Non-Derivatives 4.0 International License (CC BY-NC-ND 4.0).

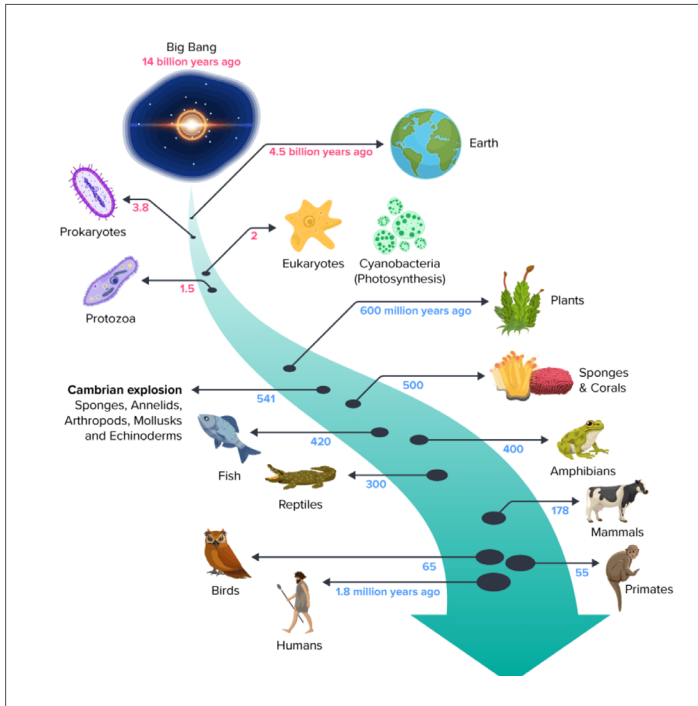


**Figure 1.** Timeline of evolution. (From Flex Books 2.0. CK-12) (6). nings of

**Box 1: Life on Earth in short**

- The world is run by microorganisms
- All creatures have to live together/help each other
- Evolution is not a chain reaction
- The engine of evolution is mutation
- Changes (mutations) can disrupt the established balance
- Change survives if it fits to the environment
- Change creates new border disputes between living beings
- Immune systems protect the borders

life on Earth and supporting the conditions of symbiotic life (5), we might reduce unnecessary suffering.

I think humanity has a lot to learn from the microorganisms that are neither our enemies nor our friends. We do not have to hate or love them; we only need to understand them because all other life forms need them. It is only through a deep understanding of the evolutionary process that we can appreciate the value of symbiotic life.



**Figure 2.** A teaspoon of soil probably contains more life than humans on Earth (9).

**Evolution in Short**

As shown in Figure 1, the world's first owners are tiny creatures. We have 3.8 billion years of joined history with these first owners of Earth, and their evolutionary superiority continues because microorganisms not only reproduce rapidly but also mutate frequently and exchange genes (by mechanisms such as conjugation, transformation, and transduction). Thus, they keep their superiority in natural selection. They still rule the world for this and other reasons, such as the production of our food and oxygen (algae).

**Metagenomic Revolution**

Metagenomics refers to the application of sequencing techniques to analyze the totality of the genomic material present in a sample (7). It allows us to characterize the entire communities of microbes in any given environment. Thus, it enables us to understand the complex interactions between different micro/macro-organisms and their environments, including our bodies.

The vital value of Earth has been recognized very early in Turkish culture; “My faithful half is black soil,” said the late Turkish folk poet Aşık Veysel (blinded by smallpox infection, 1894 –1973), who is famous for his love for nature, soil, and people (8). Thanks to the metagenomic revolution, we now know that Earth's value mainly comes from microorganisms; one teaspoon of soil contains more living organisms than people in the world (Figure 2).

Thanks to metagenomic technologies, we now have an idea of the number of microorganisms found in our soil, sea, and atmosphere (Figure 3).

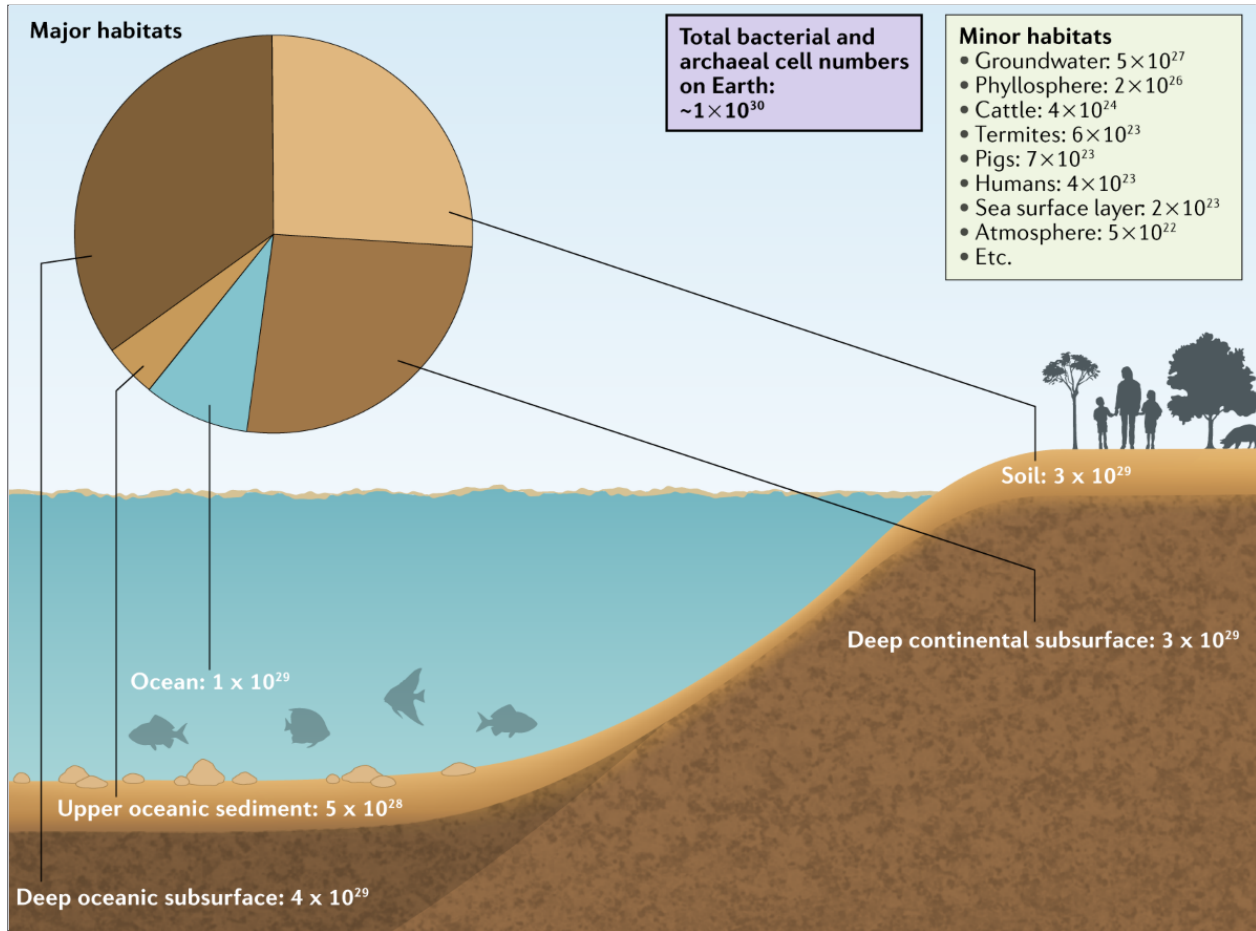


**Figure 3.** Estimated numbers of microorganisms found in our soil, sea, and atmosphere (10).

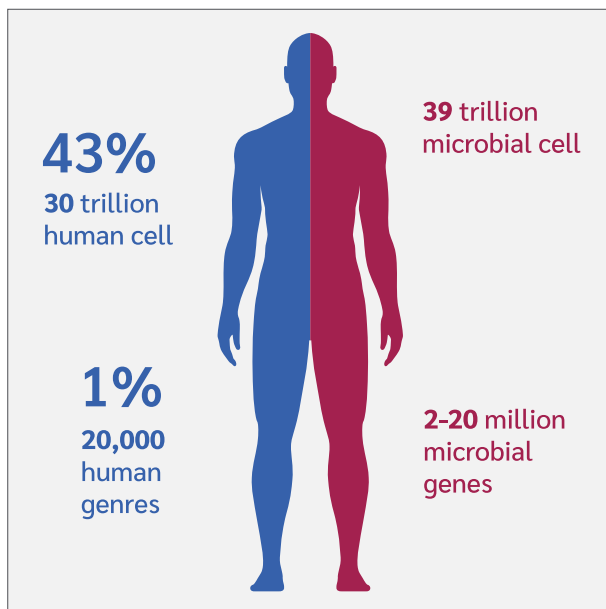


**Figure 4.** A normal human body contains more foreign cells and much more foreign genetic material than mammalian cells (13).

## Microbiome/ Microbiota

These two words are sometimes used interchangeably, but they have subtle differences. **Microbiome** refers to the collection of **genomes** from all the microorganisms in a given environment. Meanwhile, **microbiota** refers to microorganisms that are found within a specific environment. Think of our bodies; there are localized differences in each person's microbiota. Also, our gut microbiota differs greatly from the skin, mouth, etc. Predominant bacterial genera in the oral cavity, respiratory tract, skin, gut, and vagina are unique (11).

The human body consists of an estimated about 40 trillion cells (Figure 4), and only about 40 % belong to us (12). If we look at genetic material in our bodies, 99% of it belongs to microbiota.

Our microbiome is crucial to our health (13). Our microbiota is in symbiosis with us, contributing to homeostasis

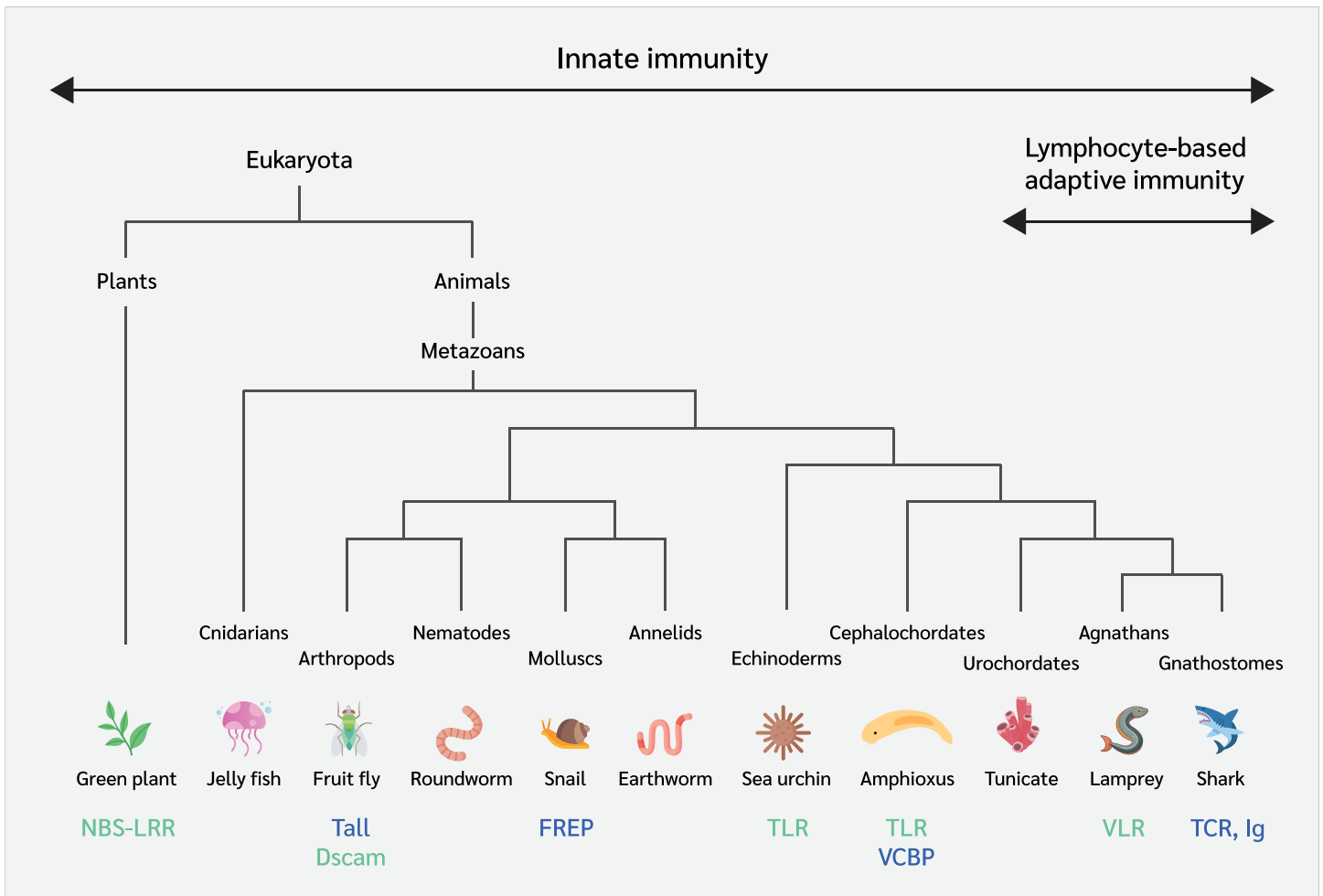


**Figure 5.** Evolution of defense systems (20).

and regulating immune function. Microbiota dysbiosis can lead to dysregulation of bodily functions and cause diseases. These microbes shape our metabolism and susceptibility to allergic and inflammatory diseases. As it became clear that microorganisms are no longer common germs or pathogens to be avoided—they are a crucial part of what makes us human, there is an explosion of literature that deals with why the gut microbiota is so important, its impact on human health, effect on allergies, or we use microbiota to treat disease, etc. Since the microbiota topic has been intensely reviewed, I only refer to some recent review articles (14-17).

## Immunity- A Peace Keeping Organ?

The interaction of different life forms on Earth can be described as a) commensalism, b) mutualism, or c) par-

### Box 2: Immunity in short

- Gathers information
- Solves problems; fast (innate) and slow (acquired)
- Keeps records (short and long-term memory)
- Communicates with brain using a common language; hormones, cytokines
- Evolves; changes, is selected, matures over

asitism. Since all organisms need to protect their cell/body borders, they must have defense systems. In fact, the first immune defence mechanism started in bacteria against viruses millions of years ago. Recently discovered CRISPR system protects bacteria against invading viruses (*bacteriophages*). CRISPR has become a powerful gene editing technology that is now revolutionizing biomedical research and clinical medicine (18). This kind of trillions of years of old protective mechanism,

i.e., foreign RNA/DNA recognition, still operates in our mammalian cells. If a mammalian cell is infected with a virus, that cell protects its neighbor cells by releasing interferon molecules (19).

As shown in Figure 5, starting from plants, metazoans all have an innate immune system that recognizes self and non-self. Only after fish, animals developed adaptive immunity. All jawed vertebrates assemble their antigen-receptor genes through combinatorial rearrangement of different immunoglobulin or T cell receptor gene segments. In humans, this sophisticated mechanism of “somatic mutations” has become so good that they can recognize an almost limitless number of antigens.

## Conclusion

“There is no ‘final knowledge obsession’ in science...”

**R. Feynman**

If one wishes to understand what life is, one must look at the world under the light of evolution (21, 22). Fast-evolving microorganisms and very slowly evolving multicellular organisms like us must live together. In

fact, our bodies are multispecies cell society living together. Therefore, there will always be border disputes (diseases).

Viruses and microorganisms are always one step ahead in evolution. Viruses are always at the center of inheritance (gene) wars and are strong, blind, and ruthless representatives of natural selection in evolution. Since the beginning of life on Earth, viruses and other microorganisms probably have shaped the evolution of all creatures. Recognizing strangers and protecting oneself started in single-celled organisms, evolved over time, and became more complex. The human immune system constantly evolves under the pressure of microbes. The immune system can be viewed as an army that lives together, watches over the borders, and tries to keep peace between multispecies cell populations.

In the natural world, an intricate and diverse web of life exists. It encompasses the interconnectedness of all living organisms, their habitats, and the ecosystems they form (23, 24). If this harmony is destroyed by the current rate of pollution, climate change, etc., consequences will be more frequent pandemics, which most people’s immune systems cannot handle.

**Ethics Committee Approval:** N.A

**Informed Consent:** N.A

**Peer-review:** : Externally peer-reviewed

**Author Contributions:** Concept – Ş.Ş.A; Design – Ş.Ş.A; Supervision –; Fundings –; Materials –; Data Collection and/

or Processing –; Analysis and/or Interpretation – Ş.Ş.A; Literature Review – Ş.Ş.A; Writer – Ş.Ş.A; Critical Reviews –Ş.Ş.A.

**Conflict of Interest:** The author declare no conflict of interest.

**Financial Disclosure:** The author declared that this study has received no financial support.

## References

- 1 Alkan SS. Coronavirus is still talking...You! Humankind, first know the universe, evolution and thysel! Turk J Immunol. 2020; 8(2):65-72.
- 2 Alkan SS. COVID-19 immunity. In: Canatan D, Alkan SS, editors. COVID-19 bağışıklığı. Ankara: Türkiye Klinikleri; 2021. p. 32-8.
- 3 COVID-19 epidemiological update – 12 March 2025 [Internet]. Geneva: World Health Organization. [cited February 24, 2025]. Available from: <https://www.who.int/publications/m/item/covid-19-epidemiological-update-edition-177>
- 4 Fan H, Tian M, Liu S, Ye C, Li Z, Wu K, et al. Strategies used by SARS-CoV-2 to evade the innate immune system in an evolutionary perspective. Pathogens. 2024;13(12):1117. [CrossRef]
- 5 Margulis L. Symbiotic planet: a new look at evolution. New York: Basic Books; 1999.
- 6 Wikin D, Brainard J. Evolution of life [Internet]. In: FlexBooks 2.0; 2024. [cited February 24, 2025]. Available from: <https://flexbooks.ck12.org/cbook/ck-12-biology-flexbook-2.0/section/1.8/primary/lesson/evolution-of-life-bio/>
- 7 Vasudeva K, Kaur P, Munshi A. High-throughput sequencing technologies in metagenomics. In: Munshi A, editor. Metagenomics to Bioremediation. 1st ed. Cambridge: Academic Press; 2023. p. 685-708.
- 8 Yildirim A. [An axiological analysis of Âşık Veysel’s poem Black earth (Kara Toprak)]. RumeliDE Dil ve Edebiyat Araştırmaları Dergisi. 2023;(36):533-40. Turkish. [CrossRef]

- 9 Financial Times. Metagenomics: mapping the mysteries of soil. FT Food Revolution [Internet]. [cited Apr 3, 2025]. Available from: <https://www.ft.com>
  - 10 Flemming HC, Wuertz S. Bacteria and archaea on Earth and their abundance in biofilms. *Nat Rev Microbiol*. 2019;17(4):247-60. [CrossRef]
  - 11 Hou K, Wu ZX, Chen XY, Wang JQ, Zhang D, Xiao C, et al. Microbiota in health and diseases. *Signal Transduct Target Ther*. 2022;7(1):135. [CrossRef]
  - 12 Hatton IA, Galbraith ED, Merleau NSC, Miettinen TP, Smith BM, Shander JA. The human cell count and size distribution. *Proc Natl Acad Sci U S A*. 2023;120(39):e2303077120. [CrossRef]
  - 13 AHW Endowment. Bacteria and the microbiome: why bacteria is crucial to our health [Internet]. Milwaukee (WI): AHW Endowment Blog; February 8, 2024 [cited February 24, 2025]. Available from: <https://blog.ahwendowment.org/bacteria-and-the-microbiome-why-bacteria-is-crucial-to-our-health>
  - 14 Noecker C, McNally CP, Eng A, Borenstein E. High-resolution characterization of the human microbiome. *Transl Res*. 2017;179:7-23. [CrossRef]
  - 15 Wood M. What role does the gut microbiome play in why more women develop Alzheimer's disease? [Internet]. Chicago (IL): The University of Chicago; February 8, 2024 [cited February 24, 2025]. Available from: <https://news.uchicago.edu/story/what-role-does-gut-microbiome-play-why-more-women-develop-alzheimers-disease>
  - 16 Burrows K, Ngai L, Chiaranunt P, Watt J, Popple S, Forde B, et al; A gut commensal protozoan determines respiratory disease outcomes by shaping pulmonary immunity. *Cell*. 2025;188(2):316-330.e12. [CrossRef]
  - 17 Nishijima S, Stankevic E, Aasmets O, Schmidt TSB, Nagata N, Keller MI, et al; GALAXY and MicrobLiver Consortia. Fecal microbial load is a major determinant of gut microbiome variation and a confounder for disease associations. *Cell*. 2025;188(1):222-36.e15. [CrossRef]
  - 18 Davis DJ, Yeddula SGR. CRISPR advancements for human health. *Mo Med*. 2024;121(2):170-6.
  - 19 Lu LY, Feng PH, Yu MS, Chen MC, Lin AJ, Chen JL, et al. Current utilization of interferon alpha for the treatment of coronavirus disease 2019: A comprehensive review. *Cytokine Growth Factor Rev*. 2022;63:34-43. [CrossRef]
  - 20 Hirano M, Das S, Guo P, Cooper DM. The evolution of adaptive immunity in vertebrates. In: Frederick WA, editor. *Advances in immunology*. Vol. 109. Cambridge (MA): Academic Press; 2011. p. 125-57.
  - 21 Dennett D. *Darwin's dangerous idea: evolution and the meaning of life*. New York: Simon & Schuster; 1995.
  - 22 Shubin N. *Some assembly required: decoding four billion years of life, from ancient fossils to DNA*. New York: Pantheon Books; 2020.
  - 23 Reaser JK, Linakis L, Perry S, Hartley DM, Hofmeister E, Mumma RO, et al. Looking left: ecologically based biosecurity to prevent pandemics. *Health Secur*. 2024;22(1). [CrossRef]
  - 24 Qiu J. The Next Viral Plague: A newly identified-and deadly-combination of climate and habitat crises, coupled with immune system stress, is driving more bat-borne viruses to afflict humanity. *Sci Am*. 2025;332(1):36. [CrossRef]
-